Sensing Human Sentiment via Social Media Images: Methodologies and Applications

by

Yilin Wang

A Dissertation Presented in Partial Fulfillment
of the Requirements for the Degree
Doctor of Philosophy

Approved July 2018 by the
Graduate Supervisory Committee:

Baoxin Li, Chair
Huan Liu
Hanghang Tong
Yi Chang

ARIZONA STATE UNIVERSITY

August 2018

ABSTRACT

Social media refers computer-based technology that allows the sharing of information and building the virtual networks and communities. With the development of internet based services and applications, user can engage with social media via computer and smart mobile devices. In recent years, social media has taken the form of different activities such as social network, business network, text sharing, photo sharing, blogging, etc. With the increasing popularity of social media, it has accumulated a large amount of data which enables understanding the human behavior possible. Compared with traditional survey based methods, the analysis of social media provides us a golden opportunity to understand individuals at scale and in turn allows us to design better services that can tailor to individuals needs. From this perspective, we can view social media as sensors, which provides online signals from a virtual world that has no geographical boundaries for the real world individual's activity.

One of the key features for social media is social, where social media users actively interact to each via generating content and expressing the opinions, such as post and comment in Facebook. As a result, sentiment analysis, which refers a computational model to identify, extract or characterize subjective information expressed in a given piece of text, has successfully employs user signals and brings many real world applications in different domains such as e-commerce, politics, marketing, etc. The goal of sentiment analysis is to classify a users attitude towards various topics into positive, negative or neutral categories based on textual data in social media. However, recently, there is an increasing number of people start to use photos to express their daily life on social media platforms like Flickr and Instagram. Therefore, analyzing the sentiment from visual data is poise to have great improvement for user understanding.

In this dissertation, I study the problem of understanding human sentiments from large scale collection of social images based on both image features and contextual social network features. We show that neither visual features nor the textual features are by themselves sufficient for accurate sentiment prediction. Therefore, we provide a way of using both of them, and formulate sentiment prediction problem in two scenarios: supervised and unsupervised. We first show that the proposed framework has flexibility to incorporate multiple modalities of information and has the capability to learn from heterogeneous features jointly with sufficient training data. Secondly, we observe that negative sentiment may related to human mental health issues. Based on this observation, we aim to understand the negative social media posts, especially the post related to depression e.g., self-harm content. Our analysis, the first of its kind, reveals a number of important findings. Thirdly, we extend the proposed sentiment prediction task to a general multi-label visual recognition task to demonstrate the methodology flexibility behind our sentiment analysis model.

DEDICATION

I dedicate my dissertation work to my loving parents, Haibo Wang and Yipan Zhang, for making me be who I am!

I also dedicate this dissertation to my girlfriend, Yi Qin, for supportng me all the way! Without her help and encouragement, this journey would have not been possible.

ACKNOWLEDGMENT

This dissertation is impossible without the help from my advisor Dr. Baoxin Li. I would like to thank him, for his guidance, encouragement, and support during my Phd career. I would also like to thank him to give me large freedom through my Ph.D. to explore various research problems and his excellent advising skills combining patience and guidance make my Ph.D. experience colorful, exciting and productive. Six year experience with him are my lifelong tresure. I learnt many abilities from him that I can benefit all my life: how to write papers and give presentations, how to find and address challenging problems, and how to establish your career and see the big vision. Dr. Li, I cannot thank you enough.

I would like to thank my committee members, Dr. Huan Liu, Dr. Hanghang Tong, and Dr. Yi Chang, for helpful suggestions and insightful comments. I take the social media course from Dr. Huan Liu, who opens a new door for my reseach world. Without taking his course, I would not even know my dissertation topic: sentiment anlaysis. His insightful discussions and commits provide me new angles to rethink about my research. I always consider Dr. Liu as my secondary advisor because many research ideas were initialized with his discussions. Dr. Yi Chang is my intern manager, he gave me lots of constructive comments and would like to share his industy experience to me, which I couldn't learn it from school. I also want to thank Dr. Hanghang Tong, who gives valuable comments and suggestion on dissertation.

I was lucky to work as interns in Yahoo!Labs and Adobe Research with amazing colleagues and mentors: Neil O'Hare, Jiliang Tang, Zhaowen Wang, Zhe Lin, Xin Lu and Xiaohui Shen. I enjoyed two wonderful and productive summers; and because of you, I was able to contribute my knowledge to exciting projects. Thank you for everything.

During my Ph.D. study, my friends and colleagues provided me consistent support and encouragement and they deserve a special thank. I am thankful to my colleagues at ASU: Qiang Zhang, Qiongjie Tian, Lin Chen, Suhang Wang, Kai Shu, Jundong Li, Liang Wu,

Xinsheng Li, Xilun Chen, Shengyu Huang, Xiang Zhang, Yao Zhou, Dawei Zhou, Chen Chen, Liangyue Li, Ziming Zhao, Mengxue Liu, Yuzhen Ding, Kevien Ding, Yikang Li, Tianshu Yu, Parag, Ragav, Xu Zhou, Jiayu Zhou, Xia Hu, Huiji Gao and Yuheng Hu. I would also like to thanks Dr. Subbarao Kambhampati to advise me on my first research work. I will remember a lot of memories when I spent on Brickyard fifth floor. They are my friends who have provide me very helpful suggestions insight comments, and encouagement.

Finally, I am deeply indebted to my dear mother and father for their love and strong support during my graduate study. I would like to thank my dear girlfriend Yi Qin for her strong support through all these years to my study. How fortunate I am having her in my life! This dissertation is dedicated to them.

TABLE OF CONTENTS

CHAPTER Page

LIST OF TABLES

LIST OF FIGURES

Chapter 1

INTRODUCTION

Social media which allows people to participate in online activities and shatters the barrier for online users to create and share information in any place at any time generates massive data in an unprecedented rate. With such a large amount of social media user activity records, it makes the analysis of online social media user possible. Mining the user online activities patterns will greatly improve the Internet based services and enable many real world applications such as content/item recommendation, personalized information retrieval, event prediction and etc. From application perspective, social media provides online signals that can sense people physical world activities.

Recently, an increasing number of people start to use photos to express their daily life on social media platforms like Facebook, Snapchat and Instagram. For example, in every minute of 2016 [1] , 38,194 photo uploaded to Instagram, 527,760 shared on Snapchat and 37,722 tweets posted on Twitter. Meanwhile, people likely to post image in social media. Since by sharing photos, users could also express opinions or sentiments, social media images provide a potentially rich source for understanding public opinions/sentiments. Similar to textual sentiment analysis, sentiment analysis for social media images could benefit many applications such as advertisement, recommendation, marketing, health-care and etc. To this end, I am motivated to take advantage of both data mining and computer vision techniques to better understand the content of social media images. However, different with recent intensively studied textual based sentiment analysis Pang *et al.* (2008); Pak and Paroubek (2010); Wilson *et al.* (2005); Pang and Lee (2004); Taboada *et al.* (2011) and visual based

[1] http://www.visualcapitalist.com/what-happens-internet-minute-2016/

sentiment analysis Borth *et al.* (2013b,a); Hussain *et al.* (2017), characteristic of sentiment analysis for social media images presents new challenges.

1.1 Research Challenges

Sentiment analysis for social media images aims to infer human sentiment: positive, negative and neutral, from the photos shared on social media websites such Flickr and Instagram. Two examples with text descriptions are shown in Figure 1.1.

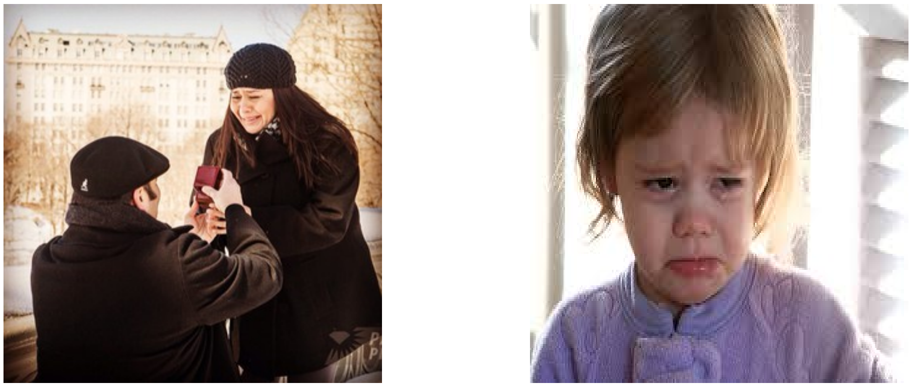

(a) A Women Cries.

(b) My Cute Baby is Crying.

Figure 1.1: An Example of Social Media Images.

Compared to the intensive studied on sentiment analysis of textual data such as Tweets Pang and Lee (2004); Pang *et al.* (2008), sentiment analysis of images is still in its infancy. A popular approach is to identify visual features from a photo that are related to human sentiments Borth *et al.* (2013b,a). For example, detecting and recognizing objects (e.g., toys, birthday cakes, gun), human actions (e.g., crying or laughing), and other low level visual features such as color temperature, brightness and etc. However, such an approach is often insufficient because the same objects/actions may convey different sentiments in different photo contexts. For example, consider Figure 1: one can easily detect the crying lady and girl (using computer vision algorithms such as face detection and expression recognition).

However, the same crying action conveys two clearly different sentiments: the crying in Figure 1a is obviously positive as the result of a successful marriage proposal. In contrast, the tearful girl in Figure 1b looks quite unhappy thus expresses negative sentiment. In other words, the so-called visual affective gap Machajdik and Hanbury (2010) exists between rudimentary visual features and human sentiment embedded in a photo. On the other hand, one may also consider inferring the sentiment of a photo via its textual descriptions (e.g., titles) using existing off-the shelf text-based sentiment analysis tools [3]. Although these descriptions can provide very helpful context information of the photos, solely relying on them while ignoring the visual features of the photos can lead to poor performance as well. Consider Figure 1 again: by analyzing only the text description from caption, we can conclude that both Figure 1a and 1b convey negative sentiment as the keyword crying is often classified as negative sentiment in standard sentiment lexicon. Last, both visual feature-based and text-based sentiment analysis approaches require massive amounts of training data in order to learn high quality models. However, manually annotating the sentiment of a vast amount of photos and/or their textual descriptions is time consuming and error-prone, presenting a bottleneck in learning good models. Last but not least, image sentiment analysis should be a special case of image classification, the methodology used for sentiment analysis should has flexibility to extend to general image classification task.

1.2 Contributions

The aforementioned challenges present a series of unsolved research questions: (1) How can we model the textual information and visual information jointly for sentiment analysis of social media images? (2) how can we adapt weakly supervised or unsupervised learning to avoid labor effort for the sentiment annotation of social media images? (3) By applying sentiment analysis on social media images, could we discover interest pattern for social media users? (4) is there a unified framework to extend sentiment analysis for general multi-label image classification? One of the main objectives of this dissertation aims to figure out these questions via innovated algorithms. The contribution of this dissertation can be summarized as following:

- The unique property of social media images determine that new algorithms should be innovated in order to precisely understand the sentiment. We design two sentiment analysis algorithm for two scenarios: supervised and unsupervised. Our first attempt is an efficient supervised sentiment analysis method RSAI Wang *et al.* (2015b), It designed to fill the visual affective gap by extracting the visual features and mapping them to different sentiment meanings. In our second attempt, we study unsupervised sentiment analysis for social media images with textual information, which is designed for learning sentiment from data than human annotation.

- We propose a new research task, i.e., self harm understanding, which is discovered from negative sentiment social media images. We make a number of important findings about self harm users on social media and develop a unified framework in both supervised and unsupervised fashion to predict self harm content.

- We generalize research about image based sentiment analysis to multi-label image classification task for computer vision. In particular, we find that beyond sentiment label, the above mentioned methods can easily extend to tag recommendation and attribute classification in computer vision, which expands the boundaries of the research in sentiment analysis of images.

1.3 Organization

The reminder of this dissertation is organized as follows.In Chapter 2, I review the related work. In Chapter 3, I discuss the proposed unified model for supervised sentiment analysis for social media images. In Chapter 4, I propose a framework for unsupervised sentiment analysis. In Chapter 5, I present a new research problem for negative sentiment discovery with a study case on self harm content analysis. In Chapter 6, I propose to extend sentiment analysis prediction task to general image classification task. In Chapter 7, I conclude and present the future work.

Chapter 2

RELATED WORK

Sentiment analysis for social media images is a novel and practical problem. Recently,with increasing popularity of social networks, it attracts a lot of attention from academia and industry. In this dissertation, I firstly provide a systematic and in depth literature review in the literature.

Sentiment analysis on text and images: Recently, sentiment analysis has shown its success in opinion mining on textual data, including product reviewLiu (2012); Hu and Liu (2004), newspaper articles Pang *et al.* (2002), and movie rating Pang and Lee (2004). Besides, there have been increasing interests in social media data Borth *et al.* (2013b); Yang *et al.* (2014); Jia *et al.* (2012); Yuan *et al.* (2013), such as Twitter and Weibo data. Unlike text-based sentiment prediction approaches, Borth *et al.* (2013b); Yuan *et al.* (2013) employed mid-level attributes of visual feature to model visual content for sentiment analysis. Yang *et al.* (2014) provides a method based on low-level visual features and social information via a topic model. While Jia *et al.* (2012) tries to solve the problem by a graphical model which is based on friend interactions. In contrast to our approach, all such methods restrict sentiment prediction to the specific data domain. For example, in Figure 1, we can see that approaches using pure visual information Borth *et al.* (2013b); Yuan *et al.* (2013) may be confused by the subtle sentiment embedded in the image. e.g., two crying people convey totally different sentiment. Jia *et al.* (2012); Yang *et al.* (2014) assume that the images belong to the same sentiment share the same low-level visual features is often not true, because positive and negative images may have similar low-level visual features, e.g., two black-white images contain smiling and sad faces respectively. Recent, deep learning has shown its success in feature learning for many computer vision problem, You *et al.* (2015)

provides a transfer deep neutral network structure for sentiment analysis. However, for deep learning framework, millions of images with associated sentiment labels are needed for network training. In real world, such label information is not available and how to deal with overfitting for small training data remains a challenging problem.

Multimodal classification for social media: Multimodal classification techniques can be classified into two main classes: early fusion and late fusion, which are depending on how the information from multiple modalities are combined. In early fusion, features are extracted from different modalities are combined together. Then the combined features are feed into a classification framework. Various early fusion methods have been proposed to classify social media content. In You *et al.* (2016a), the proposed algorithm first learns the joint embedding for both text and image, then applied LSTM (long short term memory) for sentiment classification. In Zeppelzauer and Schopfhauser (2016), the hierarchical structure is proposed to learn the concatenated features. Compared to early fusion, late fusion methods are more widely used. In late fusion, separated classification result or representation is obtained on each modality independently. Then all the result or feature is combined at decision level. There are only a few works on analyzing sentiment using multi-modal features, such as text and images. Wang *et al.* (2014) employed both text and images for sentiment analysis, where late fusion is employed to combine the prediction results of using n-gram textual features and mid-level visual features. You *et al.* (2016b) proposed a cross-modality scheme for joint sentiment analysis. Their approach employed deep visual and textual features to learn a regression model.

Our work is built on non-negative matrix factorization, where we joint learn the textual -visual feature together. Our method belongs to late fusion for multimodal classification problem.

Non-negative matrix factorization(NMF): Our proposed framework is also inspired by recent progress in matrix factorization algorithms. NMF has been shown to be useful in computer vision and data mining applications including face recognitionWang *et al.* (2005), object detection Lee and Seung (1999) and feature selection Das Gupta and Xiao (2011), etc. Specifically, the work in Lee and Seung (2001) brings more attention to NMF in the research community, where the author proposed a simple multiplicative rule to solve the problem and showed the factor coherence of original image data. Ding *et al.* (2005) shows that if adding orthogonal constrains, the NMF is equivalent to K-means clustering. Further, Ding *et al.* (2006) presents a work that shows, when incorporating freedom control factors, the non-negative factors will achieve a better performance on classification. In this paper, motivated by previous NMF framework for learning the latent factors, we extend these efforts significantly and propose a comprehensive formulation which incorporates more physically-meaningful constraints for regularizing the learning process in order to find a proper solution. In this respect, our work is similar in spirit to Hu *et al.* (2013) which develops a factorization approach for sentiment analysis of social media responses to public events.

In the dissertation, we discovery self harm user patterns from negative sentiment. Therefore, in the following, we review related work on self ham and public health.

Selfharm research from psychology and medicine: Some work from psychology and medicine have been done on understanding and characterizing the deliberate self-harm patients. In Hawton *et al.* (1997), it investigates $8,950$ deliberate self-harm (DSH) patients from 1990 to 2000 in Oxford, UK to capture their behavior trends. It shows that from 1997 to 2000, gender and age became a large portion of DSH – DSH rates in female and aged in 15 to 24 and 34 to 54 have been significantly increased. The major reasons of DSH are alcohol abuse, violence and misusing drugs. In Chapman *et al.* (2006), the authors reported that DSH helps the patients escape or regulate the emotions and most self-injurious behaviors are along with cognitive disabilities. In recent years Daine *et al.* (2013); Dyson *et al.* (2016); Robinson *et al.* (2015), more and more attention has been paid on social media platforms and studies Robinson *et al.* (2015) have shown that self-harm and suicide can be prevented from social supports from other social media users. However, the limitation of these studies is that they are typically based on surveys and self-reports about emotion. Most assessments are designed to collect the data about DSH experiences over long periods of time (1 to 5 years). Few studies are on the short term since the resources and invasiveness are required to observe individuals' behaviors over days and months.

Social Media and Public Health: In the last few years, the interests of studying public health in social media are keep growing in the research community. Sadilek *et al.* (2012) explored how to find diseases based on the posts in Twitter. Chancellor *et al.* (2016) studied the eating-disorder community on Tumblr and finds that the tags for eating-disorder community are keep evolving. In De Choudhury *et al.* (2013, 2016), authors investigated the patterns of activities for depression groups on web by analyzing the posts from Twitter and Reddit, respectively. However, research on self-harm understanding in social media is still in its infancy.

Chapter 3

SUPERVISED SENTIMENT ANALYSIS FOR SOCIAL MEDIA IMAGES

In this chapter, I focus on the problem of exploiting textual and visual information for sentiment prediction from social media images. Due to the distinct characteristics of social media data, I focus on supervised learning method in this chapter. I will firstly review the background of this problem, and then formally define the problem and present the proposed method. The real-world dataset from Flickr and Instagram will be used to evaluate the effectiveness of the proposed method by comparing with the state-of-the-art baselines.

3.1 Supervised sentiment analysis for Social Media Images

A picture is worth a thousand words. It is surely worth even more when it comes to convey human emotions and sentiments. Examples that support this are abundant: great captivating photos often contain rich emotional cues that help viewers easily connect with those photos. With the advent of social media, an increasing number of people start to use photos to express their joy, grudge, and boredom on social media platforms like Flickr and Instagram. Automatic inference of the emotion and sentiment information from such ever-growing, massive amounts of user-generated photos is of increasing importance to many applications in health-care, anthropology, communication studies, marketing, and many sub-areas within computer science such as computer vision. Think about this: Emotional wellness impacts several aspects of people's lives. For example, it introduces self-empathy, giving an individual greater awareness of their feelings. It also improves one's self-esteem and resilience, allowing them to bounce back with ease, from poor emotional health, and physical stress and difficulty. As people are increasingly using photos to record their daily lives [1] , we can assess a person's emotional wellness based on the emotion and sentiment inferred from her photos on social media platforms (in addition to existing emotion/sentiment analysis effort, e.g., see De Choudhury *et al.* (2012) on text-based social media).

As mentioned in Chapter 1. Both text based methods and visual content based methods are not suit for social media images. For example, re-consider Figure 1.1: visual feature usually has no contextual information on the visual content such as the action of ”proposal” in figure 1.1a. On the other hand, textual feature in the social media images usually not contain enough content information as the text messages are very short. For example, Twitter allows users to post message up to 140 characters. Moreover, such textual messages are also very unstructured and noisy. For example, users often prefer to use popular abbreviation words. Since the slang words don't usually appear on conventional text documents. Therefore the textual sentiment lexicon seldom contains them.

The weaknesses discussed in the foregoing motivate the need for a more accurate automated framework to infer the sentiment of photos, with 1) considering the photo context to bridge the "visual affective gap", 2) considering a photo's visual features to augment text-based sentiment, and 3) considering the availability of textual information, thus a photo may have little or no social context (e.g., friend comments, user description). While such a framework does not exist, we can leverage some partial solutions. For example, we can learn the photo context by analyzing the photo's social context (text features). Similarly, we can extract visual features from a photo and map them to different sentiment meanings. Last, while manual annotation of all photos and their descriptions is infeasible, it is often possible to get sentiment labeling for small sets of photos and descriptions. In essence, I investigate the following three questions:cm

- How do we model heterogeneous information sources, i.e., the visual information and textual information, properly in a unified framework.

[1] http://www.pewinternet.org/2015/01/09/social-media-update-2014/

- How do we seamlessly exploit both sources of information for the problem?
- How do we alleviate limited label information for efficient training?

Technical Contribution: We propose an efficient and effective framework, named *RSAI* (Robust Sentiment Analysis for Images), for inferring human sentiment from photos that leverages these partial solutions. Figure 3.1 depicts the procedure of RSAI. Specifically, to fill the visual affective gap, we first extract visual features from a photo using low-level visual features (e.g., color histograms) and a large number of mid-level (e.g., objects) visual attribute/object detectors Yuan *et al.* (2013); Tighe and Lazebnik (2013). Next, to add sentiment meaning to these extracted non-sentimental features, we construct Adjective Noun Pairs (ANPs)Borth *et al.* (2013b). Note that ANP is a visual representation that describes visual features by text pairs, such as “cloudy sky”, “colorful flowers”. It is formed by merging the low-level visual features to the detected mid-level objects and mapping them to a dictionary (more details on ANP are presented in Section 3). On the other hand, to learn the image’s context, we analyze the image’s textual description and capture its sentiment based on sentiment lexicons. Finally, with the help from ANPs and image context, RSAI infers the image’s sentiment by factorizing an input image-features matrix into three factors corresponding to image-term, term-sentiment and sentiment-features. The ANPs here can be seen as providing the initial information (“prior knowledge”) on sentiment-feature factors. Similarly, the learnt image context can be used to constrain image-term and term-sentiment factors. Last, the availability of labeled sentiment of the images can be used to regulate the product of image-term, term-sentiment factors. We pose this factorization as an optimization problem where, in addition to minimizing the reconstruction error, we also require that the factors respect the prior knowledge to the extent possible. We derive a set of multiplicative update rules that efficiently produce this factorization, and provide empirical comparisons with several competing methodologies on two real datasets of photos from Flickr and

Instagram. We examine the results both quantitatively and qualitatively to demonstrate that our method improves significantly over baseline approaches.

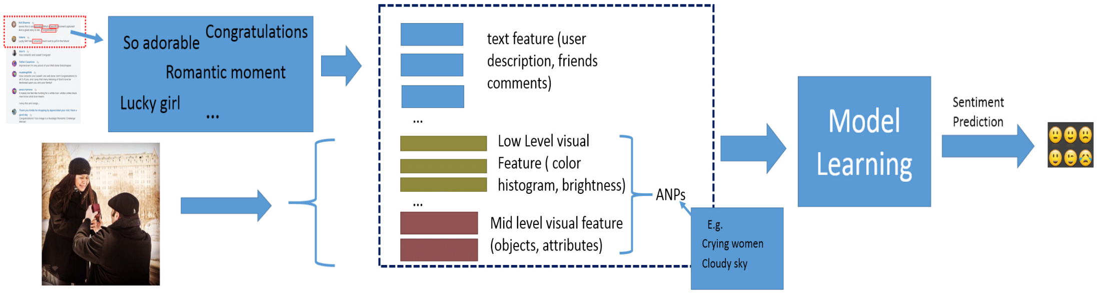
So adorable
Congratulations
Romantic moment
Lucky girl
...
text feature (user description, friends comments)
...
Low Level visual Feature (color histogram, brightness)
...
Mid level visual feature (objects, attributes)
ANPs
E.g.
Crying women
Cloudy sky
Model Learning
Sentiment Prediction

Figure 3.1: The Framework of RSAI.

3.2 The Proposed RSAI Framework

In this section, we first propose the basic model of our framework. Then we show the details of how to generate the ANPs. After that, we describe how to obtain and leverage the prior knowledge to extend the basic model. We also analyze the algorithm in terms of its correctness and convergence. Table 1 lists the mathematical notation used in this paper.

3.2.1 Basic Model

Assuming that all the images can be partitioned into K sentiment ($K = 3$ in this paper as we focus on positive, neutral and negative. However, our framework can be easily extended to handle more fine-grained sentiment.) Our goal is to model the sentiment for each image based on visual features and available text features. Let n be the number of images and the size of contextual vocabulary is t. We can then easily cluster the images with similar word frequencies and predict the cluster's sentiment based on its word sentiment. Meanwhile, for each image, which has m-dimensional visual features (ANPs, see below), we can cluster the images and predict the sentiment based on the feature probability. Accordingly, our basic framework takes these n data points and decomposes them simultaneously into three factors:

Table 3.1: Notations

Notation	Dimension	Description
X	$n \times m$	Input data matrix
T	$n \times t$	Data-term matrix
S	$t \times k$	Term-sentiment matrix
V	$m \times k$	Feature-sentiment matrix
T_0	$n \times t$	Prior knowledge on T
S_0	$t \times k$	Prior knowledge on S
V_0	$m \times k$	Prior knowledge on V
R_0	$n \times k$	Prior knowledge on the labels

photo-text, text-sentiment and visual feature-sentiment. In other words, our basic model tries to solve the following optimization problem:

$$\begin{aligned} \min_{TSV} \quad & \left\|X - TSV^T\right\|_F^2 + \|T - T_0\|_F^2 \\ \text{subject to} \quad & T \geq 0, S \geq 0, V \geq 0; , \end{aligned} \tag{3.1}$$

where $X \in \mathbb{R}^{n \times m}$ represents input data matrix, and $T \in \mathbb{R}^{n \times t}$ indicates the text features. That is, the ith row of matrix T corresponds to the posterior probability of the ith image's contextual social network information referring to the t text terms (vocabulary). Similarly, $S \in \mathbb{R}^{t \times k}$ indicates the posterior probability of a text belonging to k sentiments. Finally, $V \in \mathbb{R}^{m \times k}$ represents the sentiment for each ANP. The regularization term T_0 is the term-frequency matrix for the whole word vocabulary (which is built based on textual descriptions of all photos). It is worth noting that the non-negativity makes the latent components easy to interpret.

As a result of this factorization, we can readily predict the image sentiment whether the contextual information (comments, user descriptions,etc.) is available or not. For example, if there is no social information associated with the image, then we can directly derive the image sentiment by applying non-negative matrix factorization for the input data X, when we characterize the sentiment of each image through a new matrix $R = T \times S$. Specifically, our basic model is similar to the probabilistic latent semantic indexing (PLSI) Hofmann (1999) and the orthogonal nonnegative tri-matrix factorization Ding *et al.* (2006). In their work, the factorization means the joint distribution of documents and words.

3.2.2 Extracting and Modeling Visual Features

In Tighe and Lazebnik (2013); Tu *et al.* (2005); Yuan *et al.* (2013), visual content can be described by a set of mid-level visual attributes, however, most of the attributes such as “car”, “sky”,“grass”, etc., are nouns which make it difficult to represent high level sentiments. Thus, we followed a more tractable approach Borth *et al.* (2013b), which models the correlation between visual attributes and visual sentiment with adjectives, such as “beautiful” , “awesome”, etc. The reason for employing such ANPs is intuitive: the detectable nouns (visual attributes) make the visual sentiment detection tractable, while the adjectives add the sentiment strength to these nouns. In Borth *et al.* (2013b), a large scale ANPs detectors are trained based on the features extracted from the images and the labeled tags with SVM. However, we find that such pre-defined ANPs are very hard to interpret. For example the pairs like “warm pool” , “abandoned hospital”, and it is very difficult to find appropriate features to measure them. Moreover, in their work, during the training stage, the SVM is trained on the features extracted from the image directly, the inability of localizing the objects and scales bounds the detection accuracy. To address these problems, we have a two stage approach to detect ANPs based on the Visual Sentiment Ontology Borth *et al.* (2013b) and train a one vs all classifier for each ANP.

Noun Detection: The nouns in ANPs refer to the objects presented in the image. As one of fundamental tasks in computer vision, object detection has been studied for many years. One of most successful works is Deformable Part Model (DPM) Felzenszwalb *et al.* (2010) with Histogram of Oriented Gradient (HOG) Dalal and Triggs (2005) features. In Felzenszwalb *et al.* (2010), the deformable part model has shown its capability to detect most common objects with rigid structure such as: car, bike and non-rigid objects such as pedestrian, dogs. Pandey and Lazebnik (2011) further demonstrates that DPM can be used to detect and recognize scenes. Hence we adopt DPM to for nouns detection. The common objects(noun) are trained by the public dataset ImageNetDeng *et al.* (2009). The scene detectors are trained on SUN dataset Xiao *et al.* (2010). It is worth noting that selfie is one of most popular images on the web Hu *et al.* (2014) and face expression usually conveys strong sentiment, consequently, we also adopt one of state-of-the-art face detection methods proposed in Zhu and Ramanan (2012).

Adjective Detection: Modeling the adjectives is more difficult than nouns due to the fact that there are no well defined features to describe them. Following Borth *et al.* (2013b), we collect 20,000 images associate with specific adjective tags from Web. The a set of discriminative global features, including Gist, color histogram and SIFT, are applied for feature extraction. Finally the adjective detection is formulated as a traditional image classification problem based on Bag of words(BOW)model. The dictionary size of BOW is 1,000 with the feature dimension size 1,500 after dimension reduction based on PCA.

3.2.3 Constructing Prior Knowledge

So far, our basic matrix factorization framework provides potential solution to infer the sentiment regarding the combination of social network information and visual features. However, it largely ignores the sentiment prior knowledge on the process of learning each component. In this part, we introduce three types of prior knowledge for model regularization: (1) sentiment-lexicon of textual words, (2) the normalized sentiment strength for each ANP, and (3) sentiment labels for each image.

Sentiment Lexicon The first prior knowledge is from a public sentiment lexicon named MPQA corpus [2] . In this sentiment lexicon, there are 7,504 human labeled words which are commonly used in the daily life. The number of positive words (e.g."happy", "terrific") is 2,721 and the number of negative words (e.g. "gloomy", "disappointed") is 4,783. Since this corpus is constructed without respect to any specific domain, it provides a domain independent prior on word-sentiment association. It should be noted that the English usage in social network is very casual and irregular, we employ a stemmer technique proposed in Han and Baldwin (2011). As a result, the ill-formed words can be detected and corrected based on morphophonemic similarity, for example "good" is a correct version of "gooooooooooooood". Besides some abbreviation of popular words such as "lol"(means laughing out loud) is also added as prior knowledge. We encode the prior knowledge in a word sentiment matrix S_0 where if the i_{th} word belongs to j_{th} sentiment, then $S_0(i, j) = 1$, otherwise it equals to zero.

Visual Sentiment In addition to the prior knowledge on lexicon, our second prior knowledge comes from the Visual Sentiment Ontology (VSO) Borth *et al.* (2013b), which is based on the well known previous researches on human emotions and sentiments Darwin (1998); Plutchik (1980). It generates 3000 ANPs using Plutchnik emotion model and associates the sentiment strength (range in[-2:2] from negative to positive) by a wheel emotion interface [3] . The sample ANP sentiment scores are shown in Table 2. Similar to the word sentiment

[2] http://mpqa.cs.pitt.edu/

[3] http://visual-sentiment-ontology.appspot.com

Table 3.2: Sentiment Strength Score Examples

ANP	Sentiment Strength
innocent smile	1.92
happy Halloween	1.81
delicious food	1.52
cloudy mountain	-0.4
misty forest	-1.00
...	...

matrix S_0, the prior knowledge on ANPs V_0 is the sentiment indicator matrix.

Sentiment labels of Photos Our last prior knowledge focuses on the prior knowledge on the sentiment label associated with the image itself. As our framework essentially is a semi-supervised learning approach, this leads to a domain adapted model that has the capability to handle some domain specific data. The partial label is given by the image sentiment matrix R_0 where $R_0 \in \mathbb{R}^{n \times k}$. For example if the i_{th} image belongs to j_{th} sentiment, the $R_0(i, j) = 1$ otherwise $R_0(i, j) = 0$. The improvement by incorporating these label data is empirically verified in the experiment section.

3.2.4 Incorporating Prior Knowledge

After defining the three types of prior knowledge, we incorporate them into the basic model as regularization terms in following optimization problem:

$$\begin{aligned}\min_{TSV} & \left\| X - TSV^T \right\|_F^2 + \alpha \left\| V - V_0 \right\|_F^2 \\ & + \beta \left\| T - T_0 \right\|_F^2 + \gamma \left\| S - S_0 \right\|_F^2 \\ & + \delta \left\| TS - R_0 \right\|_F^2 \\ \text{subject to } & T \geq 0, S \geq 0, V \geq 0\end{aligned} \tag{3.2}$$

where $\alpha \geq 0$, $\beta \geq 0$, $\gamma \geq 0$ and $\delta \geq 0$ are parameters controlling the extent to which we enforced the prior knowledge on the respective components. The model above is generic and allows flexibility . For example, if there is no social information available for one image, we can simply set the corresponding row of T_0 to zeros. Moreover, the square loss function leads to an unsupervised problem for finding the solutions. Here, we re-write Eq (2) as :

$$\begin{aligned} L =& Tr(X^T X - 2X^T TSV^T + VS^T T^T TSV^T) \\ & + \alpha Tr(V^T V - 2V^T V_0 + V_0^T V) \\ & + \beta Tr(T^T T - 2T^T T_0 + T_0^T T_0) \\ & + \gamma Tr(S^T S - 2S^T S_0 + S_0^T S_0) \\ & + \delta Tr(S^T T^T TS - 2S^T T^T R_0 + R_0^T R_0) \end{aligned} \tag{3.3}$$

From Eq 3.3 we can find that it is very difficult to solve T, S and V simultaneously. Thus we employ the alternating multiplicative updating scheme shown in Ding *et al.* (2006) to find the optimal solutions. First, we use fixed V and S to update T as follows:

$$T_{ij} \leftarrow T_{ij} \sqrt{\frac{[XVS^T + \beta T_0 + \delta R_0 S^T]_{ij}}{[TSV^T VS^T + \beta T + \delta TSS^T]_{ij}}} \tag{3.4}$$

Next, we use the similar update rule to update S and V:

$$S_{ij} \leftarrow S_{ij} \sqrt{\frac{[T^T XV + \gamma S_0 + \delta T^T R_0]_{ij}}{[T^T TSV^T V + \gamma S + \delta T^T TS]_{ij}}} \tag{3.5}$$

$$V_{ij} \leftarrow V_{ij}\sqrt{\frac{[X^TTS+\alpha V_0]_{ij}}{[VS^TT^TTS+\alpha V]_{ij}}} \tag{3.6}$$

The learning process consists of an iterative procedure using Eq 3.4, Eq 3.5 and Eq 3.6 until convergence. The description of the process is shown in Algorithm 1.

Algorithm 1 Multiplicative Updating Algorithm

```
**Input:** $X, T_0, S_0, V_0, R_0, \alpha, \beta, \gamma, \delta$
**Output:** $T, S, V$
**Initialization:** $T, S, V$
**while** Not Converge **do**
    Update $T$ using Eq(4) with fixed $S, V$
    Update $S$ using Eq(5) with fixed $T, V$
    Update $V$ using Eq(6) with fixed $T, S$
**end whileEnd**
```

3.2.5 Algorithm Correctness and Convergence

In this part, we prove the guaranteed convergence and correctness for Algorithm 1 by the following two theorems.

Theorem 1. *When Algorithm 1 converges, the stationary point satisfies the Karush-Kuhn-Tuck(KKT) condition, i.e., Algorithm 1 converges correctly to a local optima.*

Proof of Theorem 1. We prove the theorem when updating V using Eq 3.6, similarly, all others can be proved in the same way. First we form the gradient of L regards V as Lagrangian form:

$$\frac{\partial L}{\partial V} = 2(VS^TT^TTS+\alpha V) - 2(X^TTS+\alpha V_0) - \mu \tag{3.7}$$

Where μ is Lagrangian multiplier μ_{ij} enforces the non-negativity constraint on V_{ij}. From the complementary slackness condition, we can obtain

$$(2(VS^TT^TTS + \alpha V) - 2(X^TTS + \alpha V_0))_{ij}V_{ij} = 0 \tag{3.8}$$

This is the fixed point relation that local minima for V must hold. Given the Algorithm 1., we have the convergence point to the local minima when

$$V_{ij} = V_{ij}\sqrt{\frac{[X^TTS + \alpha V_0]_{ij}}{[VS^TT^TTS + \alpha V]_{ij}}} \tag{3.9}$$

Then the Eq 3.9 is equivalent to

$$(2(VS^TT^TTS + \alpha V) - 2(X^TTS + \alpha V_0))_{ij}V_{ij}^2 = 0 \tag{3.10}$$

This is same as the fixed point of Eq 3.9,i.e., either $V_{ij} = 0$ or the left factor is 0. Thus if Eq 3.10 holds the Eq 3.9 must hold and vice versa.

Theorem 2. *The objective function is nondecreasing under the multiplicative rules of Eq (4), Eq (5) and Eq (6), and it will converge to a stationary point.*

Proof of Theorem 2. First, let $H(V)$ be:

$$H(V) = Tr((VS^TT^TTS + \alpha V)V^T - (X^TTS + \alpha V_0 + \mu)V^T) \tag{3.11}$$

and it is very easy to verify that $H(V)$ is the Lagrangian function of Eq 3.3 with KKT condition. Moreover, if we can verify that the update rule of Eq 3.4 will monotonically decrease the value of $H(V)$, then it means that the update rule of Eq 3.4 will monotonically decrease the value of $L(V)$(recall Eq 3.3). Here we complete the proof by constructing the following an auxiliary function $h(V, \widetilde{V})$.

$$\begin{aligned} h(V, \widetilde{V}) =& \sum_{ik} \frac{(\widetilde{V}(VS^TT^TTS + \alpha V))_{ik}V_{ik}^2}{\widetilde{V_{ik}}} \\ & - \sum_{ik}(X^TTS + \alpha V_0 + \mu)_{ik}V_{ik}(1 + \log \frac{V_{ik}}{\widetilde{V_ik}}) \end{aligned} \tag{3.12}$$

Since $z \geq (1 + \log z), \forall z > 0$ and similar in Ding *et al.* (2006), the first term in $h(V, \widetilde{V})$ is always larger than that in $H(V)$, then the inequality holds $h(V, \widetilde{V}) \geq H(V)$. And it is easy to see $h(V, \widetilde{V}) = H(V)$, thus $h(V, \widehat{V})$ is an auxiliary function of $H(V)$. Then we have the following inequality chain:

$$H(V^0) = h(V^0, V^0) \geq h(V^0, V^1) = H(V^1).... \tag{3.13}$$

Thus, with the alternate updating rule of V, S and T, we have the following inequality chain:

$$L(V^0, T^0, S^0) \geq L(V^1, T^0, S^0) \geq L(V^1, T^1, S^0).... \tag{3.14}$$

Since $L(V, S, T) \geq 0$. Thus $L(V, S, T)$ is bounded and the Algorithm 1 converges , which completes the proof.

3.3 Empirical Evaluation

We now quantitatively and qualitatively compare the proposed model on image sentiment prediction with other candidate methods. We also evaluate the robustness of the proposed model with respect to various training samples and different combinations of prior knowledge. Finally, we perform a deeper analysis of our results.

3.3.1 Experiment Settings

We perform the evaluation on two large scale image datasets collected from Flickr and Instagram respectively. The collection of Flickr dataset is based on the image IDs provided by Yang *et al.* (2014), which contains 3,504,192 images from 4,807 users. Because some images are unavailable now, and without loss of generality, we limit the number of images from each user. Thus, we get 120,221 images from 3921 users. For the collection of the Instagram dataset, we randomly pick 10 users as seed nodes and collect images by traversing the social network based on breadth first search. The total number of images from Instagram is 130,230 from 3,451 users.

Establishing Ground Truth: For training and evaluating the proposed method, we need to know the sentiment labels. Thus, 20,000 Flickr images are labeled by three human subjects, the majority voting is employed. However, manually acquiring the labels for these two large scale datasets is expensive and time consuming. Consequently, the rest of more than 230,000 images are labeled by the tags, which was suggested by the previous works Yang *et al.* (2014); Go *et al.* (????) [4] . Since labeling the images based on the tags may cause noise issue, and for better reliability we only label the images with primary sentiment labels, which include: positive, neutral and negative. It is worth noting that the human labeled images have both primary sentiment labels and fine grained sentiment labels. The fine grained labels, including: happiness, amusement, anger, fear, sad and disgust, are used to for fine grained sentiment prediction.

The comparison methods include: Senti API [5] , SentiBank Borth *et al.* (2013b), ELYang *et al.* (2014) and the baseline method.

- Senti API is a text based sentiment prediction API, it measures the text sentiment by

[4] More details can be found inYang *et al.* (2014) and Go *et al.* (????)

[5] http://sentistrength.wlv.ac.uk/,a text based sentiment prediction API

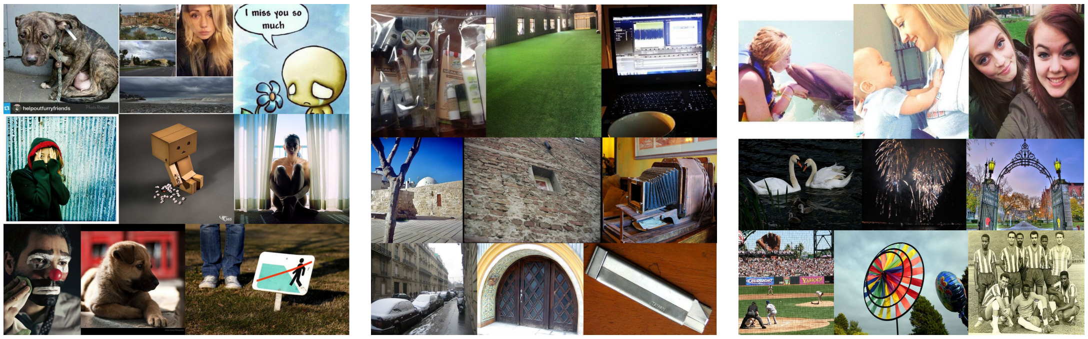

(a) Negative

(b) Neutral

(c) Positive

Figure 3.2: Sample Tag Labeled Images from Flickr and Instagram.

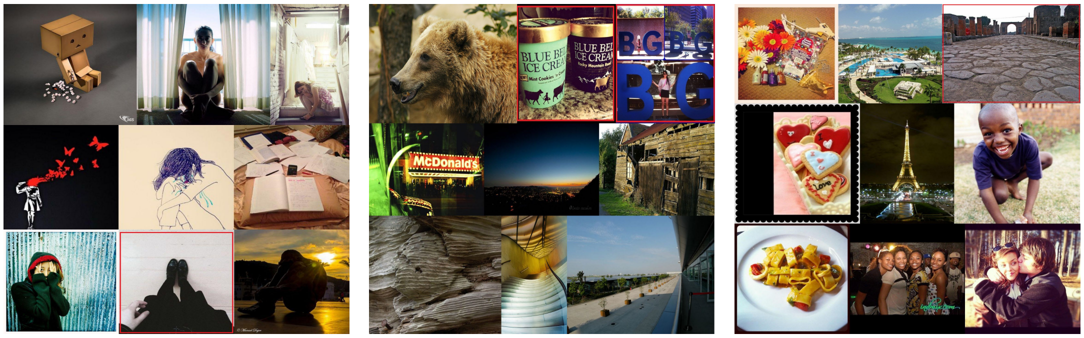

(a) Negative

(b) Neutral

(c) Positive

Figure 3.3: Sample Visual Results from RSAI.

counting the sentiment strength for each text term.

- SentiBank is a state-of-the-art visual based sentiment prediction method. The method extracts a large number of visual attributes and associates them with a sentiment score. Similar to Senti API, the sentiment prediction is based on the sentiment of each visual attributes.

- EL is a graphical model based approach, it infers the sentiment based on the friend interactions and several low level visual features.

- Baseline: The baseline method comes from our basic model. To compare it fairly, we also introduce R_0 with the basic model which makes the baseline method have the ability to learn from training data.

3.3.2 Performance Evaluation

Large scale image sentiment prediction: As mentioned in Sec 3, the proposed model has the flexibility to incorporate the information and capability to jointly learn from the visual features and text features. For each image, the visual features are formed by the confidence score of each ANP detector, the feature dimension is 1200, which is as large as VSO (prior knowledge V_0). For the text feature, it is formed based on the term frequency and the dimension relies on the input data. To predict the label, the model input is unknown data $X \in \mathbb{R}^{n \times m}$ and its corresponding text feature matrix $T_0 \in \mathbb{R}^{n \times t}$, where n is the number of images, $m = 1200$ and t is the vocabulary size, we decompose it via Aglorithm 1 and get the label based on max pooling each row of $X * V$. *It is worth noting that in the proposed model,* ***tags are not included as input feature****.*

The results of comparison are shown in Table 3. We employ 30% data for training and remaining for testing. To verify the reliability of tags labeled images, we also included 20000 labeled Flickr images with primary sentiment label. Especially, the classifier setting for SentiBank and EL followed the original papers. The classifier of Sentibank is logistic regression and for EL it is SVM. From the results we can see that, the proposed method performs best in both datasets. Noting that proposed method improved 10% and 6% over state-of-the-art methods Borth *et al.* (2013b). Results from proposed method are shown in Figure 4. Noting that the number we reported in Table 3 is the prediction accuracy for each method.

From the table, we can see that, even though noise exists in the Flickr and Instagram dataset, the results are similar to the performance on human labeled dataset. Another interesting observation is that the performance of EL on Instagram is worse than on Flickr,

Table 3.3: Sentiment Prediction Results.

	Senti API	SentiBank	EL	Baseline	Proposed method
20000 Flickr	0.32	0.42	0.47	0.48	**0.52**
Flickr	0.34	0.47	0.45	0.48	**0.57**
Instagram	0.27	0.56	0.37	0.54	**0.62**

one reason could be that the wide usage of ”picture filters” lowers discriminative ability of the low level visual features, while the models based on the mid level attributes can easily avoid this filter ambiguity. Another interesting observation is that our basic model performs fairly well even if it does not incorporate the knowledge from sentiment strength of ANPs, which indicates that the object based ANPs by our method are more robust than the features used in Borth *et al.* (2013b).

Fine Grained Sentiment Prediction: Although our motivation is to predict the sentiment (positive, negative) on the visual data, to show the robustness and extension capability of the proposed model, we further evaluate the proposed model on a more challenging task in social media; predicting human emotions. Based on the definition of human emotion Ekman (1992), our fine grained sentiment study labels the user posts with following human emotion categories including: happiness, amusement, disgust, anger, fear and sadness. The results on 20000 manually labeled flickr post are shown in Figure 5. Compared to sentiment prediction, fine grained sentiment prediction would give us more precise user behavior analysis and new insights on the proposed model.

As Figure 5 shows, compared to SentiBank and EL, the proposed method has the highest average classification accuracy and the variance of proposed method on these 6 categories is smaller than that of the baseline methods, which demonstrates the potential social media applications of the proposed method such as predicting social response. We noticed that the

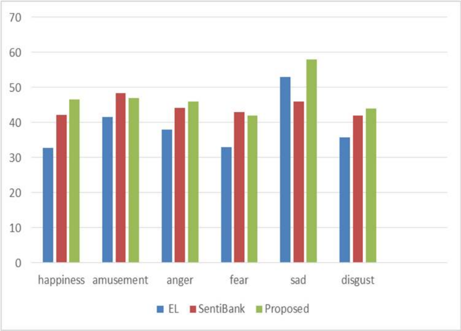

Figure 3.4: Fine Grained Sentiment Prediction Results (Y-axis represents the accuracy for each method).

sad images have the highest prediction accuracy, and both disgust and anger are difficult to predict. Another observation is the average performance of positive categories, happiness and amusement, is similar to the negative categories. Explaining reason for this drives us to dig deeper into sentiment understanding in the following section.

3.3.3 Analysis and Discussion

In this section, we present an analysis of parameters for the proposed method and the results of the proposed method. Specifically, in last section we have studied the performance of different methods. In this part, our objective is to have deeper understanding on the datasets and the correlation between different features and the sentiments embedded in the images. Without loss of generality, we collected additional 20k images from Flickr and Instagram respectively (totally 40K) and we address the following research questions:

- **RQ1:**What is the relationship between visual features and visual sentiments?
- **RQ2:**Since the proposed method is better than pure visual feature based method, How does the model gain?

First, we start with RQ1 by extracting the visual features used in Borth *et al.* (2013b) and Yang *et al.* (2014) for each image in the Flickr and Instagram datasets. Then we use k-means

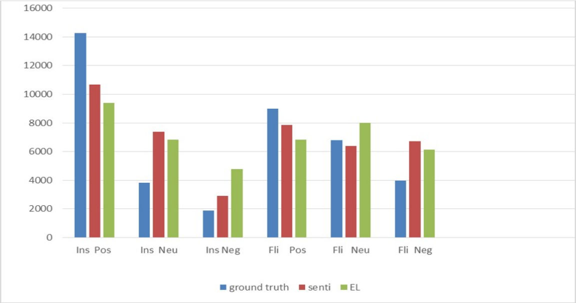

Figure 3.5: Sentiment Distribution based on Visual Features (From left to rigth is number of positive, neutral, negative images in Instagram and Flickr, receptively. Y axis represents the number of images).

clustering to obtain 3 clusters of images for each dataset, where the image similarity is measured as Euclidean distance in the feature spaces. Based on each cluster center, we used the classfier trained in the previous experiment for cluster labeling. The results are shown in Figure 6. The x-axis is the different class label for each dataset and the y-axis is the number of images that belong to each cluster. From the results, we notice that the "visual affective gap" does exist between human sentiment and visual features. For the state-of-the art method Borth *et al.* (2013b), the neural images are largely misclassified based on the visual features. While for Yang *et al.* (2014), we observe t the low level features, e.g., color histogram, contrast and brightness, are not closely related to human sentiment as visual attributes.

We further analyze the performance of the proposed method based on these 40,000 images.

Parameter study: In the proposed model, we incorporate three types of prior knowledge: sentiment lexicon, sentiment labels of photos and visual sentiment for ANPs. It is important and interesting to explore the impact of each of them on the performance of the proposed model. Figure 7 presents the average results (y-axis) of two datasets on sentiment prediction

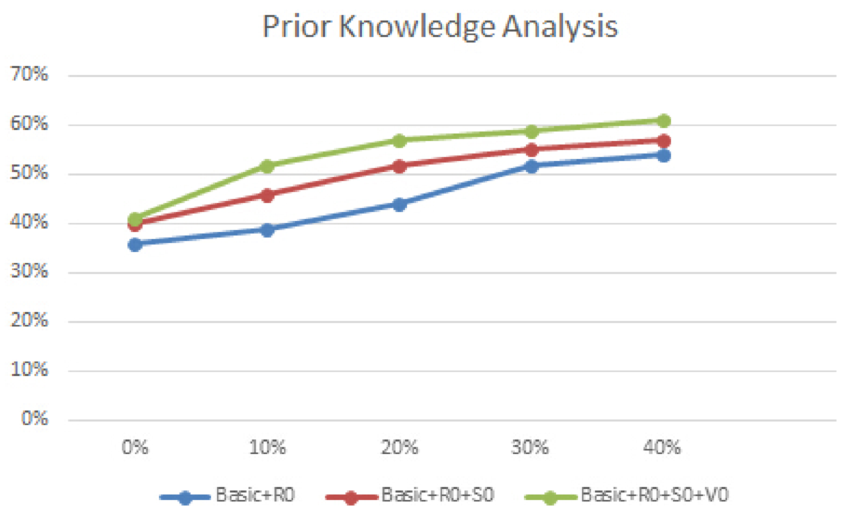

Figure 3.6: Performance Gain by Incorporating Training Data.

with different amount of training data (x-axis) [6] , where the judgment is on the same three sentiment labels with different combinations respectively. It should be noted that each combination is optimized by Algorithm 1, which has similar formulations. Moreover, we set the same parameter for α,β, γ and δ (0.9, 0.7, 0.8 and 0.7). Results give us two insights. First, employing more prior knowledge will make the model more effective than using only one type of prior knowledge. For our matrix factorization framework, T and V have independent clustering freedom by introducing S, thus it is natural to add more constraints for desired decomposed component. Second, when no training data, the basic model with S_0 performs much better than SentiAPI (refer Table 3), which means incorporating ANPs significantly improves image sentiment prediction. It is worth noting that there is no training stage for the proposed method. Thus when compared to fully supervised approaches, our method is more applicable in practice when the label information is unavailable.

Bridging the Visual Affective Gap (RQ2): Figure 1 and Figure 7 demonstrate that a visual affective gap exists between visual features and human sentiments (i.e., the same

[6] The experiments setting is as same as discussed above.

visual feature may correspond to different sentiments in different context). To bridge this gap, we show that one possible solution is to utilize heterogeneous data and features available in social media to augment the visual feature-based sentiment. In the previous parameter study, we have studied the importance of the prior knowledge. Furthermore, we study importance of β which contains the degree of contextual social information used in the proposed model. From Figure 8, we can observe that the performance of the proposed model increases along the value of β. However, when β is greater than 0.8, the performance drops. This is because textual information in social media data is usually incomplete. Larger β will cause negative effects on the prediction accuracy where there is none or little information available.

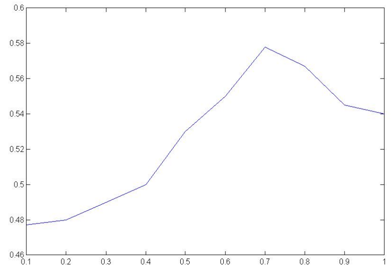

Figure 3.7: The Value of β versus Model Performance (X axis is β value, y axis is value of model performance).

3.4 Summary

In this chapter, we proposed a novel approach for visual sentiment analysis by leveraging several types of prior knowledge including: sentiment lexicon, sentiment labels and visual sentiment strength. To bridge the “affective gap” between low-level image features and high-level image sentiment, we proposed a two-stage approach to general ANPs by detecting mid-level attributes. For model inference, we developed a multiplicative update algorithm to find the optimal solutions and proved the convergence property. Experiments on two large-scale datasets show that the proposed model is superior to other state-of-the-art models in both inferring sentiment and fine grained sentiment prediction.

Chapter 4

UNSUPERVISED SENTIMENT ANALYSIS

In this chapter, I focus on the problem of exploiting textual features to enable unsupervised sentiment analysis for social media images. I will firstly review the background of this problem that address why textual feature could be potentially useful for visual sentiment analysis. And then I formally define the problem and introduce the proposed method. Real world datasets from Flickr and Instagram are used to evaluate the effectiveness of the proposed methods.

4.1 Motivation

Current methods of sentiment analysis for social media images include low-level visual feature based approaches Jia *et al.* (2012); Yang *et al.* (2014), mid-level visual feature based approaches Borth *et al.* (2013b); Yuan *et al.* (2013) and deep learning based approaches You *et al.* (2015). The vast majority of existing methods are supervised, relying on labeled images to train sentiment classifiers. Unfortunately, sentiment labels are in general unavailable for social media images, and it is too labor- and time-intensive to obtain labeled sets large enough for robust training. In order to utilize the vast amount of unlabeled social media images, an unsupervised approach would be much more desirable. This paper studies *unsupervised sentiment analysis*.

Typically, visual features such as color histogram, brightness, the presence of objects and visual attributes lack the level of semantic meanings required by sentiment prediction. In supervised case, label information could be directly utilized to build the connection between the visual features and the sentiment labels. Thus, unsupervised sentiment analysis for social media images is inherently more challenging than its supervised counterpart. As images from social media sources are often accompanied by textual information, intuitively such information may be employed. However, textual information accompanying images is often incomplete (e.g., scarce tags) and noisy (e.g., irrelevant comments), and thus often inadequate to support independent sentiment analysis Hu and Liu (2004); Hu *et al.* (2013). On the other hand, such information can provide much-needed additional semantic information about the underlying images, which may be exploited to enable unsupervised sentiment analysis. How to achieve this is the objective of our approach.

In this chapter, we study unsupervised sentiment analysis for social media images with textual information by investigating two related challenges: (1) how to model the interaction between images and textual information systematically so as to support sentiment prediction using both sources of information, and (2) how to use textual information to enable unsupervised sentiment analysis for social media images. In addressing these two challenges, we propose a novel Unsupervised SEntiment Analysis (USEA) framework, which performs sentiment analysis for social media images in an unsupervised fashion. Figure 4.1 schematically illustrates the difference between the proposed unsupervised method and existing supervised methods. Supervised methods use label information to learn a sentiment classifier; while the proposed method does not assume the availability of label information but employ auxiliary textual information. Our main contribution can be summarized as below:

- A principled approach to enable unsupervised sentiment analysis for social media images.
- A novel unsupervised sentiment analysis framework USEA for social media images, which captures visual and textual information into a unifying model. To our best knowledge, USEA is the first unsupervised sentiment analysis framework for social media images; and

- Comparative studies and evaluations using datasets from real-world social media image-sharing sites, documenting the performance of USEA and leading existing methods, serving as benchmark for further exploration.

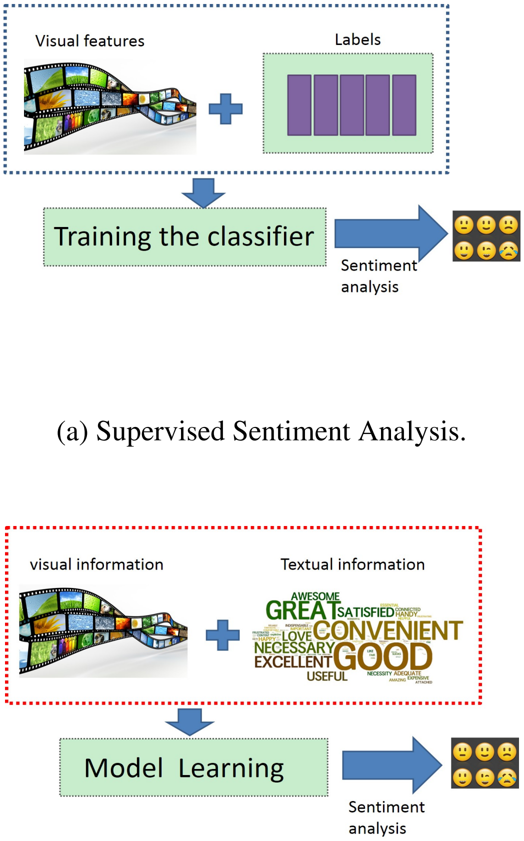

(a) Supervised Sentiment Analysis.

(b) The Proposed Unsupervised Sentiment Analysis.

Figure 4.1: Sentiment Analysis for Social Media Images.

4.2 Problem Statement

In this chapter, scalars are denoted by lower-case letters (a, b, . . . ; α, β, . . .), vectors are written as lower-case bolded letters (**a**, **b**, . . .), and matrices correspond to boldfaced uppercase letters (**A**, **B**, . . .). Let $\mathcal{I} = \{I_1, I_2, \ldots, I_n\}$ be the set of images where n is the number of images. We use $\mathcal{P} = \{p_1, p_2, \ldots, p_n\}$ to denote associated textual information about images where p_i is the textual information about I_i. Let $\mathcal{F}_v$ be set of m_v visual features and $\mathcal{F}_t$ be set of m_t textual features. We use $\mathbf{X}_v \in \mathbb{R}^{n \times m_v}$ and $\mathbf{X}_t \in \mathbb{R}^{n \times m_t}$ to denote visual and textual information about images, respectively. Let $\mathcal{C} = \{c_1, c_2, \ldots, c_k\}$ be the set of sentiment labels. Note that in this work we only consider positive, neutral and negative sentiments with $k = 3$ but the generalization of the proposed framework to multi-class sentiment analysis is straightforward.

With the aforementioned notations/definitions, the problem of unsupervised sentiment analysis for social media images with textual information is formally defined as:

Given n images with visual information $\mathbf{X}_v$ and textual information $\mathbf{X}_t$, to predict sentiment labels in $\mathcal{C}$ for the given n images.

4.3 Unsupervised Sentiment Analysis for Social Media Images

In this section, we first present our method for exploiting text information and then introduce the unsupervised sentiment analysis framework with an optimization method.

4.3.1 Exploiting Textual Information

Without label information, it is challenging for unsupervised sentiment analysis to connect visual features with sentiment labels. Textual information associated with social media images may be exploited to help, as it provides semantics about the underly images and in particular rich sentiment signals such as sentiment words and emotion symbols may be found in the textual fields. Hence, to exploit textual information, we investigate (1) how to incorporate textual information into visual information; and (2) how to model sentiment signals in textual information.

Since visual and textual information are two views about the same set of images, it is reasonable to assume that they share the same sentiment label space. More specifically, the sentiment of I_i should be consistent with that of its associated textual information p_i. Let $\mathbf{U}_0 \in \mathbb{R}^{n \times k}$ be the sentiment label space where $\mathbf{U}_0(i,j) = 1$ if the i-th data instance belongs to c_j, and $\mathbf{U}_0(i,j) = 0$ otherwise. We propose the following formulation to incorporate visual information with textual information based on nonnegative matrix factorization:

$$\begin{aligned} \min_{\mathbf{UV}} & \left\|\mathbf{X}_v - \mathbf{U}_v \mathbf{V}_v^T\right\|_F^2 + \alpha \left\|\mathbf{X}_t - \mathbf{U}_t \mathbf{V}_t^T\right\|_F^2 \\ & + \beta(\|\mathbf{U}_v - \mathbf{U}_0\|_F^2 + \|\mathbf{U}_t - \mathbf{U}_0\|_F^2) \\ \text{subject to} \quad & \mathbf{U}_v \geq 0; \mathbf{U}_t \geq 0; ||\mathbf{U}_0(i,:)||_0 = 1, i \in \{1,2,..n\} \\ & \mathbf{U}_0(i,j) \in \{0,1\}\, j \in \{1,2,..k\} \end{aligned} \tag{4.1}$$

where α controls how textual information contributes to the model and $||\cdot||_0$ is ℓ_0, which counts the number of nonzero entries in the vector. $\mathbf{U}_v \in \mathbb{R}^{n \times k}$ and $\mathbf{U}_t \in \mathbb{R}^{n \times k}$ are the sentiment label spaces learned from visual information and textual information, respectively. The term of $\beta(\|\mathbf{U}_v - \mathbf{U}_0\|_F^2 + \|\mathbf{U}_t - \mathbf{U}_0\|_F^2)$ ensures that these two types of information should share the sentiment label space $\mathbf{U}_0$. $\mathbf{V}_v \in \mathbb{R}^{m_v \times k}$ and $\mathbf{V}_t \in \mathbb{R}^{m_t \times k}$ indicate the sentiment polarities of visual and textual features, respectively.

Textual information contains rich sentiment signals. First, some words may contain sentiment polarities. For example, some words are positive such as “happy” and “terrific”; while others are negative such as “gloomy” and “disappointed”. The sentiment polarities of words can be obtained via some public sentiment lexicons. For example, the sentiment lexicon MPQA contains 7,504 human labeled words which are commonly used in the daily life with 2,721 positive words and 4,783 negative words. Second, some abbreviations and emoticons are strong sentiment indicators. For example, ”lol”(means laughing out loud) is a positive indicator while “:(” is a negative indicator. Let $\mathbf{V}_{t0} \in \mathbb{R}^{m_v \times k}$ be the matrix coding sentiment signals in textual information where $\mathbf{V}_{t0}(i,j) = 1$ if i-th word belongs to

c_j and $\mathbf{V}_{t0}(i,j) = 0$ otherwise. To model sentiment signals, we force the learned sentiment polarities of textual features to be consistent with those indicated by sentiment signals. Furthermore, not all textual features in $\mathcal{F}_t$ contain sentiment polarities and $\mathbf{V}_t$ should be sparse. We propose the following formulation to achieve these two goals as:

$$\min \quad \|\mathbf{V}_t - \mathbf{V}_{t0}\|_{2,1} \tag{4.2}$$

$\|\mathbf{X}\|_{2,1}$ is the $\ell_{2,1}$ of the matrix $\mathbf{X}$, which ensures the row sparsity of $\mathbf{X}$ Nie *et al.* (2010).

The significance of textual information in unsupervised sentiment analysis for social media images is two-fold. First, textual information bridges the semantic gap between visual features and sentiment labels. Second, we are allowed to do sentiment analysis for social media images in an unsupervised scenarios by modeling textual information via Eqs. (4.1) and (4.2).

4.3.2 The Framework: USEA

By combining the above discussion, we can have the following initial framework, which provides a potential solution to inferring sentiments by jointly considering visual information and corresponding contextual information:

$$\begin{aligned}
\min_{\mathbf{UV}} & \left\|\mathbf{X}_v - \mathbf{U}_v\mathbf{V}_v^T\right\|_F^2 + \alpha\left\|\mathbf{X}_t - \mathbf{U}_t\mathbf{V}_t^T\right\|_F^2 \\
& + \beta(\|\mathbf{U}_v - \mathbf{U}_0\|_F^2 + \|\mathbf{U}_t - \mathbf{U}_0\|_F^2) \\
& + \gamma\|\mathbf{V}_t - \mathbf{V}_{t0}\|_{2,1} \\
\text{s.t.} \quad & \mathbf{U}_v \geq 0; \mathbf{U}_t \geq 0; ||\mathbf{U}_0(i,:)||_0 = 1, i \in \{1,2,..n\} \\
& \mathbf{U}_0(i,j) \in \{0,1\}\, j \in \{1,2,..k\}
\end{aligned} \tag{4.3}$$

The parameter γ controls the sparsity of regularization term. However, the constrains of $\mathbf{U}_0$ in Eq. (3), mixed vector zero norm with integer programming, make the problem difficult to solve. To tackle this problem, we consider the relaxation of $\mathbf{U}_0$ by adding the extra orthogonal constraint on the value of $\mathbf{U}_0$. With the relaxation, the proposed framework (USEA) is to solve the following optimization problem:

$$\begin{aligned} \min_{\mathbf{UV}} & \left\|\mathbf{X}_v - \mathbf{U}_v\mathbf{V}_v^T\right\|_F^2 + \alpha\left\|\mathbf{X}_t - \mathbf{U}_t\mathbf{V}_t^T\right\|_F^2 \\ & + \beta(\|\mathbf{U}_v - \mathbf{U}_0\|_F^2 + \|\mathbf{U}_t - \mathbf{U}_0\|_F^2) \\ & + \gamma\|\mathbf{V}_t - \mathbf{V}_{t0}\|_{2,1} \\ \text{s.t.} \quad & \mathbf{U}_v \geq 0; \quad \mathbf{U}_t \geq 0; \\ & \mathbf{U}_0^T\mathbf{U}_0 = I; \mathbf{U}_0 \geq 0 \end{aligned} \tag{4.4}$$

4.3.3 An Optimization Method

There are 5 components, i.e. $\mathbf{U}_v, \mathbf{V}_v$, $\mathbf{U}_t, \mathbf{V}_t$ and $\mathbf{U}_0$, in Eq. (4). Thus it is difficult to optimize all the components simultaneously. In the following parts, we demonstrate an alternating algorithm to optimize the objective function by updating each component iteratively.

Update $\mathbf{V}_t$: If $\mathbf{U}_0$, $\mathbf{U}_v$, $\mathbf{V}_v$ and $\mathbf{U}_t$ are fixed, then the objective function is decoupled and the constrains are independent of $\mathbf{V}_t$. Thus we can optimize $\mathbf{V}_t$ separately and ignore the term without V_t, leading to the following:

$$\min_{V_v} \mathcal{J}(\mathbf{V}_t) = \left\|\mathbf{X}_t - \mathbf{U}_t\mathbf{V}_t^T\right\|_F^2 + \delta\left\|\mathbf{V}_t - \mathbf{V}_{t0}\right\|_F^2 \tag{4.5}$$

where $\delta = \frac{\gamma}{\alpha}$. Taking the derivation of $\mathcal{J}(\mathbf{V}_t)$ and setting it to zero, we can obtain the following form:

$$(-\mathbf{X}_t^T\mathbf{U}_t + \mathbf{V}_t\mathbf{U}_t^T\mathbf{U}_t) + \delta\mathbf{D}_t(\mathbf{V}_t - \mathbf{V}_{t0}) = 0 \tag{4.6}$$

where $\mathbf{D}_t$ is a diagonal matrix with jth element on the diagonal $\mathbf{D}(j,j) = \frac{1}{2\|\mathbf{V}_t(j,:) - \mathbf{V}_t0(j,:)\|_2}$. In Eq. (6), solving $\mathbf{V}_t$ directly is intractable. Since $\mathbf{D}_t$ and $\mathbf{U}_t^T\mathbf{U}_t$ are symmetric and positive definite, we employ eigen decomposition for them as:

$$\begin{aligned} \mathbf{U}_t^T\mathbf{U}_t &= \mathbf{U}_1\mathbf{\Lambda}_1\mathbf{U}_1^T \\ \mathbf{D}_t &= \mathbf{U}_2\mathbf{\Lambda}_2\mathbf{U}_2^T \end{aligned} \tag{4.7}$$

where $\mathbf{U}_1, \mathbf{U}_2$ are eigen vectors and $\mathbf{\Lambda}_1, \mathbf{\Lambda}_2$ are diagonal matrices with eigen values on the diagonal. Substituting $\mathbf{U}_t^T\mathbf{U}_t$ and $\mathbf{D}_t$ in Eq. (6), we have:

$$\mathbf{V}_t\mathbf{U}_1\mathbf{\Lambda}_1\mathbf{U}_1^T + \delta\mathbf{U}_2\mathbf{\Lambda}_2\mathbf{U}_2^T\mathbf{V}_t = X_t^T\mathbf{U}_t + \delta\mathbf{D}_t\mathbf{V}_{t0} \tag{4.8}$$

Multiplying $\mathbf{U}_2^T$ and $\mathbf{U}_1$ from left to right on both sides:

$$\mathbf{U}_2^T\mathbf{V}_t\mathbf{U}_1\Lambda_1 + \delta\Lambda_2\mathbf{U}_2^T\mathbf{V}_t\mathbf{U}_1 = \mathbf{U}_2^T(\mathbf{X}_t\mathbf{U}_t + \delta\mathbf{D}_t\mathbf{V}_{t0})\mathbf{U}_1 \tag{4.9}$$

Let $\widetilde{\mathbf{V}_t} = \mathbf{U}_2^T\mathbf{V}_t\mathbf{U}_1$ and $\mathbf{Q} = \mathbf{U}_2^T(\mathbf{X}_t\mathbf{U}_t + \delta\mathbf{D}_t\mathbf{V}_{t0})\mathbf{U}_1$, Eq. (9) becomes $\widetilde{\mathbf{V}_t}\mathbf{\Lambda}_1 + \delta\mathbf{\Lambda}_2\widetilde{\mathbf{V}_t} = \mathbf{Q}$, then we can obtain the $\widetilde{\mathbf{V}_t}$ and $\mathbf{V}_t$ as:

$$\begin{aligned} \widetilde{\mathbf{V}_t}(s,l) &= \frac{\mathbf{Q}(s,l)}{\delta\lambda_2^s + \lambda_1^l} \\ \mathbf{V}_t &= \mathbf{U}_2\widetilde{\mathbf{V}_t}\mathbf{U}_1^T \end{aligned} \tag{4.10}$$

where λ_2^s is the s-th eigen value of $\mathbf{D}_t$ and λ_1^l is l-th eigen value of $\mathbf{U}_t^T\mathbf{U}_t$. The following theorem shows that the updating rule in Eq(10) can monotonically decrease the objective function $\mathcal{J}(\mathbf{V}_t)$.

Theorem 1. *The update rule in Eq. (10) can monotonically decrease the value of* $\mathcal{J}(\mathbf{V}_t)$

Proof. The proof is similar to that in Nie *et al.* (2010), due to space limit, we omit the details of the proof.

Update $\mathbf{V}_v$. If $\mathbf{U}_0$, $\mathbf{U}_t$, $\mathbf{V}_t$ and $\mathbf{U}_v$ are fixed, by setting the derivation of the objective function to zero, $\mathbf{V}_v$ can be easily obtained as $\mathbf{V}_\mathbf{v} = \mathbf{X}_v^T\mathbf{U}_v(\mathbf{U}_v^T\mathbf{U}_v)^{-1}$. Moreover, we can easily verify updating $\mathbf{V}_v$ will monotonically decrease the objective function.

Update $\mathbf{U}_v$: If $\mathbf{V}_v$, $\mathbf{U}_t$, $\mathbf{V}_t$ and $\mathbf{U}_0$ are fixed, $\mathbf{U}_v$ can be obtained by the following optimization problem:

$$\begin{aligned} \min_{\mathbf{U}_v} \mathcal{J}(\mathbf{U}_v) &= \left\|\mathbf{X}_v - \mathbf{U}_v\mathbf{V}_v^T\right\|_F^2 + \beta\left\|\mathbf{U}_v - \mathbf{U}_0\right\|_F^2 \\ s.t. \qquad & \mathbf{U}_v \geq 0 \end{aligned} \tag{4.11}$$

The Lagrangian function of Eq. (11) is :

$$\begin{aligned} \min_{\mathbf{U}_v} \mathcal{L}(\mathbf{U}_v) &= \left\|\mathbf{X}_v - \mathbf{U}_v\mathbf{V}_v^T\right\|_F^2 + \beta\left\|\mathbf{U}_v - \mathbf{U}_0\right\|_F^2 \\ & - Tr(\Gamma\mathbf{U}_v) \end{aligned} \tag{4.12}$$

where Γ is Lagrangian multiplier. Taking the deviation of $\mathcal{J}(\mathbf{U}_v)$ and using the KKT condition ($\Gamma(s,l)U_v(s,l) = 0$), we can obtain:

$$(-\mathbf{X}_v\mathbf{V}_v + \mathbf{U}_v\mathbf{V}_v^T\mathbf{V}_v + \beta\mathbf{U}_v - \beta\mathbf{U}_0)_{sl}(\mathbf{U}_v)_{sl} = 0 \tag{4.13}$$

which leads to the following update rule for $\mathbf{U}_v$:

$$(\mathbf{U}_v)_{sl} \leftarrow (\mathbf{U}_v)_{sl}\sqrt{\frac{((\mathbf{X}_v\mathbf{V}_v)^+ + \mathbf{U}_v(\mathbf{V}_v^T\mathbf{V}_v)^- + \beta\mathbf{U}_0)_{sl}}{((\mathbf{X}_v\mathbf{V}_v)^- + \mathbf{U}_v(\mathbf{V}_v^T\mathbf{V}_v)^+ + \beta\mathbf{U}_v)_{sl}}} \tag{4.14}$$

where $\mathbf{X}(s,l)^+ = (|\mathbf{X}(s,l)| + \mathbf{X}(s,l))/2$, $\mathbf{X}(s,l)^- = (|\mathbf{X}(s,l)| - \mathbf{X}(s,l))/2$ and $\mathbf{X} = \mathbf{X}^+ - \mathbf{X}^-$.

Theorem 2. *Let*

$$\begin{aligned}
H(\mathbf{U}_v) &= Tr(-2\mathbf{X}_v\mathbf{V}_v\mathbf{U}_v^T + \mathbf{U}_v\mathbf{V}_v^T\mathbf{V}_v\mathbf{U}_v^T) \\
&+ \beta Tr(-2\mathbf{U}_v^T\mathbf{U}_0 + \mathbf{U}_v^T\mathbf{U}_v) \\
h(\mathbf{U}_v, \widetilde{\mathbf{U}_v}) &= \sum_{sl}((\mathbf{X}_v\mathbf{V}_v)^-(s,l)\frac{\widetilde{\mathbf{U}_v^2}(s,l) + \mathbf{U}_v^2(s,l)}{\widetilde{\mathbf{U}_v}(s,l)} \\
&+ \beta\frac{\widetilde{\mathbf{U}_v}(s,l)\mathbf{U}_v^2(s,l)}{\widetilde{\mathbf{U}_v}(s,l)} \\
&+ (\mathbf{V}_v^T\mathbf{V}_v)^+(s,l)\frac{\widetilde{\mathbf{U}_v}(s,l)\mathbf{U}_v^2(s,l)}{\widetilde{\mathbf{U}_v}(s,l)}) \\
&- \sum_{sl}(2(\mathbf{X}_v\mathbf{V}_v)^+\widetilde{\mathbf{U}_v}(s,l)(1 + \log\frac{\mathbf{U}_v(s,l)}{\widetilde{\mathbf{U}_v}(s,l)}) \\
&+ 2\beta\mathbf{U}_0(s,l)\widetilde{\mathbf{U}_v}(s,l)(1 + \log\frac{\mathbf{U}_v(s,l)}{\widetilde{\mathbf{U}_v}(s,l)})) \\
&- \sum_{k,s,l}(\mathbf{V}_v^T\mathbf{V}_v)^-(s,l)\widetilde{\mathbf{U}_v}(k,s)\widetilde{\mathbf{U}_v}(k,l) \\
&(1 + \log\frac{\mathbf{U}_v(k,s)\mathbf{U}_v(k,l)}{\widetilde{\mathbf{U}_v}(k,s)\widetilde{\mathbf{U}_v}(k,l)})
\end{aligned} \tag{4.15}$$

The auxiliary function $h(\mathbf{U}_v\widetilde{\mathbf{U}_v})$ of $H(\mathbf{U}_v)$ is convex and the global minimum of $h(\mathbf{U}_v, \widetilde{\mathbf{U}_v})$is: $(\mathbf{U}_v)_{sl} \leftarrow (\mathbf{U}_v)_{sl}\sqrt{\frac{((\mathbf{X}_v\mathbf{V}_v)^+ + \mathbf{U}_v(\mathbf{V}_v^T\mathbf{V}_v)^- + \beta\mathbf{U}_0)_{sl}}{((\mathbf{X}_v\mathbf{V}_v)^- + \mathbf{U}_v(\mathbf{V}_v^T\mathbf{V}_v)^+ + \beta\mathbf{U}_v)_{sl}}}$

Proof: The proof is similar to Ding *et al.* (2006) and Ding *et al.* (2010), due to space limit, we omit the details.

Theorem 3. *Updating $\mathbf{U}_v$ in Eq. (14) will monotonically decrease the value of objective function $\mathcal{J}(\mathbf{U}_v)$*

Proof: $H(\mathbf{U}_v)$ is the KKT condition of the Lagrangian function for Eq. (11). Based on the definition of auxiliary function and **Theorem 2** we can obtain the following equations:

$$H(\mathbf{U}_v^0) = h(\mathbf{U}_v^0, \mathbf{U}_v^0) \geq h(\mathbf{U}_v^0, \mathbf{U}_v^1) \geq h(\mathbf{U}_v^1, \mathbf{U}_v^1) \geq H(\mathbf{U}_v^1)... \tag{4.16}$$

This shows the update rule will monotonically decrease the objective function $H(\mathbf{U}_v)$, which complete the proof.

Update $\mathbf{U}_t$: It is worth noting that the procedure of solving $\mathbf{U}_t$ is exactly the same as that of $\mathbf{U}_v$. Thus, we omit the solution of $\mathbf{U}_t$ here.

Update $\mathbf{U}_0$: With $\mathbf{U}_v$, $\mathbf{U}_t$, $\mathbf{V}_t$ and $\mathbf{V}_v$ fixed, the sentiment label $\mathbf{U}_0$ can be obtained by solving the following optimization problem:

$$\begin{aligned} \min_{U} \mathcal{J}(\mathbf{U}_0) &= \|\mathbf{U}_v - \mathbf{U}_0\|_F^2 + \|\mathbf{U}_t - \mathbf{U}_0\|_F^2 \\ s.t. \quad & \mathbf{U}_0^T \mathbf{U}_0 = I; \mathbf{U}_0 \geq 0 \end{aligned} \tag{4.17}$$

The Lagrangian function of Eq. (17) is:

$$\begin{aligned} \min_{U} \mathcal{J}(\mathbf{U}_0) &= \|\mathbf{U}_v - \mathbf{U}_0\|_F^2 + \|\mathbf{U}_t - \mathbf{U}_0\|_F^2 \\ &+ Tr(\Lambda(\mathbf{U}_0^T \mathbf{U}_0 - I)) - Tr(\Gamma \mathbf{U}_0) \end{aligned} \tag{4.18}$$

where Λ and Γ are Lagrangian multipliers. Taking the derivation of $\mathcal{J}(\mathbf{U}_0)$ and using KKT conditions we can obtain

$$(\mathbf{U}_0 - \mathbf{U}_v + \mathbf{U}_0 - \mathbf{U}_t + \mathbf{U}_0 \Lambda)_{sl} (U_0)_{sl} = 0 \tag{4.19}$$

which leads the following update rule for $\mathbf{U}_0$:

$$(\mathbf{U}_0)_{sl} \leftarrow (\mathbf{U}_0)_{sl} \sqrt{\frac{(\mathbf{U}_v + \mathbf{U}_t + (\mathbf{U}_0 \mathbf{\Lambda})^-)_{sl}}{((\mathbf{U}_0 \mathbf{\Lambda})^+ + 2\mathbf{U}_0)_{sl}}} \tag{4.20}$$

Note that updating $\mathbf{U}_0$ needs updating the Lagrangian multiplier Λ as well. To obtain Λ, we sum over s and get $\Lambda(s,s) = (\mathbf{U}_0^T \mathbf{U}_v - I + \mathbf{U}_0^T \mathbf{U}_t - I)_{s,s}$. The offdiagonal elements of Λ are approximately obtained from non-negative value of U_0, leading to $\Lambda(s,t) = (\mathbf{U}_0^T \mathbf{U}_v - I + \mathbf{U}_0^T \mathbf{U}_t - I)_{st}$. Overall, we can obtain Λ by combining the diagonal values and off-diagonal values.

With the update rules for all the components in the proposed model, we summarize the solution in Algorithm 1. The convergence of Algorithm 1 is demonstrated as below:

Theorem 4.*With Algorithm 1, the objective function Eq. (4) will converge.*

Proof From **Theorem 1** and **Theorem 2**, the object function monotonically decreases:

$$\mathcal{J}(\mathbf{V}_v^0, \mathbf{U}_v^0) \geq \mathcal{J}(\mathbf{V}_v^1, \mathbf{U}_v^0) \geq \mathcal{J}(\mathbf{V}_v^1, \mathbf{U}_v^1)\mathcal{J}(\mathbf{V}_v^2, \mathbf{U}_v^1)... \geq 0 \tag{4.21}$$

Similarly, we can have the inequality chain for $\mathcal{J}(V_t, U_t)$. Thus we complete the proof.

Algorithm 2 The proposed USEA

```
  **Input:** ${\mathbf{X}_v, \mathbf{X}_t, \mathbf{V}_{t0}} \quad \alpha, \beta, \gamma$
  **Output:** $k$ sentiment label for each data.
  **Initialization:** $\mathbf{U_t}, \mathbf{U_v}, \mathbf{V_v}, \mathbf{V_t}$
  **while** Not Converge **do**
    Update $\mathbf{V}_t$ using Eq.(10) and compute $\mathbf{V}_v = \mathbf{X}_v^T\mathbf{U}_v(\mathbf{U}_v^T\mathbf{U}_v)^{-1}$.
    Computing $(\mathbf{X}_v\mathbf{V}_v)^{+,-}$, $(\mathbf{X}_t\mathbf{V}_t)^{+,-}$, $(\mathbf{V}_v^T\mathbf{V}_v)^{+,-}$ and $(\mathbf{V}_t^T\mathbf{V}_t)^{+,-}$
    Update $\mathbf{U}_v$ using Eq. (14), similarly update $\mathbf{U}_t$
    Computing $\Lambda$
    Update $\mathbf{U}_0$
  **end whileEnd**
  Using max-pooling for $\mathbf{U}_0$ to predict sentiment label.
```

4.4 Experiments

In this section, we conduct experiments to answer the following questions - (1) can the proposed framework do sentiment analysis in an unsupervised scenario? and (2) how does the textual information affect the performance of the proposed framework? We begin by giving details about the experimental settings.

4.4.1 Experiment Settings

We collect datasets from Flickr and Instagram for this study and we give more details below,

Flickr: On Flickr, an image-hosting Website, users can provide tags and descriptions for each uploaded image. Thus the textual information could be comments, image caption, user profile and tags. The collection of Flickr dataset is based on the image id provided by Yang *et al.* (2014), which contains 350,4192 images from 4807 users. Some images are unavailable when we crawled the data; hence we limit the number of images from one user as 50, which leads to a dataset with 140,221 images from 4341 users.

Instagram: Instagram is a service supporting photo-sharing via mobile app, where users take pictures and share them on social networking platforms like Facebook and Twitter. Similar to Flickr, we crawl at most 50 images for each user and get totally 131,224 images from 4853 users. Although the textual information as same as that on Flickr, for some images the number of comments is much bigger than that in Flickr, e.g., the images from celebrities usually contain thousands of comments, and we only consider the latest 50 comments for each image in Instagram.

Establishing Ground Truth: For evaluation purpose, we need to create sentiment labels of images. We follow the scheme in Yang *et al.* (2014); Liu (2012) and create labels for images via images' tags. Since we use tags to create labels of images, we do not consider tag information as textual information in the proposed framework. Labeling each post solely relying on tags may cause noise in the ground truth. Therefore we additionally select 20000 images from Flickr and ask three human subjects to manually create labels for them.

Feature extraction: the proposed method has the ability to incorporate visual and textual information. For visual information, we follow the recent approaches Yuan *et al.*

Table 4.1: The comparison results of different methods for sentiment analysis.

Method	Flickr (#20,000)	Flickr (#140,221)	Instagram (#131,224)
Senti API	32.30%	34.15%	37.80%
SentiBank-K	41.32%	41.12%	46.31%
EL-K	36.39%	42.90%	43.21%
USEA-T	37.90%	40.22%	36.41%
USEA	**55.22%**	**56.18%**	**59.94%**
Random	32.81%	33.12%	33.05%

(2013); Borth *et al.* (2013b) by using mid-level visual features. The visual features are extracted by a large-scale visual attribute detectors Borth *et al.* (2013b) and the feature dimension is 1200. Text-based features are formed by the term frequency in user profiles, image captions and comments. It is worth noting that textual features, which contain user descriptions, friends' comments and image captions, are preprocessed by stop word removing and stemming. MPQA [1] lexicon is employed as sentiment signals.

4.4.2 Performance Evaluation

The proposed framework USEA is compared with the following sentiment analysis algorithms:

- **Senti API**: [2] . This API is natural language processing API that performs unsupervised sentiment prediction using word-based sentiment. The method only uses textual information.

- **Sentibank**: As a mid-level visual feature based sentiment analysis approach, it uses

[1] `http://mpqa.cs.pitt.edu/`

[2] http://sentistrength.wlv.ac.uk/

large-scale visual attribute detectors and low-level visual features to form the Adjective and Nouns visual sentiment description pairs Borth *et al.* (2013b).

- **EL**: A topical graphical model based sentiment analysis approach, which models the sentiment by low-level visual features and friends information Yang *et al.* (2014).

- **USEA-T**: A variant of the proposed method that only considers the textual information including user profiles, image captions and friends' comments.

- **Random**: It predicts sentiment labels of images by randomly guessing.

Noting that SentiBank Borth *et al.* (2013b) and ELYang *et al.* (2014) are originally proposed for supervised sentiment analysis. We extend them to unsupervised scenarios by replacing original classifiers such as SVM or logistic regression with K-means. However, the clusters identified by K-means have no sentiment labels and we determine their sentiment labels with the Euclidean distance to the ground truth. We use SentiBank-K, and EL-K to represent these modifications.

Table 4.1 lists the comparison results and we make several key observations:

- Most of the time, textual based approaches obtain slight better performance than Random. These results support - (1) textual information is often incomplete and noisy and thus often inadequate to support independent sentiment analysis; and (2) textual information contains important cues for sentiment analysis.

- The proposed framework often obtains better performance than baseline methods. There are two major reasons. First textual information provides semantic meanings and sentiment signals for images. Second we combine visual and textual information for sentiment analysis. The impact of textual information on the proposed framework will be discussed in the following subsection.

In summary, compared to the performance Random, the proposed framework can significantly improve the sentiment analysis performance in a unsupervised scenario.

4.4.3 Impact of Textual Information

We introduce two parameters α and γ to control contributions from textual information. In this subsection, we investigate the impact of textual information on the proposed framework by examining how the performance of USEA varies with the changes of these parameters.

To study the impact of α, we fix $\gamma = 0.7$ and vary the value of α as $\{0.001, 0.1, 0.2, 0.3, 0.5, 0.7, 1.5, 2, 10\}$. The performance variance of USEA w.r.t. α is demonstrated in Figure 4.2. Note that we only show results in Flickr with manual labels since we have similar observations for other datasets. In general, with the increase of α, the performance first increases greatly, reach its peak value and then decrease dramatically. When we increase α from 0.001 to 0.1, the performance increases from 43.21% to 48.07%, which suggests the importance of textual information. With larger values of α (> 1.5), textual information dominates the learning process and the learnt parameters may overfit.

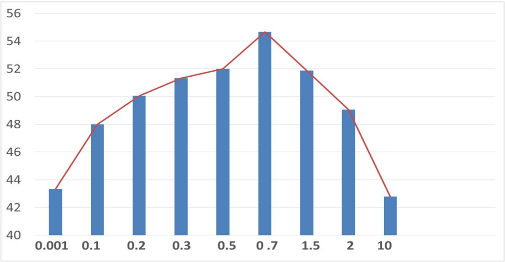

Figure 4.2: Performance Variance w.r.t. α (Y axis is the accuracy performance and X axis is the value of α).

Similarly, to study the impact of γ, we fix $\alpha = 0.7$ and vary the value of γ as $\{0.1, 0.2, 0.3, ..., 0.9, 1\}$. The performance variance of USEA w.r.t. γ is demonstrated in Figure 4.3. We also only show results in Flickr with manual labels since similar observations are made for other datasets. When γ increases from 0.1 to 0.6, the performance increases a lot, which further supports the importance of sentiment signals from textual information. After 0.8, the increase of γ will reduce the performance dramatically because the proposed framework may overfit to sentiment signals from textual information.

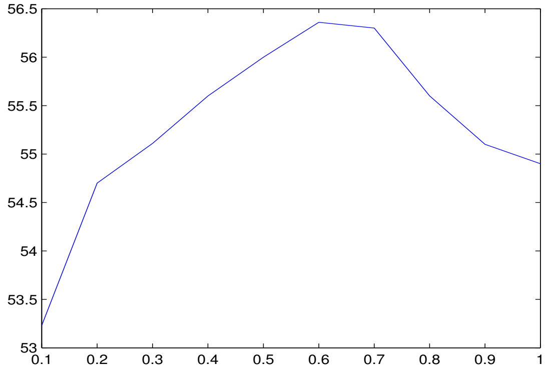

Figure 4.3: Performance Variance w.r.t. γ (Y axis is the accuracy performance and X axis is the value of γ).

4.5 Summary

In this chapter, we proposed a novel unsupervised sentiment analysis framework USEA by leveraging textual information and visual information in a unified model. Moreover, USEA provides a new viewpoint for us to better understand how textual information helps bridge the "semantic gap" between visual feature and image sentiment. Experiments on three large-scale datasets demonstrated 1) the advantages of the proposed methods in unsupervised sentiment analysis; 2) the importance of textual information. In the future, we will exploit more social media sources, such as link information, user history, geo-location, etc., for sentiment analysis.

Chapter 5

SELF-HARM SOCIAL MEDIA IMAGE UNDERSTANDING

In this chapter, I will reveal my discovery on the social media images from negative sentiment label. Especially, I focus on the understanding of self harm visual content in social media. I will firstly review the background of this problem and explain my findings that why online communities have such negative content. Then, I formally detailed my data collection and introduce the user pattern from my data. Last, I propose a framework to automatically discover self harm content. Data collected from Flickr is used to evaluate the proposed method.

5.1 Introduction

A central challenge in public health revolves around how to identify individuals who are at risk for taking their own lives. Deliberate self-injury is a behavior that some people use to cope with difficulties or painful feelings, and it has become the second leading cause of death for young people aged 15 to 19 years, and the tenth leading cause of death among those aged 10 to 14 Muehlenkamp *et al.* (2012). It has been reported by the National Alliance on Mental Illness [1] that there are around 2 million young adults and teenagers who have injured themselves. Another research from Britain Hawton *et al.* (2002) reported that among 400 pupils aged 14$\sim$16, more than 6.5% confirmed they harmed themselves in the last year. Self-harm prevention is challenging since it is a multi-faceted problem, with different categories of self-harm behaviors due to different social/personal reasons, pathogenesis, and/or underlying illnesses Hawton *et al.* (1997).

[1] www.nami.org

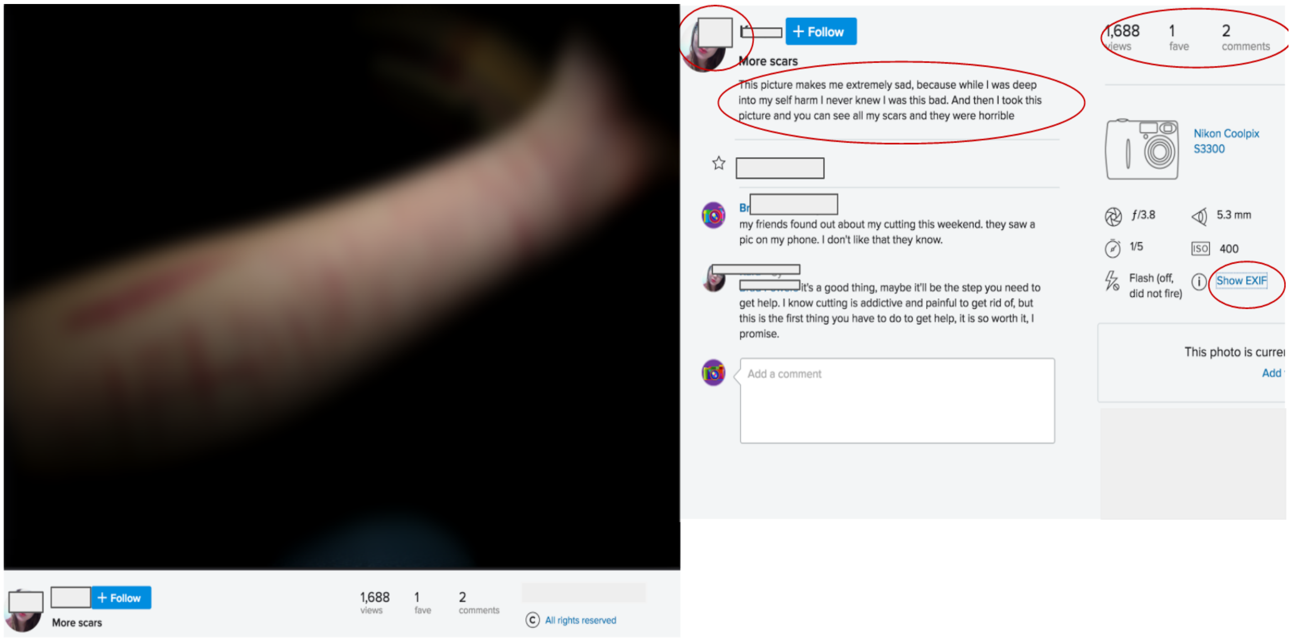

More scars

This picture makes me extremely sad, because while I was deep into my self harm I never knew I was this bad. And then I took this picture and you can see all my scars and they were horrible

Br[redacted]
my friends found out about my cutting this weekend. they saw a pic on my phone. I don't like that they know.

[redacted]
[redacted] it's a good thing, maybe it'll be the step you need to get help. I know cutting is addictive and painful to get rid of, but this is the first thing you have to do to get help, it is so worth it, I promise.

Figure 5.1: An example of Self-harm Posts from Flickr (Due to the privacy issue, we blurred the visual content in this post).

Existing efforts toward discovering and caring self-harm people. especially adolescents, have primarily relied on self report or friends/family Muehlenkamp *et al.* (2012); Hawton *et al.* (2002, 1997). However, such efforts face tremendous methodological challenges. First, self-harm people often find it difficult to discuss their feelings Gratz *et al.* (2002) and that is why they use self-harm to express their emotions. Most self-harm people suffer depression, anxiety or other mental health issues [2] which make the self-harm behavior difficult to be discovered by their friends/families Kairam *et al.* (2016). Second, although it is estimated that 7%-14% of adolescents may inflict self-harm at some time in their lives, and 20%-45% of older adolescents have been reported to have suicidal thoughts at some timeHawton and James (2005), the relatively rare occurrence of completed self-harm treatment and the stigma associated with self-harm reports have made studies challenging and expensive to conduct.

[2] http://www.mayoclinic.org/diseases-conditions/self-injury/symptoms-causes/dxc-20165427

In addition, extremely long follow-up intervals are typically required for effective study. As consequence, there are limited research efforts on examining factors associated with the development of future self-harm thoughts among self-harm-prone people Hawton and James (2005).

Nowadays people are increasingly using social media platforms, such as Twitter and Flickr, to share their thoughts and daily activities. The ubiquity of smart phones/tablets has also made such sharing easy and often instantaneous. As a result, social media provides a means to capture behavioral attributes that are relevant to an individual's thinking, mood, personal and social activities, and so on. In the physical world, people in need of help on mental issues usually do not know who to ask for help, and they often afraid that their trust could be betrayed, or they fear that asking for help may lead to more problems for themselves Houghton and Joinson (2012); Hawton and James (2005). On the other hand, they could be very active and open on social media when it comes to communication of the self-harm problem Dyson *et al.* (2016). Given the enormous volume of social media data that is created daily, a crucial step to enable the voices of self-harm users to be heard is to identify self-harm content that could be buried by the vast amount of normal content. A self-harm post from Flickr is demonstrated in Figure 5.1, which consists of multiple sources including text, photo, temporal information and meta information of its owner (highlighted by red circles in Figure 5.1). It appears that, while this problem has not been well-studied before, the rich information in social media posts may provide unprecedented opportunities for us to understand self-harm content.

In this chapter, we aim to understand and discover self-harm content in social media. To achieve this goal, we need to (1) reveal the distinct characteristics of self-harm content from normal content; and (2) leverage these characteristics to build models to automatically discover self-harm content. We conduct a comprehensive analysis on self-harm social media content using textual, owner-related, temporal and visual information, and our major understandings are summarized as: (1) The language of self-harm content has different structures compared with normal content, and the self-harm content expresses much more negative sentiments; (2) On average, owners of self-harm content are likely to have more activities, more social responses and less online friends compared to owners of normal content; (3) Posting time of self-harm content presents hourly patterns different from those of normal content, and self-harm content is likely to be posted during the night especially late night; and (4) Photos in self-harm content are more gloomy and tend to focus on the salient body image patterns. In summary, the key contributions of this work are:

- **Findings**: A first and comprehensive study on deliberate self-harm posts on social media by analyzing more than 1 billion posts on Flickr. We find that the self-harm users have different patterns on social media platform on: language structure and usage, online activity, temporal variation and visual content preference.

- **Applications**: We develop a scalable framework that can discover self-harm content automatically for both supervised and unsupervised scenarios. The features from our findings are used to boost the prediction performance. The solution we developed may be used for public health monitoring and/or directly helping the self-harm users by providing advices when they post self-harm related content.

5.2 Data Analysis

In this section, we first introduce the dataset for our study and then perform analysis to understand self-harm-related social media content.

5.2.1 Data

In this investigation, we use data from Flickr which is one of the largest image hosting websites owned by Yahoo! Inc. In Flickr, users can upload images along with short textual descriptions and tags as a post to share with others. In addition to posting some content, users can also engage in different interest groups.

Since the user's contact information is private, in order to avoid user bias, we collect data from Flickr by checking the visual content of the posts. For our initial data collection, we adopted an approach used in prior work on examination of eating disorders and anorexia in social media sites Chancellor *et al.* (2016). We first examine more than 1 billion public Flickr posts and select those public posts that annotated with "selfharm" and "selfinjury" tags. It results $15,729$ posts from $3,328$ distinct users. Then five experienced researchers manually check 2000 random selected Flickr posts that annotated with self-harm or self-injury tags. Based on the snowball sampling approach Goodman (1961) during the inspection phase, we obtain an initial 30 tags of the highest frequencies along with selfharm content [3] . Some examples include "selfhate", "suicide", "depressed", etc. By removing common tags such as wounds, scares, cut, we use 15 seed tags as shown in Table 5.1 to further retrieve posts from Flickr. In this stage, we want collect self-harm data as a complementary of first stage and it may help to make the bias as small as possible. For example "secretsociety123" and its variations are widely used by self-harm users Moreno *et al.* (2016) .

During the process, we collect $383,614$ Flickr posts from $63,949$ users. According to the findings from prior work on expression of self-harm tendencies in social media, frequently used tags can be a strong indication that a user has mental issues Chancellor *et al.* (2016); Moreno *et al.* (2016); Yom-Tov *et al.* (2012). Therefore, to obtain a set of relatively reliable self-harm users, we remove users who use selfharm related tags in less than five posts [4] , resulting in $93,286$ self-harm posts from $20,495$ potential self-harm users. Also, we collect a set of $19,720$ users from YFCC dataset Thomee *et al.* (2015), which is a 100 million open access dataset published by Flickr. We check all the historical posts of these $19,720$ users to

[3] The post contains intentional, direct injuring of body tissue content

[4] If only few self-harm related posts, the user could post them by chance

ensure that their posts do not contain any self-harm related content. We refer these users as normal users. We randomly sample 93,286 normal posts from these normal users for the following analysis. For each user, we crawled some statistical information such as the number of total posts and their user profiles; while for each post, we collected its associated information including the photos, the textual descriptions, user id of the owner, tags, and timestamps when the photo was taken and when the post was uploaded. Finally, we evaluate whether posts in the dataset contain signs of self-harm. Five experienced researchers familiar with social media and selfharm content evaluate the the correctness of the aforementioned method. In particular, each researcher randomly checked the posts and found that 95% of the posts with 'selfharm' and 'selfinjury' are correctly identified; while 83% of other tags are correctly identified. The Cohen kappa coefficient Cohen (1968) is 0.85 which suggests the high rate of agreement on our data collection method.

eatingdisorder	suicide	anxious	anorexia
mental-illness	depressed	killme	depression
selfhate	anamia	anxious	secretesociety123
bruised	bulimia	bleeding	

Table 5.1: A Set of Extended Tags that Help Identify Selfharm Posts.

5.2.2 Understanding Self-harm Content

A typical flickr post contains information from four dimensions including textual, owner, visual and temporal information. Therefore we analyze self-harm content from these four perspectives.

	Self-harm	Normal
Linguistic		
Nouns	0.158	0.268
Verbs	0.127	0.021
Adjective	0.035	0.084
Adverbs	0.032	0.023
readability	0.41	0.69
Sentiment		
Positive	0.06	0.29
Neutral	0.15	0.53
Negative	0.79	0.18

Table 5.2: Textual Analysis (the number stands for the ratio).

Textual Analysis. Linguistic style in texts is related to an individual's underlying psychological and cognitive states. It can reveal cues about their social coordination Rude *et al.* (2003); De Choudhury *et al.* (2013); Stirman and Pennebaker (2001); **?**); Wang *et al.* (2015b). Therefore we compute the distributions of nouns, verbs and adverbs in texts of social media posts, including the descriptions, titles and comments via the CMUTweetTagger Gimpel *et al.* (2011). Also, we calculate readability scores to estimate the complexity and readability [5] of texts. Individuals in self-harm or depression conditions trend to use negative words or express negative sentiments. Therefore, we compute the sentiment polarities of texts based on an off-the-shelf manually labeled sentiment lexicon, i.e., MPQA subjective lexicon, for self-harm and normal content, respectively. The comparison between self-harm and normal content is shown in Table 5.2.

[5] https://pypi.python.org/pypi/textstat/0.2

From Table 5.2, we can observe that self-harm content tends to include more verbs and adjectives/adverbs than nouns which is very consistent with suicidal word usage Stirman and Pennebaker (2001). The average readability score of self-harm content is lower than normal content. The poor linguistic structure usage and language suggest the decreased cognitive functioning and coherence Petrie and Brook (1992). Further, in addition to less usage of nouns, we note that a large portion of negative sentiment words are used in self-harm content. Such observation shows lower interests in objects and things from owners of self-harm content. It is also well known to appear for suicide users Pestian *et al.* (2012).

There is no lexicon to understand the usage of self-harm related terms in social media. Therefore, we build a lexicon of terms that are likely to appear in the texts of self-harm content. We first extract each term in texts and after post-processing each term, we calculate its vector via word2vec Mikolov *et al.* (2013) and cluster all the terms. Thereafter, we deploy the lexicon to calculate the frequencies of terms in self-harm content. In Table 5.3, we report sample unigrams from the self-harm lexicon. From Table 5.3, we observe that most captured expression/symptom terms indicate actions on eating habits, relations with others and sleeping. These are known to be correlated with sensitive disclosures Houghton and Joinson (2012). Owners of self-harm content more frequently use action words such as "help", "treatments", and "plans", and entity words such as "people", "girls", and "woman". These observations suggest that the self-harm users turn to social media to communicate and share the experiences with others in order to seek for help or attract attention from others.

Tags are a special type of textual information. We visualize most frequently used tags in self-harm content as shown in Figure 5.2. Despite the fact that most of the tags are self-harm related, some tags such as "secret society 123", "triggerwarning", and "svv", are not explicitly related to self-harm but indicate self-harm content. Similar to eating disorder Chancellor *et al.* (2016), self-harm users are likely to use some group tags that are merely used and can only be understood by themselves. To further verify these tags, we search

Theme	Token
Expression/ Symptom	anamia, anorexia, suicide, alone, stress, pretty, harms, stress, pain, angry, addiction, failure, beautiful, peace, illness, bulimic, individual, depressive, disorder
Disclosure	cuts, help, kill, live, die, plans, inflicted, treatments, eating, celebrates, suffer, saveme, triggers
Relationship/Noun	365days, razor, scar , blood, arms, wrist, band, knife, bathroom, bath, tattoo, girls, woman, boyfriend, people, body, night

Table 5.3: Unigrams from Self-harm lexicon that Appear with High Frequencies in the Self-harm Content.

these tags on Instagram and we find each of these tags returns lots of self-harm content [6] .

Owner Analysis. The owners of self-harm content provide crucial context to understand self-harm content. We analyze behaviors of owners from the following perspectives De Choudhury *et al.* (2013) – volume, proportion of reply, number of favorites, and number of friends. The volume is defined as the normalized number of posts per day by the

[6] The retrieving results with the tag "svv",for example, can be found via `https://www.instagram.com/explore/tags/svv/`

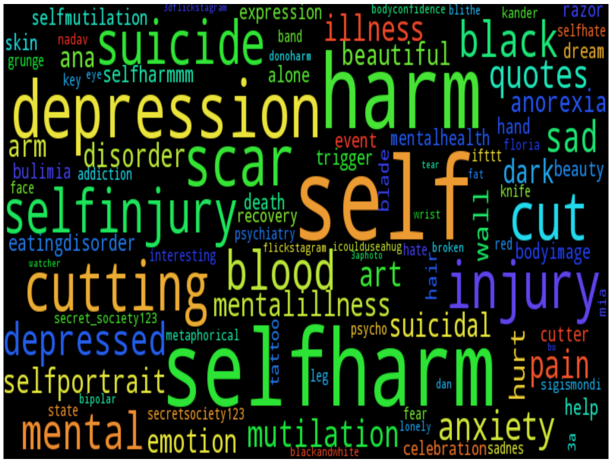

Figure 5.2: Tag Cloud for Self-harm Content

owner. Proportion of reply, number of favorites and number of friends from a user suggest the level of social interactions with other users. The results are shown in Table 5.4.

	Volume	% of reply	# favorite	# friends
Self-harm	7.76	0.15	0.56	296.89
Normal	3.79	0.11	0.23	477.57

Table 5.4: Owner Analysis.

From the table, we first note that the average volume, proportion of reply and number of favorite of owners with self-harm content are much higher than those of normal content. High volume indicates that potential self-harm users are likely to be more active than normal users in social media – they desire the public to hear their voices for help and are likely to use social media to express the emotion and satisfy self-esteem. High proportion of reply and number of favorites suggest that content from potential self-harm users are likely to attract more social responses. In addition, the owners of self-harm content are likely to have fewer number of friends than normal users.

Temporal Analysis. People with mental issues could suffer from insomnia; and they may

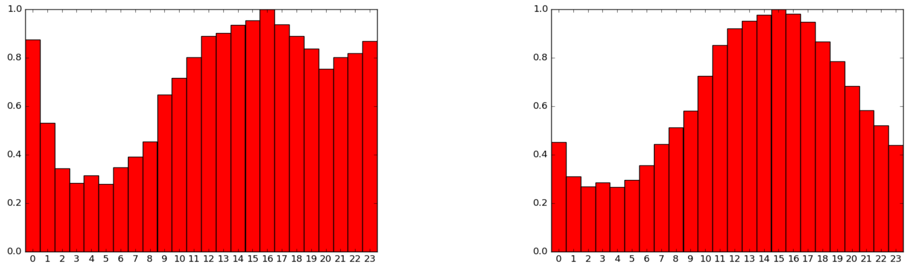

(a) Self-harm related Content

(b) Normal Content.

Figure 5.3: Temporal Analysis (Y axis represents the normalized portions of data volume of each hour. X axis is the time segment, which ranges from [0 23]).

present different temporal patterns from normal users in terms of their on-line activities. For each self-ham post, we first obtain the local time information on when the post is published, and then count the number of self-harm posts in each hour of a day. The number distributions of self-harm content over hours of a day is demonstrated in Figure 5.3a. Following a similar process, the distributions of normal content is shown in Figure 5.3b. Note that the numbers in the Figures are normalized to (0,1] for better visualization. Note that, in this study, we cluster the posts by examining the EXIF data from the user upload images, which accurately records the time when the image is taken.

For normal content, in general, they are more likely to be published during the daytime instead of night. In particular, (1) fewer number is published later in the night (i.e., post-midnight) and early in the morning; (2) the number generally increases through the day; and (3) afternoon and early night show peaks. For self-harm content, a large number is posted during nights especially late in the night (22pm to 1am), while fewer number in the morning (7am to 8 am). As mentioned earlier, people with mental issues could suffer from insomnia and their mood tends to worsen during the night Lustberg and Reynolds (2000).

Visual analysis. Color patterns are important cues to understand the emotion and affective value of a picture Kairam *et al.* (2016). Therefore, we first compute a global contrast metric

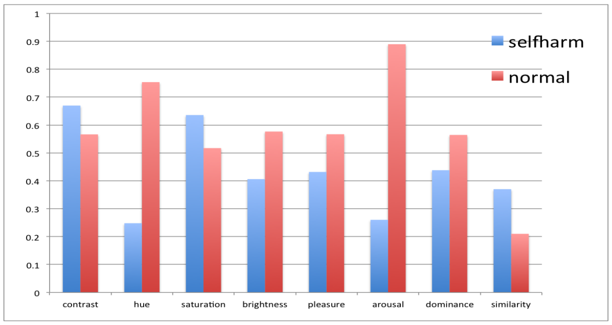

Figure 5.4: Visual Analysis.

Cheng *et al.* (2015) that: (1) provides saliency information from the distinguish ability of colors based on the magnitude of the average luminance; and (2) exposes the image regions that are more likely to grasp the attention of the human eyes. Then we extract the average of the Hue, Saturation, Brightness (H,S,V) channels. By combining average Saturation (S) and Brightness (V) values, we also extract three indicators of emotional dimensions, i.e., pleasure, arousal and dominance, as suggested by previous work on affective image analysis Machajdik and Hanbury (2010). Last, we extract some local image features including SIFT, LBP and GIST Tuytelaars and Mikolajczyk (2008), which are widely used in image matching and visual search related tasks. Based on these features, we calculate the average similarities for photos in self-harm and normal content, separately. The comparison results are presented in Figure 5.4. Note that each score in the figure is normalized to (0,1] for visualization.

In general, photos in the self-harm content have lower average values in brightness, pleasure, arousal and dominance. As suggested by the previous findings Siersdorfer *et al.* (2010); Wang *et al.* (2015b), lower values tend to express more negative sentiments. The higher global contrast demonstrates that photos in self-harm content have higher saliency value regions, e.g., body parts, possibly for attracting attention Itti and Koch (2001). Photos in self-harm content are much more similar to each other than those in normal content.

5.3 Self-harm Content Prediction

Our findings in the previous section indicate that potential self-harm users inclined to express their feelings and emotions in social media, with the purpose of seeking for help and attention. Social media content is generated at an unprecedented rate, and self-harm content is likely to be buried by the majority of normal content. Hence a crucial step to help their voices be heard by the public is to identify self-harm content. A social media post consists of multiple types of information. As suggested by our previous analysis, each type provides useful and complementary patterns to characterize self-harm content. Therefore combining multiple sources could provide a more comprehensive view about social media posts and has the potential to improve performance.

Typically supervised methodsWang *et al.* (2016, 2015b) can achieve better performance because the label information can guide the learning performance. However, most social media posts are unlabeled and annotating their labels is expensive and time consuming. Therefore an unsupervised method is also desired. In the following subsections, we will introduce frameworks to discover self-harm content automatically with and without labeled data. Before presenting the details, we first introduce the notations and definitions we will use in the proposed frameworks.

Let $\mathcal{P} = \{p_1, p_2, p_3, ..., p_n\}$ be a set of posts where n is the number of social media posts. Assume that the set of posts i.e., $\mathcal{P}$, can be represented by m heterogeneous feature spaces corresponding to m available sources. For Flickr posts in the studied dataset, m is 4 including textual, owner, temporal and visual sources. Let $\mathcal{F} = \{f_1, f_2, f_3, ..., f_m\}$ be a set of m feature spaces where $f_i \in \mathbb{R}^{l_i}$ denotes the feature space for the i-th source and l_i is the number of features in f_i. We use $\mathcal{X} = \{X_i \in \mathbb{R}^{n \times l_i}\}_{i=1}^{m}$ as the set of data matrices and X_i is the matrix representation of the i-th source. Note that for each source, we extract a set of features based on the previous analysis to augment the set of traditional features because these features cannot be captured by traditional ones but have abilities to discriminate self-harm content from normal content. For instance, we augment traditional word embedding features for the textual source by extracting features such as linguistic style and sentiments according to the textual analysis. More details about the traditional features can be found in the experiments section.

5.3.1 A Supervised Self-harm Content Prediction Framework

Under the supervised setting, we assume the availability of the label information of posts in $\mathcal{P}$. Let $\mathbf{Y} \in \mathbb{R}^{n\times 2}$ denote the label information of the n posts in $\mathcal{P}$ where $\{\mathbf{Y}_{i1} = 1, \mathbf{Y}_{i2} = 0\}$ and $\{\mathbf{Y}_{i1} = 0, \mathbf{Y}_{i2} = 1\}$ if the post p_i is labeled as self-harm and normal content, respectively. We concatenate $\{X_i \in \mathbb{R}^{n\times l_i}\}_{i=1}^m$ into one matrix $\mathbf{X} \in \mathbb{R}^{n\times \sum_{i=1}^m l_i}$. The goal is to learn a function $\mathbf{W} \in \mathbb{R}^{\sum_{i=1}^m l_i \times 2}$ that can map $\mathbf{X}$ to $\mathbf{Y}$. In this work, the basic method learns $\mathbf{W}$ via solving the following least square problem as:

$$\min_{\mathbf{W}} \|\mathbf{X}\mathbf{W} - \mathbf{Y}\|_F^2 \tag{5.1}$$

However, after concatenating m feature spaces, the feature dimension of $\mathbf{X}$ is $\sum_{i=1}^m l_i$ and $\mathbf{X}$ could be very high-dimensional. Therefore the basic method in Eq. (5.1) could suffer from the curse of dimensionality. Meanwhile not all features especially these traditional features are useful to distinguish self-harm content and normal content. Therefore it is desired to incorporate feature selection into the framework that is achieved via adding $\ell_{2,1}$-norm regularization on $\mathbf{W}$. With the feature selection component, the supervised self-harm content prediction framework SCP is to solve the following optimization problem:

$$\min_{\mathbf{W}} \|\mathbf{X}\mathbf{W} - \mathbf{Y}\|_F^2 + \alpha\|\mathbf{W}\|_{2,1} \tag{5.2}$$

where $\|\mathbf{W}\|_{2,1}$ ensures that $\mathbf{W}$ is sparse in rows, making it particularly suitable for feature selection. The parameter α controls the sparsity of $\mathbf{W}$.

Taking the derivative of the objective function in Eq. (5.2) and setting it to be zero, we can obtain the closed-form solution for $\mathbf{W}$ as:

$$\mathbf{W} = (\mathbf{X}^\top \mathbf{X} + \alpha \mathbf{D})^{-1} \mathbf{X}^\top \mathbf{Y} \tag{5.3}$$

where $\mathbf{D}$ is a diagonal matrix with its j-th diagonal element as $\mathbf{D}(j,j) = \frac{1}{2\|\mathbf{W}(j,:)\|_2}$.

5.3.2 An Unsupervised Self-harm Content Prediction Framework

Under the unsupervised scenario**?**, we do not have label information to guide the learning process. However, in our studied problem, we have multiple sources that could make it possible to develop advanced framework for self-harm content prediction. The immediate challenge is how to capture relations among sources. Since we have the same set of posts for different sources, hence no matter which source we rely on to cluster posts, we should obtain similar cluster affiliations. This intuition paves us a way to capture relations among sources by assuming that all sources share the same cluster affiliations. We assume that $\mathbf{Z} \in \mathbb{R}^{n \times 2}$ is the shared cluster indicator matrix. Each post belongs to only one cluster where $\mathbf{Z}(i,1) = 1$ if p_i belongs to the first cluster, otherwise $\mathbf{Z}(i,1) = 0$. Thus $\mathbf{Z}$ should satisfy the following constraints:

$$\mathbf{Z}(i,:) \in \{0,1\}^k, \|\mathbf{Z}(i,:)\|_0 = 1, \quad 1 \leq i \leq n. \tag{5.4}$$

where $\|*\|_0$ is the vector zero norm, which counts the number of non-zero elements in the vector.

With the shared cluster indicator matrix $\mathbf{Z}$, we are further allowed to take advantages of information from multiple sources. First, we assume that similar data instances should have similar cluster indicators and then $\mathbf{Z}$ can be learned by spectral clustering:

$$\min_{\mathbf{Z}} \quad Tr(\mathbf{Z}^T \mathbf{L}_i \mathbf{Z}) \tag{5.5}$$

where $\mathbf{L}_i = \mathbf{V}_i - \mathbf{S}_i$ is a Laplacian matrix and $\mathbf{V}_i$ is a diagonal matrix with its elements defined as $\mathbf{V}_i(j,j) = \sum_{K=1}^{n} \mathbf{S}_i(K,j)$. $\mathbf{S}_i \in \mathbb{R}^{n \times n}$ denotes the similarity matrix based on $\mathbf{X}_i$ via a RBF kernel in this work.

Similar to the supervised framework SCP, we can learn a function $\mathbf{W}$ with the help of the shared cluster indicator matrix $\mathbf{Z}$. With these two model components, the proposed unsupervised self-harm content prediction framework USCP is to solve the following optimization problem:

$$\begin{aligned} \min_{\mathbf{W},\mathbf{Z}} \quad & \sum_{i=1}^{m} \lambda(Tr(\mathbf{Z}^T\mathbf{L}_i\mathbf{Z})) + \alpha \left\|\mathbf{X}\mathbf{W} - \mathbf{Z}\right\|_F^2 + \beta \left\|\mathbf{W}\right\|_{2,1} \\ \text{subject to} \quad & s_i \in \{0,1\}^n \\ & \left\|\mathbf{Z}(i,:)\right\|_0 = 1, i \in \{1,2,3...n\}, \\ & \mathbf{Z}(i,j) \in \{0,1\}, j \in \{1,2,...k\} \end{aligned} \tag{5.6}$$

The constraints in Eq. (5.6) is mixed vector zero norm with integer programming, making the problem hard to solve Ding *et al.* (2010). First, we need to relax the constraints on the cluster indicator matrix. By relaxing the value in $\mathbf{Z}$ to a continuous nonnegative value, we convert the constraints into:

$$\mathbf{Z}^T\mathbf{Z} = \mathbf{I}, \quad \mathbf{Z} \geq 0 \tag{5.7}$$

the constraints in Eq. (5.7) can ensure that there is only one non-negative value in each row of $\mathbf{Z}$.

With the relaxation, USCP is to solve the following optimization problem:

$$\begin{aligned} \min_{\mathbf{W},\mathbf{Z}} \quad & \sum_{i=1}^{m} \lambda_i(Tr(\mathbf{Z}^T\mathbf{L}_i\mathbf{Z})) + \alpha \left\|\mathbf{X}\mathbf{W} - \mathbf{Z}\right\|_F^2 + \beta \left\|\mathbf{W}\right\|_{2,1} \\ \text{subject to} \quad & \mathbf{Z}^T\mathbf{Z} = \mathbf{I}, \quad \mathbf{Z} \geq 0 \end{aligned} \tag{5.8}$$

We adopt an alternating optimization to solve the optimization problem of USCP and update $\mathbf{W}$ and $\mathbf{Z}$ iteratively and alternately. Since optimizing $\mathbf{W}$ is the same as that in

Eq. (5.2), we focus on how to update **Z** in the following part. Fixing **W**, **Z** can be obtained via the following optimization problem:

$$\begin{aligned} \min_{\mathbf{Z}} \quad & \sum_{i=1}^{m} \mathcal{J}(\mathbf{Z}) = \lambda_i (Tr(\mathbf{Z}^T \mathbf{L}_i \mathbf{Z})) + \alpha \left\| \mathbf{X}\mathbf{W} - \mathbf{Z} \right\|_F^2 \\ \text{subject to} \quad & \mathbf{Z}^T\mathbf{Z} = \mathbf{I}, \quad \mathbf{Z} \geq 0 \end{aligned} \tag{5.9}$$

The Lagrangian function of Eq. (5.9) is:

$$\begin{aligned} \mathbf{Z} = & Tr(\mathbf{Z}^T \mathbf{M} \mathbf{Z}) + Tr(\Gamma(\mathbf{Z}^{\mathbf{Z}} - \mathbf{I}) \\ & - Tr(\Lambda \mathbf{Z}) + \alpha Tr(-2\mathbf{A}^\top \mathbf{Z} + \mathbf{Z}^T \mathbf{Z}) \end{aligned} \tag{5.10}$$

where we use $\mathbf{M} = \sum_{i=1}^{m} \lambda_i \mathbf{L}_i$, and $\mathbf{A} = \mathbf{X}\mathbf{W}$. Γ and Λ are Lagrangian multipliers. Due to the space limit, we omit the derivations to optimize Eq. (5.10), and more details can be found in Ding *et al.* (2010). The provided updating rule for **Z** is as following:

$$\mathbf{Z}(p,q) \leftarrow \mathbf{Z}(p,q) \sqrt{\frac{(\mathbf{M}^{-}\mathbf{Z} + \alpha \mathbf{A}^{+} + \mathbf{Z}\Gamma^{-})(p,q)}{(\mathbf{M}^{+}\mathbf{Z} + \alpha \mathbf{A}^{-} + \mathbf{Z} + \mathbf{Z}\Gamma^{+})(p,q)}} \tag{5.11}$$

where $\mathbf{X}^{+}(p,q) = (|\mathbf{X}(p,q)| + \mathbf{X}(p,q))/2$, $\mathbf{X}^{-}(p,q) = (-|\mathbf{X}(p,q)| + \mathbf{X}(p,q))/2$, $\mathbf{X} = \mathbf{X}^{+} + \mathbf{X}^{-}$, and $\Gamma = \alpha(\mathbf{Z}^T \mathbf{A} - \mathbf{I}) - \mathbf{Z}^T \mathbf{M} \mathbf{Z}$

With the updating rules of **Z** and **W**, we present the detailed algorithm to optimize Eq. (5.8) in Algorithm 3.

5.4 Experiments

In this section, we conduct experiments which (a) quantify the effectiveness of the proposed frameworks, and (b) validate the importance of findings from data analysis in discovering self-harm content. We begin by introducing experimental settings.

5.4.1 Experiment Settings

Datasets. We perform the evaluation on the dataset used in the data analysis section. That dataset is balanced with equal size of self-harm and normal content. In reality, there

Algorithm 3 Pseudo Code of the USCP

```
Input: $\{\mathbf{X}_i, \lambda_i\}, \alpha, \beta$
Output: the cluster label for each instance
for i = $1$ to $m$: do
    Constructing Laplacian Matrix $\mathbf{L}_i$
end for
while Not converge do
    Update $\mathbf{W}$ by Eq. 5.3
    Compute $\mathbf{A} = \mathbf{XW}$
    Compute $\Gamma = \alpha(\mathbf{Z}^T\mathbf{A} - \mathbf{I}) - \mathbf{Z}^T\mathbf{MZ}$
    Update $\mathbf{Z}$ using Eq. (5.11)
end while
for i = $1$ to $n$: do
    Max pooling in $\mathbf{Z}$ to find the cluster label for each instance
end for
```

could be more normal content than self-harm content. To consider this situation, we sample $850,000$ more normal content from these normal users to construct an imbalanced dataset. We will assess the performance of self-harm content prediction on both balanced and imbalanced datasets under supervised and unsupervised settings.

The Finding Features. Our findings in the previous section contain multiple cues. For each finding, we regard as one feature source. (1) lingual feature (a vector of language structure ratios and normalized term frequencies in the lexicon) (2) owner feature (a vector of user information) (3) temporal feature(1-hot vector of time) (4) visual feature (a vector of averaged saliency value, averaged HSV value, averaged pleasure, arousal and dominance value, and normalized SIFT,LBP GIST feature [7])

[7] We use PCA to reduce the feature dimension of concatenated of SIFT,LBP and GIST

Traditional Features. In addition to features extracted according to our findings in the data analysis section, we also follow the state-of-the-art methods to extract traditional features for textual and visual sources as follows:

- The textual features are extracted from texts in social media posts including descriptions, titles and comments. For each word, we first transform it to a 100-dimension vector representation using a pre-trained word2vec Mikolov *et al.* (2013) model. The final feature representation is the sum of vector representation for all the words.

- The CNN features are the last layer of fully connected layer of the convolutional neutral network. In our experiment, we use AlexNetKrizhevsky *et al.* (2012) pre-trained on ImageNet. The feature size is 4096.

Note that we use both the finding features and traditional features. Thus, the m is set to be 6 in both SCP and USCP.

5.4.2 Performance Comparisons for Supervised Self-harm Content Prediction

Evaluation metrics: In imbalanced datasets, the accuracy metric under supervised settings is well known to be misleading De Choudhury *et al.* (2013). For example, given the massive data on social media, a trivial classifier that labels all the samples as non self-harm post can achieve very high accuracy. In self-harm content prediction, we aim to achieve high precision and recall over self-harm posts defined in terms of the confusion matrix of a classifier– $prescision = \frac{tp}{tp+fp}$, $recall = \frac{tp}{tp+fn}$ and $F1 = 2\frac{precision \cdot recall}{precision+recall}$. Usually precision and recall are combined into their harmonic mean, the Fmeasure; hence we will adopt F1-measure as one metric for the performance evaluation. As suggested in De Choudhury *et al.* (2013), in some scenarios, we put more emphasis on precision because

features. The final dimension of these three features is 128 the most challenging task is to seek for some self-harm posts with high probability, even at the price of increasing false negatives. Hence, we also report the precision performance.

We compare the proposed supervised framework SCP with the following baselines:

- *Word-embedding(WE)*: We represent each text as the sum of the embedding of the words it contains; and the prediction is based on a 2 layer convolutional neural network Kim (2014). This method is one of the state-of-the-arts in textual classification tasks such as sentiment classification Kim (2014);

- *CNN-image*: It is one of the state-of-the-art model for image classification Krizhevsky *et al.* (2012). We use the same architecture except the softmax layer with self-harm and normal labels;

- *CNN+WE* : We combine CNN and word embedding features and the prediction is based on a linear regression model; and

- *SCP-lite*: A lite version of SCP which only considers traditional features; while ignoring features extracted by our findings.

We use 60% of the data as training and the remaining as testing, and parameters are determined via cross-validation. The comparison results are demonstrated in Table 5.5. We make the following observations:

- CNN+WE obtains much better performance than Word-embedding and CNN-image. This result suggests that textual and visual sources contain complementary information;

- By incorporating feature selection, SCP-lite performs slightly better than CNN+WE; and

Algorithm	Balanced		Imbalanced	
	F1	precision	F1	precision
Word-embedding	57.9%	63.7%	37.9%	30.1 %
CNN-image	61.8%	64.5%	48.6%	44.7%
CNN+WE	68.3%	72.3%	53.1%	46.7%
SCP-lite	68.4%	73.1%	54.5%	47.9%
SCP	**72.1**%	**75.2**%	**56.7**%	**49.8**%

Table 5.5: Performance Comparisons for Supervised Self-harm Content Prediction.

- SCP outperforms SCP-lite in both balanced and imbalanced datasets. We conduct t-test on the results and the evidence from t-test indicates the improvement is significant. The remarkable improvement of SCP over SCP-lite is from the augmented features. These results demonstrate that (1) traditional features cannot fully cover our findings; and (2) features extracted based on our findings can boost the performance significantly.

5.4.3 Performance Comparisons for Unsupervised Self-harm Content Prediction

In this subsection, we evaluate the proposed unsupervised framework USCP. Following the common practiceVinh *et al.* (2010), we choose NMI and accuracy (ACC) to assess the clustering performance. The baseline methods are defined as follows:

- *CNN+kmeans*: We use pre-trained CNN features Krizhevsky *et al.* (2012) and then perform kmeans for clustering;

- *Word-embedding+kmeans*: We use word embedding features and then perform kmeans for clustering;

- *CNN+WE+kmeans*: We combine CNN and word embedding features and then per-

Algorithm	Balanced		Imbalanced	
	NMI	ACC	NMI	ACC
CNN+kmean	0.36	47.3%	0.15	15.3%
WE+kmeans	0.08	33.8%	0.04	10.3 %
CNN+WE+kmeans	0.46	56.2%	0.23	23.1%
USCP-lite	0.48	58.3%	0.26	24.3%
USCP	0.51	61.2%	0.31	27.4%

Table 5.6: Performance Comparisons for Unsupervised Self-harm Content Prediction.

form kmeans for clustering; and

- *USCP-lite*: It is a variant of the proposed framework USCP that ignores features extracted according to our findings.

Since kmeans can only obtain local optimal solutions, we repeat experiments for these baselines based on kmeans 10 times and report the average performance. The performance comparisons are shown in Table 5.6. From the table, we make similar observations as the supervised self-harm content prediction experiments: (1) textual and visual sources are complementary to each other; and (2) the features extracted based on our findings can significantly improve the prediction performance under the unsupervised setting.

Parameter Analysis. There is one important parameter α for the proposed unsupervised framework USCP. The parameter controls the contribution of the model component capturing relations among sources. Next we study the impact of the component on the proposed framework by investigating how the performance changes with different values of α. We vary α as $\{0.001, 0.1, 0.2, 0.3, 0.4, 0.5, 0.6, 0.7, 0.8, 0.9,$
$10\}$. The performance variance w.r.t. α in terms of ACC is shown in Figure 5.5. Note that we do not show performance in terms of NMI since we make similar observations. In

general, with the increase of α, the performance tends to first increase and then decrease. In particular, (1) the performance increases a lot when α is increased from 0.001 to 0.1 that indicates the importance of capturing relations among sources; (2) when α in certain regions, the performance is relatively stable that can ease the process of parameter selection in practice; and (3) when α increases to 10, the performance degrades significantly since the term capturing relations among sources will dominate the learning process that will lead to overfitting.

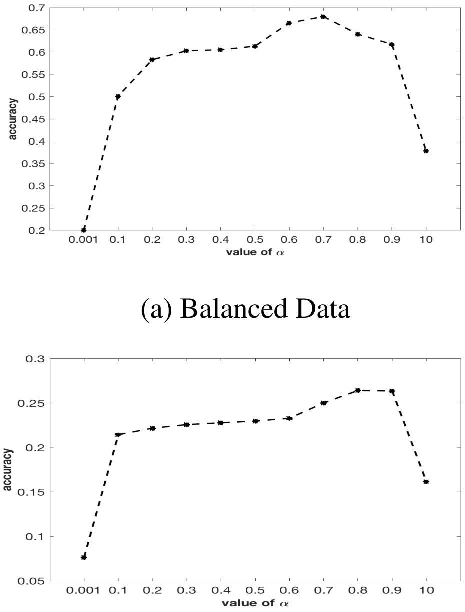

(a) Balanced Data

(b) Imbalanced Data

Figure 5.5: Parameter Analysis for Unsupervised Framework USCP.

5.5 Summary

In this paper, we aim to understand and discover self-harm content in social media since social media has become increasingly popular for self-harm users to discuss their problems. We conducted the first comprehensive analysis on self-harm content with data from the social media site Flickr. Our analysis suggests that characteristics of self-harm content are different from those of normal content, from textual, owner, temporal and visual perspectives. These findings have potentials to help us distinguish self-harm content from others, and we have thus developed frameworks by incorporating these findings to discover self-harm content automatically. Empirical results demonstrate that (1) the proposed frameworks can accurately identify self-harm content under both supervised and unsupervised settings; and (2) our findings play an important role in boosting the prediction performance.

There are several interesting directions for further investigations. First, we would like to extend our proposed models to the semi-supervised setting because in reality we can obtain a small amount of labeled data but need to deal with a large amount of unlabeled data Wang *et al.* (2016). Second, while the findings on self-harm content motivated us to develop approaches for identifying posts related to self-harm, it is interesting to further understand how such post-level analysis can be extended to automatically identify the self-harm users. Third, social networks are pervasively available in social media and it could be promising to study the impact of peer influence on self-harm user behaviors and leverage social networks to improve predictive tasks in self-harm research.

Chapter 6

BEYOND SENTIMENT ANALYSIS: A GENERAL APPROACH FOR MULTI-LABEL IMAGE LEARNING

Image classification, which tries to assign an image label to to a given image and one example is shown in Figure 6.1 [1] , is a core computer vision problem and has been well studied in past decades. In this chapter, I introduce a general multi-label image classification approach that derives from the sentiment analysis framework in previous chapters. The motivation behind our method is that sentiment analysis is a special application of a general image classification problem. It is possible to extend the method for sentiment analysis for a general image content analysis, i.e., image classification. In this chapter, I will firstly review the background of this problem that why label relationship is essential. Then I proposed a unified label relationship modelling method for multi-label image classification . Real-world Flickr and shopping datasets are used to evaluate the performance of the proposed method by comparing with the state-of-the-art baseline methods.

6.1 Introduction

The increasing popularity of social media generates massive data at an unprecedented rate. The ever-growing number of images has brought new challenges for efficient and effective image analysis tasks, such as image classification, annotation and image ranking. Based on the types of labels, we can roughly divide the supervised vision tasks into two categories – pointwise label based approaches and pairwise label based approaches. Pointwise approaches adopt pointwise labels such as image categories or tags as training targets Jiang *et al.* (2011); Toderici *et al.* (2010); Chen *et al.* (2013); Sigurbjörnsson and Van Zwol

[1] `http://cs231n.github.io/classification/`

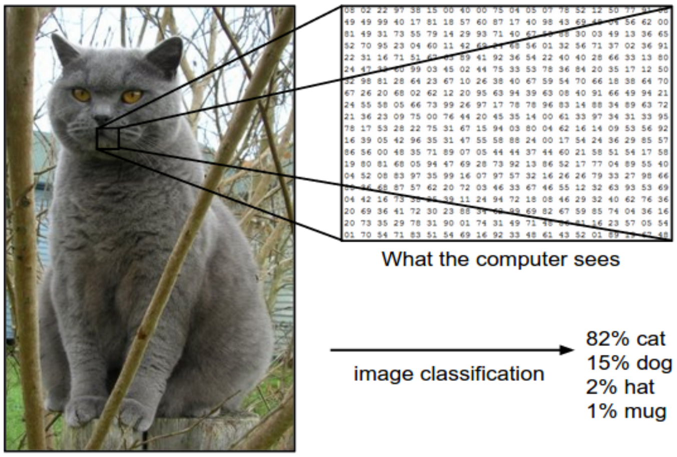

Figure 6.1: An Example of Image Classification and Image Representation

(2008); Jannach *et al.* (2010); Wang *et al.* (2015c,d). Class labels in classification often capture high-level image content, while tags in tag annotation are likely to describe a piece of information in the image, such as “high heel, buckle, leather” in a shoe image. In Wang *et al.* (2009), these two tasks are considered together because the labels and tags may have some relations in an image. Recently, due to the semantic gap between low-level image features and high-level image concepts, human nameable visual attributes are proposed to solve the vision tasksFarhadi *et al.* (2009); Lampert *et al.* (2009); Berg *et al.* (2010); Kumar *et al.* (2009). However, for a large variety of attributes, the pointwise binary setting is restrictive and unnatural. For example, it is very difficult to assign or not assign “sporty” to the middle car in Figure 6.2 because different people have different opinions. Thus, pairwise approaches Parikh and Grauman (2011); Kovashka and Grauman (2013a,b) have been proposed, which aim to learn a ranking function to predict the attribute strength for images. For example, in Figure 6.2. most of the people would agree that the middle car is more “sporty” than the left one and less “sporty” than the right one

Pointwise and pairwise labels have their own advantages as well as limitations in terms of labeling complexity and representational capability. **Labeling complexity**: given 10

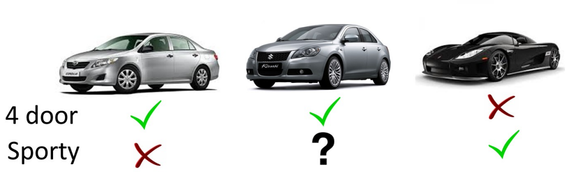

Figure 6.2: An Illustrative Example of Poinwise Labels and Pairwise Labels. (Pointwise label "4 door" is better than the pairwise label to describe presence of 4 door in a car, while "sporty" is better to use pairwise label to describe the car style, as the right is more sporty than the left. For example it is hard to label the middle (we ask 10 human viewer – 40% agree with the non sporty and 60% agree with sporty, but 100% agree with middle one is more sporty than the left one and less sporty than right one)).

images, we only need 10 sets of class categories/tags. However, we need to label at least 45 image pairs to capture the overall ordering information. (Although the ranking relation is considered as transferable, e.g. $A \succ B \& B \succ C \Rightarrow A \succ C$). **Representational capability**: pointwise labels such as tags/class labels imply the presence of content properties such as whether a shoe is made of leather, contains a heel, buckle, etc. While pairwise labels capture the relations in a same property, e.g., A has a higher heel than B. Solely relying on pointwise labels may cause ambiguity or produce noisy data for the models as in the example of assigning "sporty" to the middle car in Figure 6.2, while only using pairwise labels may also cause problems when the images have very similar properties.

As pointwise and pairwise labels encapsulate information of different types and may have different benefits for vision problems and recommendation systemsWang *et al.* (2015a) , we develop a new framework for fusing different types of training data by capturing their underlying relations. For example, in Figure 6.3, the tags, "leather, cognac, lace up" may suggest the left shoe with a higher score on the "formal" attribute, while the "high heel" may indicate the right shoe with a lower score on the "comfort" attribute. On the other hand, the higher score on "formal" and "comfort" with tag "Oxford" could help label the left image as “shoe” and enable the rare tag annotation such as “wingtip”. To the best of our knowledge, there are only a few recent works that fused pointwise and piarwise labels Sculley (2010); Chen *et al.* (2015). However, they simply combined regression and ranking in the loss functions for ranking tasks and totally ignored the relations between pointwise labels and pairwise labels.

In this paper, we investigate the problem of fusing pointwise and pairwise labels by exploiting their underlying relations for joint pointwise label prediction such as, image classification and annotation, and pairwise label prediction, e.g., relative ranking. We derive a unified bipartite graph model to capture the underlying relations among two types of labels. Since traditional approaches cannot take advantages of relations among pointwise and pairwise labels, we proceed to study two fundamental problems: (1) how to capture relations between pointwise and pairwise labels mathematically; and (2) how to make use of the relations for jointly addressing vision tasks. These two problems are tackled by the propose framework PPP and our contributions are summarized as follows:

- We provide a principled approach to modeling relations between pointwise and pairwise labels;
- we propose a novel joint framework PPP, which can predict both pointwise and pairwise labels for images simultaneously; and
- We conduct experiments on various benchmark datasets to understand the working of the proposed framework PPP.

In the remaining of the paper, we first give a formal problem definition and basic model in Section 2. Then the proposed framework and an optimization method for model learning is presented in Section 3. Experiments and results are demonstrated in Section 4, with further discussion in section 5.

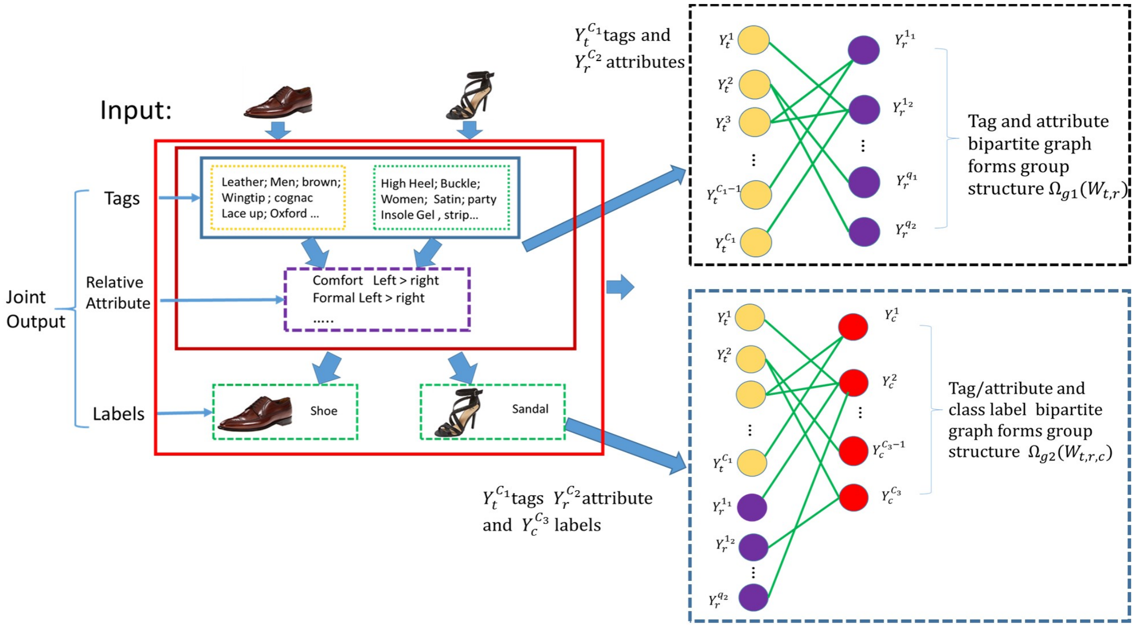
Input:
Joint Output
Tags
Relative Attribute
Labels
Leather; Men; brown; Wingtip ; cognac Lace up; Oxford ...
High Heel; Buckle; Women; Satin; party Insole Gel , strip...
Comfort Left > right
Formal Left > right
.....
Shoe
Sandal
$Y_t^{C_1}$tags and $Y_r^{C_2}$ attributes
Y_t^1
Y_t^2
Y_t^3
$Y_t^{C_1-1}$
$Y_t^{C_1}$
$Y_r^{1_1}$
$Y_r^{1_2}$
$Y_r^{q_1}$
$Y_r^{q_2}$
Tag and attribute bipartite graph forms group structure $\Omega_{g1}(W_{t,r})$
$Y_t^{C_1}$tags $Y_r^{C_2}$attribute and $Y_c^{C_3}$ labels
Y_c^1
Y_c^2
$Y_c^{C_3-1}$
$Y_c^{C_3}$
Tag/attribute and class label bipartite graph forms group structure $\Omega_{g2}(W_{t,r,c})$

Figure 6.3: The Demonstration of Capturing the Relations between Pointwise Label and Pairwise Label via Bipartite Graph (For example, the attribute "formal" with tags "leather, lace up, congnac" will form a group via the upper bipartite graph, while label "sandal" with attribute "less formal" and tags "high heel, party" will form a group via the lower bipartite graph).

6.2 The Proposed Method

Before detailing the proposed framework, we first introduce notations used in this paper. We use $\mathbf{X} \in \mathbb{R}^{n \times d}$ to denote a set of images in the database where n is the number of images and d is the number of features. Note that there are various ways to extract features such as SIFT, Gist or the features learned via deep learning frameworks. Let $\mathbf{Y}_t \in \mathbb{R}^{n \times c_1}$ and $\mathbf{Y}_c \in \mathbb{R}^{n \times c_3}$ be the data-tag and data-label matrices which represent the pointwise labels. $\mathbf{Y}(i,j) = 1$ if the i-th image is annotated/classified with j-th tag/class label, $\mathbf{Y}(i,j) = 0$ otherwise. Given a fixed training set D, a candidate pair set P can be drawn. The pair set implied by the fixed training set D uses pairwise labels. In the proposed framework, given a pair of images $< a, b >$ on the attribute q, if $y_a \succ y_b$, then a has a positive attribute score $y(a, q, 1) = |y_a - y_b|$, and a negative score $y(a, q, 2) = 0$; while b has a positive attribute $y(b, q, 1) = 0$, and a negative score $y(b, q, 2) = |y_a - y_b|$. Thus, the pairwise label is defined as $\mathbf{Y}_r \in \mathbb{R}^{m \times c_2}$, where m is the number of pairs drawn from training samples and $c_2 = 2q$ where q is the number of attributes. For example, let $< a, b >$ be the first pair, the pairwise label $\mathbf{Y}_r(1, 2(q-1)+1)$ represents how likely the $y_a \succ y_b$ and $\mathbf{Y}_r(1, 2(q-1)+2)$ represents how likely $y_a \prec y_b$ on attribute q.

6.2.1 Baseline Models

In our framework, pointwise labels are considered for classification and annotation tasks. For classification, we assume that there is a linear classifier $\mathbf{W}_c \in \mathbb{R}^{d \times c_3}$ to map $\mathbf{X}$ to the pointwise label $\mathbf{Y_c}$ as $\mathbf{Y}_c = \mathbf{X}\mathbf{W}_c$. $\mathbf{W}_c$ can be obtained by solving the following optimization problem:

$$\min_{\mathbf{W}_c} \Omega(\mathbf{W}_c) + \mathcal{L}(\mathbf{W}_c, \mathbf{Y}_c, D) \tag{6.1}$$

where $\mathcal{L}()$ is a loss function and Ω is a regularization penalty to avoid overfitting, D is the training sample set. Here we employ least square for loss function $\mathcal{L}$.

For tag annotation, we also assume that there is a linear function $\mathbf{W}_t \in \mathbb{R}^{d \times c_1}$ which captures the relation between data $\mathbf{X}$ and pointwise label $\mathbf{Y}_t$ as $\mathbf{Y}_t = \mathbf{X}\mathbf{W}_t$. Similarly, the optimization problem to learn $\mathbf{W}_t$ is:

$$\min_{\mathbf{W}_t} \Omega(\mathbf{W}_t) + \mathcal{L}(\mathbf{W}_t, \mathbf{Y}_t, D) \tag{6.2}$$

For pairwise label based approaches, a simple and successful approach to utilizing the pairwise label is Rank SVM, whose goal is to learn a model $\mathbf{W}$ that achieves little loss over a set of previously unseen data, using a prediction function. Similar to RankSVM, in our framework, the original distribution of training examples are expanded into a set of candidate pairs and the learning process is over a set of pairwise feature vectors as:

$$\min_{\mathbf{W}} \mathcal{L}(\mathbf{W}, \mathbf{Y}_r, P) + \Omega(\mathbf{W}_r) \tag{6.3}$$

where P is a set of training pairs. The loss function $\mathcal{L}$ is defined over the pairwise difference vector x:

$$\mathcal{L}(\mathbf{W}, \mathbf{Y}_r, P) = \sum_{((a,y_a,q_a),(b,y_b,q_b)) \in P} l(t(y_a - y_b), f(w, a - b)) \tag{6.4}$$

where the transformation function $t(y)$ transforms the difference of the labels Sculley (2010). In our framework, the transformation function is defined as $t(y) = sign(y)$.

Note that one may form a unified model by simply adding all the above objective functions together. Such an approach would still essentially treat the component models as independent tasks (albeit trade-off among them might be considered via weighting), since no explicit relations among them are considered.

6.2.2 Capturing Relations between Poinwise and Pairwise Labels

In the previous subsection, we defined three tasks that use pointwise and pairwise labels separately. Capturing the relations between pointwise and pairwise labels can further pave a way for us to develop a joint framework that enables interaction between classification, annotation and ranking simultaneously.

First, the relations between attributes and tags can be denoted as a bipartite graph as shown in Figure 6.3. We assume that $\mathbf{B} \in \mathbb{R}^{c_2 \times c_1}$ is the adjacency matrix of the graph where $\mathbf{B}(i, j) = 1$ if both the i-th tag and the j-th attribute co-occur in the same image and $\mathbf{B}(i, j) = 0$ otherwise. Note that in this paper, we do not consider the concurrence frequencies of tags and attributes and we would like to leave it as one future work. From the bipartite graph, we can identify groups of attributes and tags where attributes and tags in the same group could share similar properties such as semantical meanings. A feature

$\mathbf{X}(:, i)$ should be either relevant or irrelevant to the attributes and tags in the same group. For example, $\mathbf{W}_r(i, j)$ indicates the effect of the i-th feature on predicting the j-th attribute; while $\mathbf{W}_t(i, k)$ denotes the impact of the i-th feature on the k-th tag. Therefore we can impose constraints on $\mathbf{W}_t$ and $\mathbf{W}_r$ together, which are derived from group information on the bipartite graph, to capture relations between attributes and tags.

We can adopt any community detection algorithms to identify groups from the bipartite graph. In this paper, we use a very simple way to extract groups from the bipartite graph – for the j-th attribute, we consider the tags that connect to that attribute in the bipartite graph as a group, i.e., $\mathbf{B}(i, j) = 1$. Note that a tag may connect to several attributes thus extracted groups via the aforementioned process have ***overlaps***. Assume that $\mathcal{G}$ is the set of groups we detect from the attribute-tag bipartite graph and we propose to minimize the following term to capture relations between attributes and tags as:

$$\Omega_{\mathcal{G}}(\mathbf{W}_{t,r}) = \sum_{i=1}^{d} \sum_{g \in \mathcal{G}} \alpha_g \left\| \mathbf{w}_g^i \right\|_2 \tag{6.5}$$

where $\mathbf{W}_{t,r} = [\mathbf{W}_t, \mathbf{W}_r]$ and α_g is the confidence of the group g and $\mathbf{w}_g^i$ is a vector concatenating $\{\mathbf{W}_{t,r}(i, j)\}_{j \in g}$. For example, if $g = \{1, 5, 9\}$, $\mathbf{w}_g^i = [\mathbf{W}_{t,r}(i, 1), \mathbf{W}_{t,r}(i, 5), \mathbf{W}_{t,r}(i, 9)]$. Next we discuss the inner workings of Eq. (6.5). Let us check terms in Eq. (6.5) related to a specific group g, $\sum_{i=1}^{d} \left\| \mathbf{w}_g^i \right\|_2$, which is equal to adding a ℓ_1 norm on the vector $\mathbf{g} = [\mathbf{w}_g^1, \mathbf{w}_g^2, \ldots, \mathbf{w}_g^d]$, i.e., $\|\mathbf{g}\|_1$. That ensures a sparse solution of g; in other words, some elements of g could be zero. If $\mathbf{g}_i = 0$ or $\|\mathbf{w}_g^2\|_2 = 0$, the effects of the i-th feature on both the attribute and tags in the group g are eliminated simultaneously.

Similarly, we build the bipartite graph to capture the underlying relations for the attributes and class labels. In Wang *et al.* (2009), it was suggested that the co-occurrence of tags and labels should also be considered. Thus, we build a mixture bipartite graph to extract the group information between class labels, tags, and attributes. The group regularization

$\Omega_{\mathcal{G}2}(\mathbf{W}_{t,r,c})$ is similar to Eq. 6.5 and illustration is shown in Figure 6.3, where a tag or an attribute will connect to the class label if they are associated with each other. Note that a group extracted from Figure 6.3 could include a class label, a set of attributes and a set of tags.

6.2.3 The Proposed Framework

With the model component to exploit the bipartite graph structures, the proposed framework is to solve the following optimization problem:

$$\begin{aligned}\min_{\mathbf{W}} \; & \mathcal{L}(\mathbf{W}_c, \mathbf{Y}_c, D) + \mathcal{L}(\mathbf{W}_t, \mathbf{Y}_t, D) + \mathcal{L}(\mathbf{W}_r, \mathbf{Y}_r, P) \\ & + \lambda(\|\mathbf{W}_c\|_F^2 + \|\mathbf{W}_t\|_F^2 + \|\mathbf{W}_r\|_F^2) \\ & + \alpha\Omega_{\mathcal{G}1}(\mathbf{W}_{t,r}) + \beta\Omega_{\mathcal{G}2}(\mathbf{W}_{t,r,c})\end{aligned} \tag{6.6}$$

In Eq. 6.6, the first six term is from the basic models to predict the class label, tags and ranking order. The seventh and eighth term are to capture the overlapped structure of the output, which is controlled by α and β respectively. The group regularization is defined as blow:

$$\Omega_{\mathcal{G}}(\mathbf{Z}) = \sum_{i\in\mathcal{G}} \|\mathbf{Z}_g\|_2 = \sum_{i=1}^{d}\sum_{i\in\mathcal{G}} \|\mathbf{z}_g^i\|_2 \tag{6.7}$$

6.3 An Optimization Method for PPP

Since the group structures are overlapped, directly optimizing the objective function is difficult. We propose to use Alternating Direction Method of Multiplier (ADMM)(Yogatama and Smith (2014); Boyd *et al.* (2011)) to optimize the objective function. We first introduce two auxiliary variables $\mathbf{P} = [\mathbf{W}_t, \mathbf{W}_r]\mathbf{M}_1$ and $\mathbf{Q} = [\mathbf{W}_t, \mathbf{W}_r, \mathbf{W}_c]\mathbf{M}_2$. $\mathbf{M}_1 \in \{0,1\}^{(c_1+c_2)\times c_2(c_1+c_2)}$ is defined as: if $i-th$ tag connects to the jth attribute then $\mathbf{M}_1(i,(c_1+c_2)(j-1)+i) = 1$, otherwise it is zero. The definition of $\mathbf{M}_2 \in \{0,1\}^{(c_1+c_2+c_3)\times c_3(c_1+c_2+c_3)}$ is similar to $\mathbf{M}_1$. With these two variable, solving the overlapped group lasso on $\mathbf{W}$ is transfered to the non-overlapped group lasso on $\mathbf{P}$ and $\mathbf{Q}$, respectively. Therefore, the objective function becomes:

$$\begin{aligned}\min_{\mathbf{W},\mathbf{P},\mathbf{Q}} & \mathcal{L}(\mathbf{W}_c, D) + \mathcal{L}(\mathbf{W}_t, D) + \mathcal{L}(\mathbf{W}_r, P) \\ & + \alpha\Omega_{\mathcal{G}}(\mathbf{P}) + \beta\Omega_{\mathcal{G}2}(\mathbf{Q}) \\ & + \lambda(\|\mathbf{W}_c\|_F^2 + \|\mathbf{W}_t\|_F^2 + \|\mathbf{W}_r\|_F^2) \\ & s.t. \mathbf{P} = [\mathbf{W_t}, \mathbf{W_r}]\mathbf{M}_1; \mathbf{Q} = [\mathbf{W}_t, \mathbf{W}_r, \mathbf{W}_c]\mathbf{M}_2;\end{aligned} \tag{6.8}$$

which can be solved by the following ADMM problem:

$$\begin{aligned}\min_{\mathbf{W},\mathbf{P},\mathbf{Q}} & \mathcal{L}(\mathbf{W}_c, \mathbf{Y}_c, D) + \mathcal{L}(\mathbf{W}_t, \mathbf{Y}_t, D) + \mathcal{L}(\mathbf{W}_r, \mathbf{Y}_r, P) \\ & + \lambda(\|\mathbf{W}_c\|_F^2 + \|\mathbf{W}_t\|_F^2 + \|\mathbf{W}_r\|_F^2) + \alpha\Omega_{\mathcal{G}}(\mathbf{P}) \\ & + \beta\Omega_{\mathcal{G}2}(\mathbf{Q}) + \langle \mathbf{\Lambda}_1, \mathbf{P} - [\mathbf{W}_t, \mathbf{W}_r]\mathbf{M}_1 \rangle \\ & + \langle \mathbf{\Lambda}_2, \mathbf{Q} - [\mathbf{W}_t, \mathbf{W}_r, \mathbf{W}_c]\mathbf{M}_2 \rangle \\ & + \frac{\mu}{2}\|\mathbf{P} - [\mathbf{W}_t, \mathbf{W}_r]\mathbf{M}_1\|_F^2 \\ & + \frac{\mu}{2}\|\mathbf{Q} - [\mathbf{W}_t, \mathbf{W}_r, \mathbf{W}_c]\mathbf{M}_2\|_F^2\end{aligned} \tag{6.9}$$

where $\mathbf{\Lambda}$ is the Lagrangian multiplier and μ is a scaler to control the penalty for the violation of equality constrains $\mathbf{P} = [\mathbf{W}_t, \mathbf{W}_r]\mathbf{M}_1$ and $\mathbf{Q} = [\mathbf{W}_t, \mathbf{W}_r, \mathbf{W}_c]\mathbf{M}_2$. Noting that the loss function L has lots of choices, we use the least square loss function in this paper.

6.3.1 Updating W

To update $\mathbf{W}$, we fix the other variable except $\mathbf{W}$ and remove terms that are irrelevant to $\mathbf{W}$. Then the Eq. 6.9 becomes:

$$\begin{aligned}\min_{\mathbf{W}} & \sum_{x\in D}\|x\mathbf{W}_t - y_t\|_2^2 + \sum_{x\in D}\|x\mathbf{W}_c - y_c\|_2^2 \\ & + \sum_{x_i,x_j\in P}\|(x_i - x_j)\mathbf{W}_r - y_r\|_2^2 \\ & + \lambda(\|\mathbf{W}_c\|_F^2 + \|\mathbf{W}_t\|_F^2 + \|\mathbf{W}_r\|_F^2) \\ & + \frac{\mu}{2}\|(\mathbf{P} + \frac{1}{\mu}\Lambda_1) - [\mathbf{W}_t, \mathbf{W}_r]\mathbf{M}_1\|_F^2 \\ & + \frac{\mu}{2}\|(\mathbf{Q} + \frac{1}{\mu}\Lambda_2) - [\mathbf{W}_t, \mathbf{W}_r, \mathbf{W}_c]\mathbf{M}_2\|_F^2\end{aligned} \tag{6.10}$$

Setting the derivative of Eq. 6.10 w.r.t $\mathbf{W}_t$ to 0, we get:

$$\begin{aligned}&\mathbf{X}_D^T\mathbf{X}_D\mathbf{W}_t + \lambda\mathbf{W}_t + \mathbf{W}_t(\mathbf{M}_1^t\mathbf{M}_1^{tT} + \mathbf{M}_2^t\mathbf{M}_2^{tT}) \\ &= \mathbf{X}^T\mathbf{Y} + \frac{\mu}{2}[(\mathbf{P} + \frac{1}{\mu}\Lambda_1)\mathbf{M}_1^t + (\mathbf{Q} + \frac{1}{\mu}\Lambda_2)\mathbf{M}_2^t]\end{aligned} \tag{6.11}$$

where $\mathbf{M}_1^t$ is the part of $\mathbf{M}_1$ corresponding to $\mathbf{W}_t$. Directly getting the close form solution from Eq. 6.11 is intractable. On the other hand $\mathbf{X}_D^T\mathbf{X}_D + \frac{1}{2}\lambda\mathbf{I}$ and $\mathbf{M}_1^t\mathbf{M}_1^{tT} + \mathbf{M}_2^t\mathbf{M}_2^{tT} + \frac{1}{2}\lambda\mathbf{I}$ are symmetric and positive definite. Thus, we employ eigen decomposition for each of them:

$$\begin{aligned}\mathbf{X}_D^T\mathbf{X}_D + \frac{1}{2}\lambda\mathbf{I} &= \mathbf{U}_1\Sigma_1\mathbf{U}_1^T \\ \mathbf{M}_1^t\mathbf{M}_1^{tT} + \mathbf{M}_2^t\mathbf{M}_2^{tT} + \frac{1}{2}\lambda\mathbf{I} &= \mathbf{U}_2\Sigma_2\mathbf{U}_2^T\end{aligned} \tag{6.12}$$

where$\mathbf{U}_1, \mathbf{U}_2$ are eigen vectors and Σ_1, Σ_2 are diagonal matrices with eigen value on the diagonal. Substituting Eq. 6.12 into Eq. 6.11:

$$\begin{aligned}\mathbf{U}_1\Sigma_1\mathbf{U}_1^T\mathbf{W}_t{+}\mathbf{W}_t\mathbf{U}_2\Sigma_2\mathbf{U}_2^T &= \mathbf{X}_D^T\mathbf{Y}_t + \frac{\mu}{2}(\mathbf{P} + \frac{1}{\mu}\Lambda_1)\mathbf{M}_1^t \\ &+ \frac{\mu}{2}(\mathbf{Q} + \frac{1}{\mu}\Lambda_2)\mathbf{M}_2^t\end{aligned} \tag{6.13}$$

Multiplying $\mathbf{U}_1^T$ and $\mathbf{U}_2$ from left to right on both sides, and letting $\widetilde{\mathbf{W}_t} = \mathbf{U}_1^T\mathbf{W}_t\mathbf{U}_2$ and $\mathbf{Z}_t = \mathbf{U}_1^T[\mathbf{X}_D^T\mathbf{Y}_t + \frac{\mu}{2}[(\mathbf{P} + \frac{1}{\mu}\Lambda_1)\mathbf{M}_1^t + (\mathbf{Q} + \frac{1}{\mu}\Lambda_2)\mathbf{M}_2^t]]\mathbf{U}_2$, we can obtain:

$$\Sigma_1\widetilde{\mathbf{W}_t} + \widetilde{\mathbf{W}_t}\Sigma_2 = \mathbf{Z}_t \tag{6.14}$$

Then, we can get $\widetilde{\mathbf{W}_t}$ and $\mathbf{W}_t$ as:

$$\widetilde{\mathbf{W}_t}(s,t) = \frac{\mathbf{Z}_t(s,t)}{\sigma_1^s + \sigma_2^t} \tag{6.15}$$

$$\mathbf{W}_t = \mathbf{U}_1\widetilde{\mathbf{W}_t}\mathbf{U}_2^T \tag{6.16}$$

Similarly, setting the derivative of Eq. 6.10 w.r.t $\mathbf{W}_c$ to zero and apply the eigen decomposition, we have the closed form solution of $\mathbf{W}_c$:

$$\widetilde{\mathbf{W}_c}(s,t) = \frac{\mathbf{Z}_c}{\sigma_1^s + \sigma_3^t} \tag{6.17}$$

$$\mathbf{W}_c = \mathbf{U}_1\widetilde{\mathbf{W}_c}\mathbf{U}_3^T \tag{6.18}$$

where $\mathbf{Z}_c = \mathbf{U}_3^T[\mathbf{X}_D^T\mathbf{Y}_c + \frac{\mu}{2}(\mathbf{Q} + \frac{1}{\mu}\Lambda_2)]\mathbf{M}_2^c$ and $\mathbf{U}_3, \sigma_3$ are the eigen vector and eigen value for the symmetric and positive definite matrix $\mathbf{M}_2^c\mathbf{M}_2^{cT} + \frac{1}{2}\lambda\mathbf{I}$.

Noting that for $\mathbf{W}_r$, which input is data pairs, we can use the same learning process by using the transform label function mentioned above. For example, we regard the pair difference as one data sample for $\mathbf{X}_P$ and use the positive and negative label for label transformation. Setting the Eq. 6.10 w.r.t $\mathbf{W}_r$ to zero, we can obtain:

$$\begin{aligned} &\mathbf{X}_P^T\mathbf{X}_P\mathbf{W}_r + \lambda\mathbf{W}_r + \mathbf{W}_r(\mathbf{M}_1^r\mathbf{M}_1^{rT} + \mathbf{M}_2^r\mathbf{M}_2^{rT}) \\ &= \mathbf{X}_P^T\mathbf{Y}_r + \frac{\mu}{2}[(\mathbf{P} + \frac{1}{\mu}\Lambda_1)\mathbf{M}_1^r + (\mathbf{Q} + \frac{1}{\mu}\Lambda_2)\mathbf{M}_2^r] \end{aligned} \tag{6.19}$$

Similar to $\mathbf{W}_c$, with eigen decomposition, we can get the closed form solution for $\mathbf{W}_r$ as:

$$\widetilde{\mathbf{W}_r}(s,t) = \frac{\mathbf{Z}_r}{\sigma_4^s + \sigma_5^t} \tag{6.20}$$

$$\mathbf{W}_r = \mathbf{U}_4\widetilde{\mathbf{W}_r}\mathbf{U}_5^T \tag{6.21}$$

where $\mathbf{Z}_r = \mathbf{U}_4[\mathbf{X}_P^T\mathbf{Y}_r + \frac{\mu}{2}[(\mathbf{P} + \frac{1}{\mu}\Lambda_1)\mathbf{M}_1^r + (\mathbf{Q} + \frac{1}{\mu}\Lambda_2)\mathbf{M}_2^r]\mathbf{U}_5^T$, $\mathbf{U}_4, \sigma_4$ are eigen vector and eigen values for $\mathbf{X}_P^T\mathbf{X}_P + \frac{1}{2}\lambda\mathbf{I}$, and $\mathbf{U}_5, \sigma_5$ are eigen vector and eigen value for $\mathbf{M}_1^r\mathbf{M}_1^{rT} + \mathbf{M}_2^r\mathbf{M}_2^{rT} + \frac{1}{2}\lambda\mathbf{I}$.

6.3.2 Updating P

After removing terms that are irrelevant to $\mathbf{P}$, Eq. 6.9 becomes:

$$\min_{\mathbf{P}} \frac{\mu}{2}\|\mathbf{P} - [\mathbf{W}_t, \mathbf{W}_r]\mathbf{M}_1\|_F^2 + \alpha\Omega_{\mathcal{G}}(\mathbf{P}) + Tr(\Lambda_1\mathbf{P}) \tag{6.22}$$

When applied to the collection of group for the parameters, $\mathbf{P}$, $\Omega_{\mathcal{G}}(\mathbf{P}))$ no longer have overlapping groups. We denote $j - th$ group in i-th row as $\mathbf{P}_{i,j} = \mathbf{P}(i, (c_1 + c_2)(j-1) + 1 : (c_1 + c_2)j)$. Hence, we can solve the problem separately for each row of $\mathbf{P}$ within one group by the following optimization:

$$\min_{\mathbf{P}_{i,j}} \alpha\|\mathbf{P}_{i,j}\|_2^2 + \frac{\mu}{2}\|\mathbf{P}_{i,j} - (([\mathbf{W}_c, \mathbf{W}_r]\mathbf{M}_1)_{i,j} - \frac{\Lambda_{1ij}}{\mu})\|_F^2 \tag{6.23}$$

Note that Eq. 6.23 is the proximal operator Yuan *et al.* (2011) of $\frac{1}{\mu}(P)_{i,j}$ applied to $(([\mathbf{W}_c, \mathbf{W}_r]\mathbf{M}_1)_{i,j} - \frac{\Lambda_{1ij}}{\mu})$. Let $\mathbf{Z}_{i,j}^P = ([\mathbf{W}_c, \mathbf{W}_r]\mathbf{M}_1)_{i,j} - \frac{\Lambda_{1ij}}{\mu}$. The solution by applying the proximal operator used in non-overlapping group lasso to each sub-vector is:

$$\mathbf{P}_{i,j} = prox(\mathbf{Z}_{i,j}^P) = \begin{cases} 0 & if\|\mathbf{Z}_{i,j}^P\|_2 \leq \frac{\alpha}{\mu} \\ \frac{\|\mathbf{Z}_{i,j}^P\|_2 - \frac{\alpha}{\mu}}{\|\mathbf{Z}_{i,j\|_2}^P}\mathbf{Z}_{i,j}^P & otherwise \end{cases} \tag{6.24}$$

6.3.3 Updating Q

Similar to $\mathbf{P}$, we can update $\mathbf{Q}$ by proximal operator used in non-overlapping group lasso to each sub-vector of $\mathbf{Q}$:

$$\mathbf{Q}_{i,j} = prox(\mathbf{Z}_{i,j}^Q) = \begin{cases} 0 & if\|\mathbf{Z}_{i,j}^Q\|_2 \leq \frac{\beta}{\mu} \\ \frac{\|\mathbf{Z}_{i,j}^Q\|_2 - \frac{\beta}{\mu}}{\|\mathbf{Z}_{i,j\|_2}^Q}\mathbf{Z}_{i,j}^Q & otherwise \end{cases} \tag{6.25}$$

where $\mathbf{Q}_{ij} = \mathbf{Q}(i, (c_1 + c_2 + c_3)(j-1) + 1 : (c_1 + c_2 + c_3)j)$ and $\mathbf{Z}_{i,j}^Q = ([\mathbf{W_t}, \mathbf{W_r}, \mathbf{W_c}]M_2)_{i,j} - \frac{\Lambda_{i,j}}{\mu}$

6.3.4 Updating Λ_1, Λ_2 and μ

After updating the variables, we now need to update the ADMM parameters. According to Boyd *et al.* (2011), they are updated as follows:

$$\Lambda_1 = \Lambda_1 + \mu(\mathbf{P} - [\mathbf{W}_t, \mathbf{W}_r]\mathbf{M}_1) \tag{6.26}$$

$$\Lambda_2 = \Lambda_2 + \mu(\mathbf{Q} - [\mathbf{W}_t, \mathbf{W}_r, \mathbf{W}_c]\mathbf{M}_2) \tag{6.27}$$

$$\mu = min(\rho\mu, \mu_{max}) \tag{6.28}$$

Here, $\rho > 0$ is a parameter to control the convergence speed and μ_{max} is a large number to prevent μ from becoming too large.

With these updating rules, the optimization method for our proposed method is summarized in Algorithm 4

6.3.5 Convergence Analysis

Since the sub-problems are convex for $\mathbf{P}$ and $\mathbf{Q}$, respectively, Algorithm 1 is guaranteed to converge because they satisfy the two assumptions required by ADMM. The proof of the convergence can be found in Boyd *et al.* (2011). Specially, Algorithm 1 has dual variable convergence. Our empirical results show that our algorithm often converges within 100 iterations for all the datasets we used for evaluation.

6.3.6 Time Complexity Analysis

The main computation cost for $\mathbf{W}$ involves the eigen decomposition on $\mathbf{X^T X} + \frac{1}{2}\beta\mathbf{I}$, while other terms that involve eigen decomposition is very fast because the feature dimension of $\mathbf{M}\mathbf{M}^T$ is small. The time complexity for eigen decomposition is $O(d^3)$. However, in Algorithm 1 the eigen decomposition is only computed once before the loop and dimension reduction algorithm can be employed to reduce image feature dimensions d. The computation cost for $\mathbf{Z}$ is $O(nd^2)$ due to the sparsity of $\mathbf{M}$. The computation of $\mathbf{P}$ depends on the

Algorithm 4 The Algorithm for the Framwork

```
**Input**: $\mathbf{X}_D \in \mathbf{R}^{N\times d}$ and $\mathbf{X}_P \in \mathbf{R}^{m\times d}$ and corresponding label $\mathbf{Y}_t, \mathbf{Y}_c$ and $\mathbf{Y}_r$
**Output**: $c_1$ tags label $c_2$ relative score and $c_3$
class label for each data instance
Initialize random Sample training set $D$ and drawn random pair set $P$ from $D$.
Setting $\mu = 10^{-3}, \rho = 1.1, \mu_{max} = 10^8$ and building $\mathbf{M}_1$ and $\mathbf{M}_2$
Precompute the eigen decomposition
**repeat**
    Calculate $\widetilde{\mathbf{W}_t}$, $\widetilde{\mathbf{W}}_t$ and $\widetilde{\mathbf{W}_r}$
    Update $\mathbf{W}_t, \mathbf{W}_r$ and $\mathbf{W}_c$ by Eq. 6.16, Eq. 6.21, and Eq. 6.18, respectively.
    Calculate $\mathbf{Z}^P$ and $\mathbf{Z}^Q$
    Update $\mathbf{P}$ and $\mathbf{Q}$
    Update $\Lambda_1$, $\Lambda_2$ and $\mu$
**until** convergence
Using max pooling for testing use $\mathbf{XW}$ to predict tags, relative relation and labels.
```

proximal method within each group. Since there are c_2 groups which have the group size $c_1 + c_2$ for each feature dimension, the total computation cost for $\mathbf{P}$ is $O(dc_2(c_1 + c_2))$ and it is similar for $\mathbf{Q}$. It is worth noting that $\mathbf{P}$ and $\mathbf{Q}$ can be computed in parallel for each feature dimension.

6.4 Experiment

In this section, we conduct experiments to evaluate the effectiveness of PPP. After introducing datasets and experimental settings, we compare PPP with the state-of-the-art methods of tag prediction, classification and ranking.

6.4.1 Experiments Settings

The experiments are conducted on 3 publicly available benchmark datasets.

Shoe-Zappo dataset Yu and Grauman (2014): It is a large shoe dataset consisting of 50,025 catalog images collected from Zappos.com. The images are divided into 4 major categories shoes, sandals, slippers, and boots. The tags are functional types and individual brands such as high-heel, oxford, leather, lace up, and pointed toe. The number of tags is 147 and 4 relative attribute is defined as “open” , “pointy”, “sporty” and “comfortable”. The ground truth is labeled from AmazonTurk.

OSR-scene dataset Oliva and Torralba (2001): It is a dataset for out door scene recognition with 2688 images. The images are divided into 8 category named as coast, forest, highway, inside-city, mountain, open-country, street and tall-building. 6 attributes with pointwise label and pairwise label are provided by Parikh and Grauman (2011) named by natural, open, perspective, large-objects, diagonal-plane and close-depth.

Pubfig-face dataset Kumar *et al.* (2009): It is a dataset containing 800 images from 8 random identities (100 images per person) named Alex Rodriguez, Clive Owen, Hugh Laurie , Jared Leto , Miley Cyrus, Scarlett Johansson , Viggo Mortensen and Zac Efron. We use the 11 attributes with pintwise label and pairwise label provided by Parikh and Grauman (2011). The example attributes are named as masculine-looking, white, young, smiling and etc.

6.4.2 Performance Comparison

We compare PPP with the following representative algorithms:

- SVM Chang and Lin (2011): It uses the state of the art classifier SVM for classification with linear kernel; We also apply it to tag prediction by considering tags as a kind of labels;

- GLasso Yuan and Lin (2006): The original framework of group lasso is to handle high-dimensional and multi-class data. To extend it for joint classification and tag prediction, we also consider tags as a kind of labels and apply GLasso to learn the mapping of features to tags and label. Note that it does not make use of the pointwise and pairwise label bipartite graph. We use the implementation in Liu *et al.* (????);

- sLDA Wang *et al.* (2009): It is a joint framework based on topic models, which learns both class labels and annotations given latent topics;

- LS Ji *et al.* (2008): A multi-label classification method that exploits the label correlation information. To apply LS for joint classification and tag prediction, we consider tags as a kind of labels and use tag and label relations to replace the label correlation in the original model; and

- FT Chen *et al.* (2013): It is one of the state-of-the art annotation method which is based on linear mapping and co-regularized joint optimization. To apply it for classification, we consider labels as tags to annotate; and

- RD: It predicts labels and tags by randomly guessing.

- MultiRank Chen *et al.* (2014): It is a ranking method based on the assumption that the correlation exists between attributes, where the ranking function learns all attributes together via multi task learning framework.

- RA Parikh and Grauman (2011): It is the method for image ranking based on relative attributes.

Note that for all the baseline methods, none of them can utilize both pointwise and pairwise labels. Although we get the performance of the proposed framework by jointly predicting both pointwise and pairwise labels, we present our results for each task separately

Table 6.1: Performance Comparison for Classification (The number after each dataset means the class label number).

Method	Zappos(4)	OSR(8)	Pubfig (8)
SVM	67.41 %	42.21 %	50.77%
GLasso	78.31%	50.11%	59.13%
sLDA	74.32%	46.33%	56.21%
LS	84.46%	61.22%	66.56%
FT	84.69%	59.38%	67.45%
RD	25.01%	12.51%	12.50%
PPP	**89.39%**	**62.33%**	**74.95%**

for a clear comparison. Moreover, we could use more advanced features, e.g., CNN feature, however, to compare with other methods fairly, we adopt the original feature provided by each datasets, which can easily show the performance gain from the proposed model.

6.4.3 Pointwise label Prediction

For pointwise label prediction, our method is compared with SVM, Glasso, sLDA, LS, FT, and RD. For all the baseline methods with parameters, we use cross validation to determine their values. For the Shoe dataset, we use the same data split and features (990 gist and color features) in Yu and Grauman (2014). It contains 11102 data samples for training and 2400 data sample for testing. For OSR and Pubfig, we use the same data split and features in Parikh and Grauman (2011).

Since OSR and Pubfig contain a small number of attributes, we leave one random-picked attribute for pairwise prediction and use the rest for tag annotation. Especially, to evaluate the performance of tag annotation, we rank all the tags based on their relevant scores

Table 6.2: Performance Comparison in terms of Tag Recommendation.

Method	Zappo		OSR		Pubfig	
	AP@3	AP@5	AP@1	AP@3	AP@1	AP@5
SVM	50.57%	38.53%	68.51%	60.12%	46.21%	34.12%
GLasso	64.34%	55.37%	87.11%	80.87%	90.12%	86.41%
sLDA	62.57%	51.63%	90.15%	84.78%	91.12%	84.17%
LS	74.76%	61.85%	94.19%	**92.75**%	93.71%	91.91%
FT	67.37%	51.98%	**98.62**%	92.22%	92.45%	90.16%
RD	1.44%	1.44%	20.00%	20.01%	10.01%	10.01%
PPP	**77.10%**	**62.95%**	96.69%	90.14%	**94.48%**	**92.71%**

and return the top K ranked tags. We use the average precision $AP@K$ as the evaluation metric which has been widely used in the literature Chen *et al.* (2013); Wang *et al.* (2009). Meanwhile since the data samples are balanced, we use accuracy as the metric to evaluate the classification performance. The comparison results are shown in Table 6.1 and Table 6.2 for classification and tag annotation, respectively. We repeat 10 times for the training-testing process and report the average performance.

From the tables, we make the following observations:

- The proposed method that utilizes pairwise labels to predict pointwise labels tends to outperform the methods which solely rely on pointwise labels. These results support that (1) pairwise attributes can provide evidence for the pointwise label prediction; especially for the Pubfig dataset that contains 8 label classes, our method utilizes information from pairwise attributes significantly improve the classification performance. (2) The performance of tag prediction $AP@K$ indicates that the pairwise attributes contain important information for tag prediction;

- Our method with model components to capture relations between pairwise and pointwise labels outperforms those without. For example, compared to GLasso, the proposed framework, modeling the relations via the bipartite graph, gains remarkable performance improvement for both classification and tag prediction; and

- Most of the time, the proposed framework PPP performs the best among all the baselines, which demonstrates the effectiveness of the proposed algorithm. There are two major reasons. First, PPP jointly performs pointwise and pairwise label prediction. Second, PPP captures relations between labels by extracting group information from the bipartite graph, which works as the bridge for building interactions between pointwise and pairwise labels.

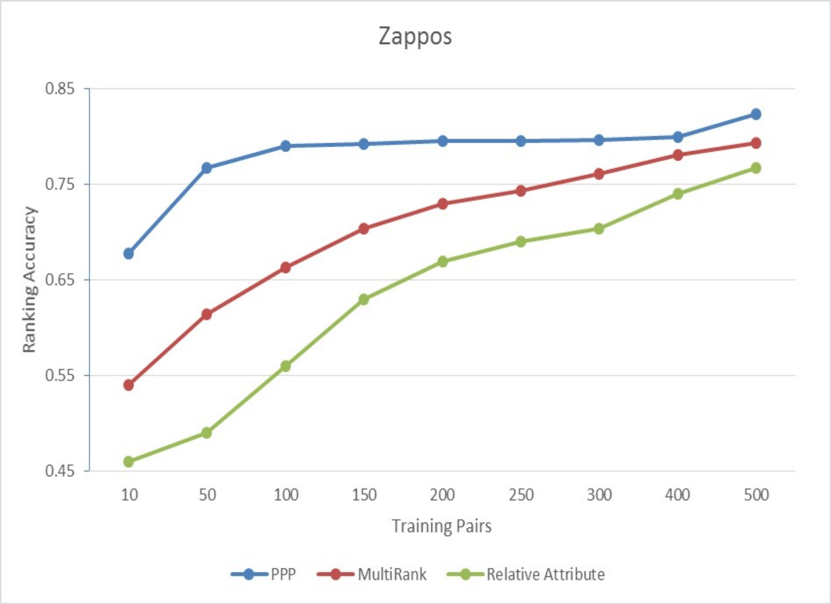

Figure 6.4: Learning Curve of Average Ranking Accuracy with Regarding to Different numbers of Training Pairs.

Table 6.3: The Average Ranking Accuracy on Three Dataset

Method	Zappos	OSR	Pubfig
RA	70.37%	76.10%	71.23%
MultiRank	76.12%	84.93%	74.91%
PPP	**79.67%**	**88.40%**	**76.32%**

6.4.4 Pairwise label Prediction

For pairwise label prediction, we generate pairs drawn from the training set used in the pointwise label prediction. For the Shoe dataset, we use 300 pairs; while for OSR and Pubfig, we use 100 pairs (the number suggested in Chen *et al.* (2014)) drawn from training set. We compute the average ranking accuracy with standard deviation by running 10 rounds of each implementation. The results are shown in Table 6.3. Moreover, we also plot in Figure 6.4 to show how average accuracy changes with different sizes of training samples on the attributes on the Shoe dataset (due to the space limits, we omit the figure on OSR and Pubfig).

From Table 6.3 and Figure 6.4, we can have the following observations:

- The proposed method that leverages pointwise labels to predict pairwise labels often outperforms the methods which only use pairwise labels. These results support that pointwise labels can help the pairwise label prediction;

- The performance of the ranking accuracy varies with the number of the training pairs. With a small amount of labeled data, e.g., 10 pairs, the proposed method significantly outperforms relative attribute methods, which demonstrates that the pointwise labels contain important information for attribute ranking;

- The comparison based on multi-task attribute learning methods and our method demonstrates that simply combining the attributes together fails to differentiate these attributes which are not related to other attributes, while our methods use group structures, which makes the correlated attributes have strong overlaps, providing a discriminative way to capture the correlation between attributes.

6.5 Summary

In this paper, we propose a novel way to capture the relations between pointwise labels and pairwise labels. Moreover, PPP provides a new viewpoint for us to have a better understanding how pointwise and pairwise labels interact with each other. Experiments demonstrated : (1) the advantages of the proposed methods for pointwise label based tasks including image classification, tag annotation and pairwise label based image ranking; and(2) the importance of considering the group correlation between pointwise labels and pairwise labels.

Chapter 7

FUTURE WORK AND CONCLUSION

In this chapter, I summarize my research results and their broader impacts, and highlighting the future directions.

7.1 Conclusion

With the growing availability of social media services, sentiment analysis is becoming an essential problem and attracts a lot of attention from academia and industry. Sentiment analysis for social media images aims to understand the sentiment of an image on social media. Successful detecting the visual sentiment in social media is important to improve the quality of user experience, and to promote the healthy use and development of a social networking system. Compared to traditional image classification problem in computer vision , sentiment analysis for social media data is more challenging. First, solely rely on the visual information is not enough as the visual content lacks of contextual information. At the mean time, due to the characteristics of social media, the textual data along the image is short and noisy. Therefore, text based sentiment analysis is also not satisfying. In this dissertation, I firstly address the key challenges of this novel problem. Then I proposed novel and effective computational model to tackle challenges and achieve good performance. Moreover, from the social media data, I am able to find user patterns or predict the activities in the physical world . In this dissertation, I propose four innovative research tasks - supervised and unsupervised sentiment analysis for social media images, understand self harm users from their image posts, and extend proposed computational model for general image classification tasks.

For supervised model of sentiment analysis , I first address the properties of social media images and find traditional approaches are not suit for this novel task. Therefore, I exploit both visual content and textual information and proposed a novel computational framework RSAI. It leverages several types of prior knowledge including: sentiment lexicon, sentiment labels and visual sentiment strength. To bridge the "affective gap" between low-level image features and high-level image sentiment, I propose a novel way to generate robust image representations. The results from the proposed computational model indicate that visual content and textual information are complementary to each other and considering both of them can improve the prediction performance.

Many supervised learning methods suffer from the lack of label information in real-world applications. It presents great challenges for sentiment analysis of social media images when there is no sufficient label data. In the dissertation, I proposed a principled approach to model the problem by utilzing textual information. Our novel strategy enable the unsupervised learning for sentiment analysis and achieve comparable performance to its supervised setting. The successful experience unsupervised sentiment analysis indicates that the importance of considering textual information.

Given the large scale of negative sentiment social media images and the anonymous nature of social media. I formally define the problem of self harm content prediction from social media images and make a number of important findings about the self harm users in social media. By investigate this novel task, first of this kind in the literature, we obtain the following observations: (1) The language of self-harm content has different structures compared with normal content, and the self-harm content expresses much more negative sentiments; (2)On average, owners of self-harm content are likely to have more activities, more social responses and less online friends compared to owners of normal content; (3) Posting time of self-harm content presents hourly patterns different from those of normal content, and self-harm content is likely to be posted during the night especially late night;

and (4) Photos in self-harm content are more gloomy and tend to focus on the salient body image patterns. These findings serve the groundwork of a supervised and an unsupervised framework, which can predict selfharm content from large amount of normal contents.

In order to generalize the methodologies used for sentiment analysis, I investigate the generalization algorithms for multi-label classification task in computer vision. To tack the problem, I investigate the problem of fusing pointwise and pairwise labels by exploiting their underlying relations. As a result, I derive a unified bipartite graph model to capture the underlying relations among two types of labels. Experimens on real Flickr and Shoe dataset show that the proposed framework can effectively integrate both kinds of information to outperform the state-of-the-art methods.

This dissertation investigates original problems that entreat unconventional computer vision and data mining tasks. They are challenging because the exists of "affective gap". Methodologies and techniques presented in this dissertation also have broader impacts:

- Social media provides a virtual world for users online activities and makes it possible to observe human behavior and interaction from tons of data. Our successful experience of using visual content and textual information pave the way for new research endeavor to study user behaviors in social media via computational model.
- Data availability is still challenging problem and our unified unsupervised sentiment analysis framework directly tack this challenges and could have impact for social scientist and computer scientists.
- A central challenge in public health revolves around how to identify individuals who are at risk for taking their own lives. Our findings from self harm content in social media could play important roles in helping public health agencies to help and assistant people who suffers depression in physical world.

7.2 Future Work

Predicting sentiment from social media images is still in its infant. Blow I present some promising research directions:

- **Weakly Supervised Methods:** Our previous study suggests that the "Affective and Noun Pairs" Borth *et al.* (2013b) achieves good representations for images in sentiment analysis tasks. While recent advanced deep learningLeCun *et al.* (2015) based image representations have shown great power in traditional computer vision tasks such as image classification and detection. Recently, You *et al.* (2016a) also demonstrate that applied deep neural network greatly improve the sentiment analysis performance. However, the deep learning based methods usually relies on a large amount of labelled data for training while the nature of social media data is unlabelled. Therefore, Using partial or limited data for robust network training for sentiment analysis of social media images is more applicable.

- **Interpreting and characterizing the Sentiment in the Visual Content:** Another key challenge in visual sentiment analysis is how to interpret the prediction model. One research direction is how to understand the dominant factors and visual content that invoke the sentiment. For example, do those image share the similar sentiment with similar objects and vice versa? or do they have similar visual features? By interpreting the image regions related to human sentiment and emotions, the computation model can pay more attention on those regions which could be potentially improve the prediction performance. Moreover, charaterizing the visual content can also benefit social scientist to understand and interpret human behavior and activities in physical world. We will investigate how to locate the objects, action or other visual features that related to human sentiment.

REFERENCES

Berg, T. L., A. C. Berg and J. Shih, “Automatic attribute discovery and characterization from noisy web data”, in “Computer Vision–ECCV 2010”, pp. 663–676 (Springer, 2010).

Borth, D., T. Chen, R. Ji and S.-F. Chang, “Sentibank: large-scale ontology and classifiers for detecting sentiment and emotions in visual content”, in “Proceedings of the 21st ACM international conference on Multimedia”, pp. 459–460 (ACM, 2013a).

Borth, D., R. Ji, T. Chen, T. Breuel and S.-F. Chang, “Large-scale visual sentiment ontology and detectors using adjective noun pairs”, in “Proceedings of the 21st ACM international conference on Multimedia”, pp. 223–232 (ACM, 2013b).

Boyd, S., N. Parikh, E. Chu, B. Peleato and J. Eckstein, “Distributed optimization and statistical learning via the alternating direction method of multipliers”, Foundations and Trends® in Machine Learning **3**, 1, 1–122 (2011).

Chancellor, S., Z. J. Lin and M. D. Choudhury, “”this post will just get taken down”: Characterizing removed pro-eating disorder social media content”, in “CHI, San Jose, CA, USA, May 7-12, 2016”, (2016).

Chang, C.-C. and C.-J. Lin, “Libsvm: A library for support vector machines”, ACM Transactions on Intelligent Systems and Technology (TIST) **2**, 3, 27 (2011).

Chapman, A. L., K. L. Gratz and M. Z. Brown, “Solving the puzzle of deliberate self-harm: The experiential avoidance model”, Behaviour research and therapy **44**, 3, 371–394 (2006).

Chen, L., P. Zhang and B. Li, “Fusing pointwise and pairwise labels for supporting user-adaptive image retrieval”, in “Proceedings of the 5th ACM on International Conference on Multimedia Retrieval”, pp. 67–74 (ACM, 2015).

Chen, L., Q. Zhang and B. Li, “Predicting multiple attributes via relative multi-task learning”, in “Computer Vision and Pattern Recognition (CVPR), 2014 IEEE Conference on”, pp. 1027–1034 (IEEE, 2014).

Chen, M., A. Zheng and K. Weinberger, “Fast image tagging”, in “Proceedings of the 30th international conference on Machine Learning”, pp. 1274–1282 (2013).

Cheng, M.-M., N. J. Mitra, X. Huang, P. H. Torr and S.-M. Hu, “Global contrast based salient region detection”, IEEE Transactions on Pattern Analysis and Machine Intelligence **37**, 3, 569–582 (2015).

Cohen, J., “Weighted kappa: Nominal scale agreement provision for scaled disagreement or partial credit.”, Psychological bulletin **70**, 4, 213 (1968).

Daine, K., K. Hawton, V. Singaravelu, A. Stewart, S. Simkin and P. Montgomery, “The power of the web: a systematic review of studies of the influence of the internet on self-harm and suicide in young people”, PloS one **8**, 10, e77555 (2013).

Dalal, N. and B. Triggs, “Histograms of oriented gradients for human detection”, in “Computer Vision and Pattern Recognition, 2005. CVPR 2005. IEEE Computer Society Conference on”, vol. 1, pp. 886–893 (IEEE, 2005).

Darwin, C., *The expression of the emotions in man and animals* (Oxford University Press, 1998).

Das Gupta, M. and J. Xiao, “Non-negative matrix factorization as a feature selection tool for maximum margin classifiers”, in “Computer Vision and Pattern Recognition (CVPR), 2011 IEEE Conference on”, pp. 2841–2848 (IEEE, 2011).

De Choudhury, M., S. Counts and M. Gamon, “Not all moods are created equal! exploring human emotional states in social media”, in “Sixth International AAAI Conference on Weblogs and Social Media”, (2012).

De Choudhury, M., M. Gamon, S. Counts and E. Horvitz, “Predicting depression via social media.”, in “ICWSM”, p. 2 (2013).

De Choudhury, M., E. Kiciman, M. Dredze, G. Coppersmith and M. Kumar, “Discovering shifts to suicidal ideation from mental health content in social media”, in “Proceedings of the 2016 CHI Conference on Human Factors in Computing Systems”, pp. 2098–2110 (ACM, 2016).

Deng, J., W. Dong, R. Socher, L.-J. Li, K. Li and L. Fei-Fei, “Imagenet: A large-scale hierarchical image database”, in “Computer Vision and Pattern Recognition, 2009. CVPR 2009. IEEE Conference on”, pp. 248–255 (IEEE, 2009).

Ding, C., T. Li and M. I. Jordan, “Convex and semi-nonnegative matrix factorizations”, Pattern Analysis and Machine Intelligence, IEEE Transactions on **32**, 1, 45–55 (2010).

Ding, C., T. Li, W. Peng and H. Park, “Orthogonal nonnegative matrix t-factorizations for clustering”, in “Proceedings of the 12th ACM SIGKDD international conference on Knowledge discovery and data mining”, pp. 126–135 (ACM, 2006).

Ding, C. H., X. He and H. D. Simon, “On the equivalence of nonnegative matrix factorization and spectral clustering.”, in “SDM”, vol. 5, pp. 606–610 (SIAM, 2005).

Dyson, M. P., L. Hartling, J. Shulhan, A. Chisholm, A. Milne, P. Sundar, S. D. Scott and A. S. Newton, “A systematic review of social media use to discuss and view deliberate self-harm acts”, PLoS one **11**, 5, e0155813 (2016).

Ekman, P., “An argument for basic emotions”, Cognition & Emotion **6**, 3-4, 169–200 (1992).

Farhadi, A., I. Endres, D. Hoiem and D. Forsyth, “Describing objects by their attributes”, in “Computer Vision and Pattern Recognition, 2009. CVPR 2009. IEEE Conference on”, pp. 1778–1785 (IEEE, 2009).

Felzenszwalb, P. F., R. B. Girshick, D. McAllester and D. Ramanan, “Object detection with discriminatively trained part-based models”, Pattern Analysis and Machine Intelligence, IEEE Transactions on **32**, 9, 1627–1645 (2010).

Gimpel, K., N. Schneider, B. O'Connor, D. Das, D. Mills, J. Eisenstein, M. Heilman, D. Yogatama, J. Flanigan and N. A. Smith, "Part-of-speech tagging for twitter: Annotation, features, and experiments", in "Proceedings of the 49th Annual Meeting of the Association for Computational Linguistics: Human Language Technologies: short papers-Volume 2", pp. 42–47 (Association for Computational Linguistics, 2011).

Go, A., R. Bhayani and L. Huang, "Twitter sentiment classification using distant supervision", (????).

Goodman, L. A., "Snowball sampling", The annals of mathematical statistics pp. 148–170 (1961).

Gratz, K. L., S. D. Conrad and L. Roemer, "Risk factors for deliberate self-harm among college students.", American journal of Orthopsychiatry **72**, 1, 128 (2002).

Han, B. and T. Baldwin, "Lexical normalisation of short text messages: Makn sens a# twitter", in "Proceedings of the 49th Annual Meeting of the Association for Computational Linguistics: Human Language Technologies-Volume 1", pp. 368–378 (Association for Computational Linguistics, 2011).

Hawton, K., J. Fagg, S. Simkin, E. Bale and A. Bond, "Trends in deliberate self-harm in oxford, 1985-1995. implications for clinical services and the prevention of suicide.", The British Journal of Psychiatry **171**, 6, 556–560 (1997).

Hawton, K. and A. James, "Suicide and deliberate self harm in young people", Bmj **330**, 7496, 891–894 (2005).

Hawton, K., K. Rodham, E. Evans and R. Weatherall, "Deliberate self harm in adolescents: self report survey in schools in england", Bmj **325**, 7374, 1207–1211 (2002).

Hofmann, T., "Probabilistic latent semantic indexing", in "Proceedings of the 22nd annual international ACM SIGIR conference on Research and development in information retrieval", pp. 50–57 (ACM, 1999).

Houghton, D. J. and A. N. Joinson, "Linguistic markers of secrets and sensitive self-disclosure in twitter", in "System Science (HICSS), 2012 45th Hawaii International Conference on", pp. 3480–3489 (IEEE, 2012).

Hu, M. and B. Liu, "Mining and summarizing customer reviews", in "Proceedings of the tenth ACM SIGKDD international conference on Knowledge discovery and data mining", pp. 168–177 (ACM, 2004).

Hu, Y., L. Manikonda and S. Kambhampati, "What we instagram: A first analysis of instagram photo content and user types", (2014).

Hu, Y., F. Wang and S. Kambhampati, "Listening to the crowd: automated analysis of events via aggregated twitter sentiment", in "Proceedings of the Twenty-Third international joint conference on Artificial Intelligence", pp. 2640–2646 (AAAI Press, 2013).

Hussain, Z., T. Patanam and H. Cate, "Group visual sentiment analysis", arXiv preprint arXiv:1701.01885 (2017).

Itti, L. and C. Koch, “Computational modelling of visual attention”, Nature reviews neuroscience **2**, 3, 194–203 (2001).

Jannach, D., M. Zanker, A. Felfernig and G. Friedrich, *Recommender systems: an introduction* (Cambridge University Press, 2010).

Ji, S., L. Tang, S. Yu and J. Ye, “Extracting shared subspace for multi-label classification”, in “Proceedings of the 14th ACM SIGKDD international conference on Knowledge discovery and data mining”, pp. 381–389 (ACM, 2008).

Jia, J., S. Wu, X. Wang, P. Hu, L. Cai and J. Tang, “Can we understand van gogh’s mood?: learning to infer affects from images in social networks”, in “Proceedings of the 20th ACM international conference on Multimedia”, pp. 857–860 (ACM, 2012).

Jiang, Y.-G., G. Ye, S.-F. Chang, D. Ellis and A. C. Loui, “Consumer video understanding: A benchmark database and an evaluation of human and machine performance”, in “Proceedings of the 1st ACM International Conference on Multimedia Retrieval”, p. 29 (ACM, 2011).

Kairam, S., J. Kaye, J. A. G. Gómez and D. A. Shamma, “Snap decisions? how users, content, and aesthetics interact to shape photo sharing behaviors”, CHI 2016 (2016).

Kim, Y., “Convolutional neural networks for sentence classification”, arXiv preprint arXiv:1408.5882 (2014).

Kovashka, A. and K. Grauman, “Attribute adaptation for personalized image search”, in “Computer Vision (ICCV), 2013 IEEE International Conference on”, pp. 3432–3439 (IEEE, 2013a).

Kovashka, A. and K. Grauman, “Attribute pivots for guiding relevance feedback in image search”, in “Computer Vision (ICCV), 2013 IEEE International Conference on”, pp. 297–304 (IEEE, 2013b).

Krizhevsky, A., I. Sutskever and G. E. Hinton, “Imagenet classification with deep convolutional neural networks”, in “Advances in neural information processing systems”, pp. 1097–1105 (2012).

Kumar, N., A. C. Berg, P. N. Belhumeur and S. K. Nayar, “Attribute and simile classifiers for face verification”, in “Computer Vision, 2009 IEEE 12th International Conference on”, pp. 365–372 (IEEE, 2009).

Lampert, C. H., H. Nickisch and S. Harmeling, “Learning to detect unseen object classes by between-class attribute transfer”, in “Computer Vision and Pattern Recognition, 2009. CVPR 2009. IEEE Conference on”, pp. 951–958 (IEEE, 2009).

LeCun, Y., Y. Bengio and G. Hinton, “Deep learning”, nature **521**, 7553, 436 (2015).

Lee, D. D. and H. S. Seung, “Learning the parts of objects by non-negative matrix factorization”, Nature **401**, 6755, 788–791 (1999).

Lee, D. D. and H. S. Seung, “Algorithms for non-negative matrix factorization”, in “Advances in neural information processing systems”, pp. 556–562 (2001).

Liu, B., “Sentiment analysis and opinion mining”, Synthesis Lectures on Human Language Technologies **5**, 1, 1–167 (2012).

Liu, J., S. Ji, J. Ye *et al.*, “Slep: Sparse learning with efficient projections”, (????).

Lustberg, L. and C. F. Reynolds, “Depression and insomnia: questions of cause and effect”, Sleep medicine reviews **4**, 3, 253–262 (2000).

Machajdik, J. and A. Hanbury, “Affective image classification using features inspired by psychology and art theory”, in “Proceedings of the 18th ACM international conference on Multimedia”, pp. 83–92 (ACM, 2010).

Mikolov, T., K. Chen, G. Corrado and J. Dean, “Efficient estimation of word representations in vector space”, arXiv preprint arXiv:1301.3781 (2013).

Moreno, M. A., A. Ton, E. Selkie and Y. Evans, “Secret society 123: understanding the language of self-harm on instagram”, Journal of Adolescent Health **58**, 1, 78–84 (2016).

Muehlenkamp, J. J., L. Claes, L. Havertape and P. L. Plener, “International prevalence of adolescent non-suicidal self-injury and deliberate self-harm”, Child and Adolescent Psychiatry and Mental Health **6**, 1, 1 (2012).

Nie, F., H. Huang, X. Cai and C. H. Ding, “Efficient and robust feature selection via joint 2, 1-norms minimization”, in “Advances in Neural Information Processing Systems”, pp. 1813–1821 (2010).

Oliva, A. and A. Torralba, “Modeling the shape of the scene: A holistic representation of the spatial envelope”, International journal of computer vision **42**, 3, 145–175 (2001).

Pak, A. and P. Paroubek, “Twitter as a corpus for sentiment analysis and opinion mining.”, in “LREc”, vol. 10 (2010).

Pandey, M. and S. Lazebnik, “Scene recognition and weakly supervised object localization with deformable part-based models”, in “Computer Vision (ICCV), 2011 IEEE International Conference on”, pp. 1307–1314 (IEEE, 2011).

Pang, B. and L. Lee, “A sentimental education: Sentiment analysis using subjectivity summarization based on minimum cuts”, in “Proceedings of the 42nd annual meeting on Association for Computational Linguistics”, p. 271 (Association for Computational Linguistics, 2004).

Pang, B., L. Lee and S. Vaithyanathan, “Thumbs up?: sentiment classification using machine learning techniques”, in “Proceedings of the ACL-02 conference on Empirical methods in natural language processing-Volume 10”, pp. 79–86 (Association for Computational Linguistics, 2002).

Pang, B., L. Lee *et al.*, “Opinion mining and sentiment analysis”, Foundations and Trends® in Information Retrieval **2**, 1–2, 1–135 (2008).

Parikh, D. and K. Grauman, “Relative attributes”, in “Computer Vision (ICCV), 2011 IEEE International Conference on”, pp. 503–510 (IEEE, 2011).

Pestian, J. P., P. Matykiewicz, M. Linn-Gust, B. South, O. Uzuner, J. Wiebe, K. B. Cohen, J. Hurdle and C. Brew, “Sentiment analysis of suicide notes: A shared task”, Biomedical informatics insights **5**, Suppl. 1, 3 (2012).

Petrie, K. and R. Brook, “Sense of coherence, self-esteem, depression and hopelessness as correlates of reattempting suicide”, British Journal of Clinical Psychology **31**, 3, 293–300 (1992).

Plutchik, R., *Emotion: A psychoevolutionary synthesis* (Harper & Row New York, 1980).

Robinson, J., G. Cox, E. Bailey, S. Hetrick, M. Rodrigues, S. Fisher and H. Herrman, “Social media and suicide prevention: a systematic review”, Early Interv Psychiatry (2015).

Rude, S. S., C. R. Valdez, S. Odom and A. Ebrahimi, “Negative cognitive biases predict subsequent depression”, Cognitive Therapy and Research **27**, 4, 415–429 (2003).

Sadilek, A., H. A. Kautz and V. Silenzio, “Modeling spread of disease from social interactions.”, (2012).

Sculley, D., “Combined regression and ranking”, in “Proceedings of the 16th ACM SIGKDD international conference on Knowledge discovery and data mining”, pp. 979–988 (ACM, 2010).

Siersdorfer, S., E. Minack, F. Deng and J. Hare, “Analyzing and predicting sentiment of images on the social web”, in “Proceedings of the 18th ACM international conference on Multimedia”, pp. 715–718 (ACM, 2010).

Sigurbjörnsson, B. and R. Van Zwol, “Flickr tag recommendation based on collective knowledge”, in “Proceedings of the 17th international conference on World Wide Web”, pp. 327–336 (ACM, 2008).

Stirman, S. W. and J. W. Pennebaker, “Word use in the poetry of suicidal and nonsuicidal poets”, Psychosomatic Medicine **63**, 4, 517–522 (2001).

Taboada, M., J. Brooke, M. Tofiloski, K. Voll and M. Stede, “Lexicon-based methods for sentiment analysis”, Computational linguistics **37**, 2, 267–307 (2011).

Thomee, B., D. A. Shamma, G. Friedland, B. Elizalde, K. Ni, D. Poland, D. Borth and L.-J. Li, “The new data and new challenges in multimedia research”, arXiv preprint arXiv:1503.01817 (2015).

Tighe, J. and S. Lazebnik, “Finding things: Image parsing with regions and per-exemplar detectors”, in “Computer Vision and Pattern Recognition (CVPR), 2013 IEEE Conference on”, pp. 3001–3008 (IEEE, 2013).

Toderici, G., H. Aradhye, M. Paşca, L. Sbaiz and J. Yagnik, “Finding meaning on youtube: Tag recommendation and category discovery”, in “Computer Vision and Pattern Recognition (CVPR), 2010 IEEE Conference on”, pp. 3447–3454 (IEEE, 2010).

Tu, Z., X. Chen, A. L. Yuille and S.-C. Zhu, “Image parsing: Unifying segmentation, detection, and recognition”, International Journal of Computer Vision **63**, 2, 113–140 (2005).

Tuytelaars, T. and K. Mikolajczyk, “Local invariant feature detectors: a survey”, Foundations and trends® in computer graphics and vision **3**, 3, 177–280 (2008).

Vinh, N. X., J. Epps and J. Bailey, “Information theoretic measures for clusterings comparison: Variants, properties, normalization and correction for chance”, JLMR pp. 2837–2854 (2010).

Wang, C., D. Blei and F.-F. Li, “Simultaneous image classification and annotation”, in “Computer Vision and Pattern Recognition, 2009. CVPR 2009. IEEE Conference on”, pp. 1903–1910 (IEEE, 2009).

Wang, M., D. Cao, L. Li, S. Li and R. Ji, “Microblog sentiment analysis based on cross-media bag-of-words model”, in “Proceedings of international conference on internet multimedia computing and service”, p. 76 (ACM, 2014).

Wang, S., J. Tang, Y. Wang and H. Liu, “Exploring implicit hierarchical structures for recommender systems”, in “Proceedings of the Twenty-Fourth International Joint Conference on Artificial Intelligence, IJCAI 2015, Buenos Aires, Argentina, July 25-31, 2015”, pp. 1813–1819 (2015a), URL `http://ijcai.org/papers15/Abstracts/IJCAI15-258.html`.

Wang, Y., Y. Hu, S. Kambhampati and B. Li, “Inferring sentiment from web images with joint inference on visual and social cues: A regulated matrix factorization approach”, in “Ninth international AAAI conference on web and social media”, (2015b).

Wang, Y., Y. Hu, S. Kambhampati and B. Li, “Inferring sentiment from web images with joint inference on visual and social cues: A regulated matrix factorization approach”, in “Proceedings of the Ninth International Conference on Web and Social Media, ICWSM 2015, University of Oxford, Oxford, UK, May 26-29, 2015”, pp. 473–482 (2015c), URL `http://www.aaai.org/ocs/index.php/ICWSM/ICWSM15/paper/view/10532`.

Wang, Y., Y. Jia, C. Hu and M. Turk, “Non-negative matrix factorization framework for face recognition”, International Journal of Pattern Recognition and Artificial Intelligence **19**, 04, 495–511 (2005).

Wang, Y., S. Wang, J. Tang, H. Liu and B. Li, “Unsupervised sentiment analysis for social media images”, in “Proceedings of the Twenty-Fourth International Joint Conference on Artificial Intelligence, IJCAI 2015, Buenos Aires, Argentina, July 25-31, 2015”, pp. 2378–2379 (2015d), URL `http://ijcai.org/papers15/Abstracts/IJCAI15-336.html`.

Wang, Y., S. Wang, J. Tang, H. Liu and B. Li, “PPP: Joint pointwise and pairwise image label prediction”, in “Proceedings of the IEEE Conference on Computer Vision and Pattern Recognition”, (2016).

Wilson, T., J. Wiebe and P. Hoffmann, “Recognizing contextual polarity in phrase-level sentiment analysis”, in “Proceedings of the conference on human language technology and empirical methods in natural language processing”, pp. 347–354 (Association for Computational Linguistics, 2005).

Xiao, J., J. Hays, K. A. Ehinger, A. Oliva and A. Torralba, “Sun database: Large-scale scene recognition from abbey to zoo”, in “Computer vision and pattern recognition (CVPR), 2010 IEEE conference on”, pp. 3485–3492 (IEEE, 2010).

Yang, Y., J. Jia, S. Zhang, B. Wu, J. Li and J. Tang, “How do your friends on social media disclose your emotions?”, (2014).

Yogatama, D. and N. Smith, “Making the most of bag of words: Sentence regularization with alternating direction method of multipliers”, in “Proceedings of the 31st International Conference on Machine Learning (ICML-14)”, pp. 656–664 (2014).

Yom-Tov, E., L. Fernandez-Luque, I. Weber and S. P. Crain, “Pro-anorexia and pro-recovery photo sharing: a tale of two warring tribes”, Journal of medical Internet research **14**, 6, e151 (2012).

You, Q., L. Cao, H. Jin and J. Luo, “Robust visual-textual sentiment analysis: When attention meets tree-structured recursive neural networks”, in “Proceedings of the 2016 ACM on Multimedia Conference”, pp. 1008–1017 (ACM, 2016a).

You, Q., J. Luo, H. Jin and J. Yang, “Robust image sentiment analysis using progressively trained and domain transferred deep networks”, (2015).

You, Q., J. Luo, H. Jin and J. Yang, “Cross-modality consistent regression for joint visual-textual sentiment analysis of social multimedia”, in “Proceedings of the Ninth ACM International Conference on Web Search and Data Mining”, pp. 13–22 (ACM, 2016b).

Yu, A. and K. Grauman, “Fine-grained visual comparisons with local learning”, in “Computer Vision and Pattern Recognition (CVPR), 2014 IEEE Conference on”, pp. 192–199 (IEEE, 2014).

Yuan, J., S. Mcdonough, Q. You and J. Luo, “Sentribute: image sentiment analysis from a mid-level perspective”, in “Proceedings of the Second International Workshop on Issues of Sentiment Discovery and Opinion Mining”, p. 10 (ACM, 2013).

Yuan, L., J. Liu and J. Ye, “Efficient methods for overlapping group lasso”, in “Advances in Neural Information Processing Systems”, pp. 352–360 (2011).

Yuan, M. and Y. Lin, “Model selection and estimation in regression with grouped variables”, Journal of the Royal Statistical Society: Series B (Statistical Methodology) **68**, 1, 49–67 (2006).

Zeppelzauer, M. and D. Schopfhauser, “Multimodal classification of events in social media”, Image and Vision Computing **53**, 45–56 (2016).

Zhu, X. and D. Ramanan, “Face detection, pose estimation, and landmark localization in the wild”, in “Computer Vision and Pattern Recognition (CVPR), 2012 IEEE Conference on”, pp. 2879–2886 (IEEE, 2012).